UNIVERSIDADE DE LISBOA
FACULDADE DE CIÊNCIAS
DEPARTAMENTO DE QUÍMICA E BIOQUÍMICA

Influence of Guava Leaf Decoctions on Cholesterol Permeation through the Intestinal Barrier and Cholesterol Biosynthesis

Maria Constança Batista da Cunha e Lorena

Mestrado em Bioquímica
Especialização em Bioquímica

Dissertação orientada por:
Professora Doutora Maria Luísa Mourato Oliveira Marques Serralheiro
Doutora Asma Ressaissi

2020

Acknowledgements

This work wouldn’t be successfully completed without the contribution of several people around me.

Firstly, I would like to show my deepest gratitude to Professor Dr. Maria Luísa Serralheiro for her guidance, knowledge, and enthusiasm throughout the entire work and for providing excellent working conditions for the development of this thesis.

I would also like to express my gratitude to Dr. Asma Ressaissi for mentoring me in the laboratory work and analysis of results. Her knowledge, critical spirit, and patience are worth mentioning.

I’m grateful to Professor Rita Pacheco for helping and encouraging me during the last months. A special thanks to my laboratory colleagues, Rebeca André, Laura Guedes, and Ana Rita Ferraz, for welcoming me and for the help and support provided.

To my family and friends, for believing in me and for supporting me through the hardest moments.

To everyone who, directly or indirectly, helped and supported me throughout this year, my sincere thanks.

Abstract

Psidium guajava L. leaf decoction has been used in traditional medicine due to its beneficial health effects, both in the prevention and treatment of diseases, namely hypercholesterolemia. This disorder consists of abnormally high levels of blood cholesterol and it's a risk factor for the development of cardiovascular diseases. Cholesterol homeostasis is maintained through the endogenous synthesis, intestinal absorption, and hepatic excretion.

The aim of this thesis was to evaluate the bioactivity and chemical composition of *P. guajava* leaf decoction and its influence on cholesterol absorption and metabolism. To do so, cholesterol permeation through the simulated intestinal barrier, inhibition of 3-hydroxy-3-methylglutaryl coenzyme A reductase (HMGR), and inhibition of cholesterol transporters was assessed under the decoction's influence. The aqueous extract (PG1) and the ethanolic precipitation supernatant (PG2) and pellet (PG3) from *P. guajava* leaf decoction were studied. It was observed that PG1 and PG2 were rich in phenolic compounds, whereas PG3 had low concentration of these bioactive molecules. The samples also possess strong antioxidant power (EC_{50} 7.5 ± 0.4, 11.9 ± 0.5, and 7.3 ± 0.6 µg/mL for PG1, PG2, and PG3, respectively) and acetylcholinesterase inhibitory activity was only achieved by PG1 and PG2 (48.66 ± 1.39 and 63.44 ± 1.13 µg/mL for PG1 and PG2, respectively). In addition, PG1 and PG2 weren't cytotoxic. Some phenolic compounds from PG1 and PG2 were able to permeate the intestinal barrier, ranging from 0.07 to 9.95%. The decoction also decreased cholesterol absorption in the simulated intestinal wall (55% and 24% for PG1 and PG2, respectively). The decoction inhibited cholesterol biosynthesis by inhibiting the HMGR activity (IC_{50} 8.4 ± 0.5 µg/mL for PG1) and decreased the expression of cholesterol transporters NPC1L1 (ranging from 16 to 94%), ABCG5 (ranging from 28 to 98%), and ABCG8 (ranging from 24 to 80%). Additionally, FTIR data suggested a decrease in protein expression related to modifications at the transcription level. In conclusion, *P. guajava* leaf decoction was reported to influence cholesterol homeostasis at several levels, which helps explain its use and effects in traditional medicine.

Keywords

Psidium guajava L., cholesterol, phenolic compounds, cholesterol transporters

Resumo

Psidium guajava L., também conhecida por goiabeira, é uma pequena árvore nativa de áreas tropicais como a América Central e do Sul. No entanto, é capaz de crescer em diversos climas. As suas folhas são muito usadas sob a forma de decocção na medicina tradicional para prevenir e tratar de várias doenças e indisposições. Foi relatado que esta decocção apresenta propriedades antioxidantes, anti-inflamatórias, antimicrobianas e anti-hipercolesterolémicas. O racional por detrás destes efeitos está relacionado com a presença de moléculas com bioatividade conhecida como os compostos fenólicos (inclui maioritariamente ácidos fenólicos, flavonoides e taninos) e derivados, terpenos, ácido ascórbico, entre outros.

Os compostos fenólicos são a maior classe de metabolitos secundários em plantas, sendo encontrados em quase todas as estruturas vegetais, como frutos, sementes, caules, folhas e raízes. Estas moléculas são dotadas de propriedades antioxidantes e anti-inflamatórias que têm efeitos positivos na saúde quando se consomem alimentos ricos neste tipo de compostos. De forma semelhante, os terpenos são moléculas com grande variedade estrutural e podem ser encontrados principalmente em frutos, vegetais e flores. São responsáveis pelo cheiro das plantas e também apresentam propriedades benéficas para a saúde ao funcionarem como agentes antimicrobianos, antihiperglicémicos e anti-inflamatórios. Estes dois grupos de moléculas, ao funcionarem como antioxidantes, resultantes das suas características estruturais, reduzem o stress oxidativo associado a várias doenças crónicas e degenerativas como cancro, doença de Alzheimer, diabetes, doenças cardiovasculares, entre outras.

As doenças cardiovasculares são responsáveis por uma grande taxa de mortalidade em países desenvolvidos, sendo a hipercolesterolemia um dos principais fatores de risco. Esta é uma doença em que os níveis de colesterol estão elevados no sangue e tal pode provocar aterosclerose, cancro, síndrome metabólico e neurodegeneração. A homeostasia do colesterol pode ser regulada a vários níveis: através da síntese endógena no fígado, da absorção intestinal de colesterol proveniente da dieta e através do efluxo hepático. Sendo assim, é comum prescreverem-se fármacos como as Estatinas e a Ezetimiba que inibem, respetivamente, o enzima regulador da síntese de colesterol 3-hidroxi-3-metillglutaril coenzima A redutase (HMGR) e a absorção de colesterol da dieta no intestino ao interferir com a atividade dos transportadores de colesterol dos enterócitos. A hipercolesterolemia é também um fator de risco para o desenvolvimento da doença de Alzheimer. De notar que o enzima acetilcolinesterase (AChE) é um dos alvos terapêuticos da doença de Alzheimer e que, devido à sua atividade também nas junções neuromusculares, a sua inibição aumenta a motilidade intestinal. Assim, existe uma contribuição para a diminuição da absorção de colesterol da dieta no intestino. Foi relatado que o consumo de infusões e decocções de plantas ricas em compostos fenólicos diminuíram os níveis de colesterol no sangue de pessoas dispostas a tomar tais bebidas. Este tipo de observações realçam o potencial de decocções de plantas, como aquela feita de folhas de goiabeira, e o seu possível uso com fins terapêuticos.

O objetivo deste estudo é determinar a bioatividade e composição química da decocção de folhas de *P. guajava* e compreender a sua influência na absorção e metabolismo do colesterol. Adicionalmente, foi estudada a influência da decocção num enzima envolvido na doença de Alzheimer e motilidade intestinal, o AChE. Para tal, vai ser avaliada a permeação de colesterol através da barreira intestinal simulada, a inibição do enzima HMGR e a inibição da expressão de transportadores de colesterol na presença de extratos provenientes da decocção de folhas de goiabeira.

Prepararam-se três extratos a partir da decocção de folhas de goiabeira, nomeadamente o extrato aquoso (PG1), que mimetiza a decocção tal e qual como é consumida; o sobrenadante da precipitação com etanol (PG2) que corresponde a uma fração sem mucilagens, que mascaram a atividade e concentração de moléculas ativas; o pellet rico em mucilagens (PG3) cuja análise ajuda a compreender se houve co-

precipitação de moléculas ativas. O conteúdo fenólico total e de flavonoides foi analisado em todas as amostras. O extrato aquoso foi o mais rico nestes dois grupos de moléculas. Estes valores refletem a presença de várias moléculas identificadas através de espetrometria de massa, nomeadamente quercetina, ácido clorogénico, ácido gálico, catequina e epigalocatequina. Também foram identificados derivados glicosídicos de quercetina como o hiperósido, a quercitrina e a guaijaverina. O terpenóide ácido jacoumárico foi também encontrado no extrato aquoso bem como alguns metabolitos primários. A atividade antioxidante foi analisada e constatou-se que as amostras são ativas e que o extrato aquoso era o mais antioxidante (EC_{50} 7.5 ± 0.4, 11.9 ± 0.5 e 7.3 ± 0.6 µg/mL para o extrato aquoso, sobrenadante e pellet, respetivamente). Já para o ensaio da inibição do enzima AChE, apenas extrato aquoso e o sobrenadante obtiveram resultados e estes mostraram-se promissores (IC_{50} 48.7 ± 1.4 e 63.4 ± 1.1 µg/mL, respetivamente). Com base nestas observações, não se utilizou mais o extrato das mucilagens. Antes de qualquer ensaio em linhas celulares, foi averiguada a citotoxicidade das amostras e chegou-se à conclusão de que nenhum era tóxico. A digestão *in vitro* com sucos gástrico e pancreático artificiais não exerceram modificações no extrato aquoso. Assim, as moléculas presentes nos extratos são capazes de chegar ao intestino sem sofrerem alterações significativas e o seu efeito neste órgão pode ser avaliado. Um destes ensaios é determinação da permeação de moléculas ativas através da barreira intestinal simulada com células Caco-2 diferenciadas num sistema *Transwell*. Esta análise permitiu observar que o ácido clorogénico, a quercetina, o ácido gálico, a catequina e a quercitrina são capazes de permear a barreira intestinal de modo a entrar na corrente sanguínea e alcançar outros alvos terapêuticos. No fígado ocorre a síntese endógena de colesterol cuja regulação é efetuada através da modulação da atividade do enzima limitante HMGR. O extrato aquoso mostrou ser capaz de inibir este enzima (IC_{50} 8.4 ± 0.5 µg/mL) e reduzir os níveis de colesterol no sangue de forma semelhante às Estatinas, um fármaco utilizado para este fim. Neste ensaio foi obtido um valor de IC_{50} baixo mas maior que o IC_{50} das Estatinas. Outra forma de reduzir o nível de colesterol no sangue é através da inibição da absorção de colesterol proveniente da dieta no intestino. Tanto o extrato aquoso como o sobrenadante diminuíram a absorção de colesterol 55% e 24%, respetivamente. Para perceber como é que esta diminuição é provocada, a expressão dos transportadores de colesterol ABCG5, ABCG8 e NPC1L1 foi analisada através de Western Blot. Observou-se que a expressão destas proteínas diminuiu em células expostas aos dois extratos. A diminuição da expressão de NPC1L1 e o aumento da expressão de ABCG5 e ABCG8 é desejada para diminuir os valores de colesterol no sangue. Sendo assim, apenas a diminuição de expressão do transportador NPC1L1 pode explicar os efeitos benéficos da decocção de folhas de goiabeira. A espetrometria de FTIR foi utilizada para analisar os metabolitos de células hepáticas (HepG2) sob o efeito dos extratos aquoso e do sobrenadante. Ambas as amostras modificaram o perfil metabólico, sendo que houve uma diminuição da síntese proteica provocada por perturbações na transcrição de genes. Os lípidos também sofreram alterações a nível da sua síntese, sendo esta menor na presença de extrato. Também da análise por SDS-PAGE das proteínas provenientes de células Caco-2 se chegou à conclusão de que os extratos diminuem a quantidade de proteína nas células.

Em conclusão, a decocção de folhas de *P. guajava* mostrou ser capaz de interferir na absorção e metabolismo de colesterol a vários níveis. Este efeito é resultante da inibição do enzima HMGR no fígado e da inibição da absorção de colesterol da dieta no intestino através da diminuição da expressão do transportador NPC1L1. Estas observações ajudam a compreender o racional por detrás do uso e justificar os efeitos observados na medicina tradicional.

Palavras chave: *Psidium guajava* L., colesterol, compostos fenólicos, transportadores de colesterol

Table of Contents

Acknowledgements III
Abstract V
Resumo VI
List of Tables XI
List of Figures XII
Abbreviations XIV
General Introduction 1
I. Introduction 2
1.1. *Psidium guajava* 3
1.1.1. Botany 3
1.1.2. Uses of *P. guajava* leaves in traditional medicine 3
1.1.3. Chemical composition *P. guajava* leaves 4
1.2. Phenolic compounds 4
1.2.1. Role in plants and in human diseases 5
1.2.2. Structure and classification 5
1.2.3. Bioavailability of phenolic compounds 9
1.3. Terpenes in plant extracts 10
1.4. Dietary plant peptides 10
1.5. Cholesterol: absorption, metabolism, and role in diseases 11
1.5.1. Cholesterol transporters 11
1.5.2. Cholesterol intestinal absorption 13
1.5.3. Cholesterol biosynthesis 14
1.5.4. Reverse cholesterol transport (RCT) and biliary cholesterol secretion 14
1.5.5. Regulation of cholesterol homeostasis 15
1.5.6. Hypercholesterolemia 15
1.5.7. Acetylcholinesterase, Alzheimer's disease, and cholesterol homeostasis 16
II. Objectives 18
III. Materials and Methods 20
3.1. Reagents 21
3.2. Decoction and sample preparation 21
3.3. Quantification of bioactive compounds in *P. guajava* leaf decoction 22
3.3.1. Quantification of total phenolic content 22

3.3.2. Quantification of flavonoids 22
3.4. Identification and quantification of compounds in *P. guajava* decoction 22
3.4.1. High-resolution liquid chromatography – high-resolution tandem mass spectrometry (LC-HRMS-MS) 22
3.4.2. High-performance liquid chromatography with diode array (HPLC-DAD) 23
3.5. Determination of *P. guajava* leaf decoction biological activity 23
3.5.1. Antioxidant activity 23
3.5.2. Acetylcholinesterase inhibition 23
3.5.3. HMG-CoA reductase inhibition 24
3.6. *In vitro* gastrointestinal digestion of *P. guajava* leaf decoction 24
3.7. Cell culture 25
3.8. Cytotoxicity of *P. guajava* leaf decoction 25
3.9. Permeation studies 25
3.10. Fourier-transform infrared spectroscopy (FTIR) analysis of HepG2 cellular components 26
3.11. Effect of *P. guajava* decoction in the protein profile of cells 26
3.11.1. Sodium dodecyl sulfate-polyacrylamide gel electrophoresis (SDS-PAGE) of cytosolic and membrane proteins from Caco-2 26
3.11.2. Effect of *P. guajava* decoction on cholesterol transporters expression 27
3.13. Data analysis 28
IV. Results and Discussion 30
4.1. Quantification of bioactive compounds in *P. guajava* leaf decoction: total phenolic and flavonoid content 31
4.2. Identification and quantification of compounds in *P. guajava* leaf decoction 32
4.2.1. High-resolution liquid chromatography – high-resolution tandem mass spectrometry (LC-HRMS-MS) analysis 32
4.2.2. High-performance liquid chromatography with diode array (HPLC-DAD) analysis 37
4.3. Determination of *P. guajava* leaf decoction biological activity 39
4.3.1. Antioxidant activity 39
4.3.2. Acetylcholinesterase inhibition 40
4.4. *In vitro* gastrointestinal digestion of *P. guajava* leaf decoction 41
4.5. Cytotoxicity of *P. guajava* leaf decoction 42
4.6. Effect of *P. guajava* decoction in cholesterol permeation and permeation of phenolic compounds 43
4.7. HMGR inhibition 45
4.8. Fourier-transform infrared (FTIR) spectroscopy analysis of HepG2 cellular components 45

4.9. Effect of *P. guajava* decoction in proteins 50
4.9.1. SDS-PAGE of cytosolic and membrane proteins from Caco-2 50
4.9.2. Effect of *P. guajava* decoction on cholesterol transporters 53
V. Conclusions and Perspectives 56
5.1. Conclusions 57
5.2. Perspectives 58
VI. References 60
VII. Annex 68
Annex 1: Identified molecules in *P. guajava* decoction in the bibliography 69
Annex 2: Identification of compounds in *P. guajava* leaf decoction through LC-HRMS-MS analysis 71
Annex 3: *In vitro* gastrointestinal digestion of *P. guajava* leaf decoction 72
Annex 4: SDS-PAGE of membrane and cytosolic proteins from Caco-2 74

List of Tables

Table 4.1: P. guajava leaf decoction – total phenols, using gallic acid (GA) as standard, and flavonoid content, using rutin (R) and catechin (C) as standards. The same letter indicates no statistical difference at 95% confidence level. 31

Table 4.2: Detected molecules in PG1 by LC-HRMS-MS in negative ion mode. 33

Table 4.3: Detected molecules in PG1 by LC-HRMS-MS in positive ion mode. 34

Table 4.4: Quantification of the identified molecules in PG1 and PG2. 37

Table 4.5: HPLC-DAD peak intensity comparison between PG1 and PG2, and heat map of the relative difference (%) normalized to PG1. 38

Table 4.6: Antioxidant activity (DPPH method) of PG1, PG2, and PG3. The same letter indicates no statistical difference at 95% confidence level. 39

Table 4.7: AChE inhibitory activity of PG1, PG2, and PG3. The same letter indicates no statistical difference at 95% confidence level. 40

Table 4.8: Cytotoxicity of PG1 and PG2 in HepG2 and Caco-2 cell lines. The same letter indicates no statistical difference at 95% confidence level between samples in each cell line. 43

Table 4.9: Permeation of cholesterol in Caco-2 cells in the absence and presence of PG1 and PG2. The same superscript letter indicates no statistical difference at 90% confidence level. 44

Table 4.10: Permeation of the molecules found in PG1 and PG2 through Caco-2 cell monolayers..... 44

Table 4.11: Heatmap of the relative difference between PG1 and control, and PG2 and control for the analyzed ratios in FTIR spectroscopy. 48

Table 4.12: Calculated molecular weight and relative difference between bands from membrane proteins of treated (PG1 0.25, 0.50,and 0.75 mg/mL, and PG2 0.25, 0.50, and 0.75 mg/mL for 24 h) and untreated Caco-2 cells. 51

Table 4.13: Calculated molecular weight and relative difference between bands from cytosolic proteins of treated (PG1 0.25, 0.50,and 0.75 mg/mL, and PG2 0.25, 0.50, and 0.75 mg/mL for 24 h) and untreated Caco-2 cells. 52

Table 7.14: Molecules identified in P. guajava leaves from literature. 69

Table 4.15: Relative difference heatmap between peak intensities from PG1 and PG2, in the negative ion mode. 71

Table 4.16: Relative difference heatmap between peak intensities from PG1 and PG2, in the positive ion mode. 72

List of Figures

Figure 1.1: P. guajava tree (a) and leaves (b). Photographed by Maria Constança Lorena in 01/11/2020 in Queluz, Lisboa, Portugal. 3

Figure 1.2: Basic flavonoid structure. Two phenyl rings (A and B) are joined by a heterocyclic pyran ring (C); carbon atoms are numbered according to IUPAC nomenclature[9]. 6

Figure 1.3: The six main families of flavonoids: flavones (A), isoflavones (B), flavonols (C), flavanones (D), flavanols (E), and anthocyanidins (F). The "R"s represent the sites where substituent groups can be added[9]. 7

Figure 1.4: The basic structure of the two main groups of phenolic acids: hydroxybenzoic acids, (A), hydroxycinnamic acids (B). The "R"s represent the sites where substituent groups can be added[9]. 8

Figure 1.5: Chemical structure of tannic acid (A) and proanthocyanidin (B)[28]. 8

Figure 1.6: Basic chemical structure of other PC: lignans (A), chalcones (B), dihydrochalcones (C), stilbenes (D), and furanocoumarins (E)[28]. 9

Figure 4.7: LC-HRMS-MS chromatogram of PG1 (a) and PG2 (b) in the negative mode. 36

Figure 4.8: LC-HRMS-MS chromatogram of PG1 (a) and PG2 (b) in the positive mode 36

Figure 4.9: HPLC-DAD chromatogram from PG1 and PG2 at 1 mg/mL. Gallic acid (5), catechin (9), chlorogenic acid (12), hyperoside (16), and quercitrin (18). 38

Figure 4.10: Structure of ACh (A), donepezil (B), chlorogenic acid (C), quercitrin (D), and hyperoside (E). 41

Figure 4.11: HPLC-DAD chromatogram of pepsin digestion assay (Pep) at t0, t2, and t4. 42

Figure 4.12: HPLC-DAD chromatogram of pancreatin digestion assay (Panc) at t0, t2, and t4 42

Figure 4.13: Structure of simvastatin. 45

Figure 4.14: FTIR spectra between 3000 and 2800 cm^{-1} of HepG2 cells and HepG2 cells exposed to 0.5 mg/mL of PG1 and exposed to 0.5 mg/mL of PG2. 46

Figure 4.15: FTIR spectra between 1800 and 900 cm^{-1} of HepG2 cells and HepG2 cells exposed to 0.5 mg/mL of PG1 and exposed to 0.5 mg/mL of PG2 46

Figure 4.16: Comparison between the ratios CH3/CH2, CH2/COOH, CH2/AmideII, AmideI/AmideII, COOH/AmideII, DNA/AmideII, RNA/AmideII, RNA/DNA, PO2-asym/PO2-sym, glyco/AmideII, and glyco/DNA resulting from FTIR analysis of control cells, cells exposed to 0.5 mg/mL of PG1 and cells exposed to 0.5 mg/mL of PG2. The ratios were normalized according to the intensity of control. Different letters (a-c) correspond to values in the same ratio that can be considered statistically different with 95% confidence level 48

Figure 4.17: Analysis of FTIR spectra of control and treated cells with PCA. Two spectral regions were considered for analysis: 1800-900 and 3000-2800 cm^{-1}. PC loadings are represented on the left and score scatter plots of the corresponding PC1 and PC2 are represented on the right. 49

Figure 4.18: SDS-PAGE of membrane proteins from Caco-2 cells treated with PG1 0.25 mg/mL (lane 2), 0.50 mg/mL (lane 3), and 0.75 mg/mL (lane 4), and treated with PG2 0.25 mg/mL (lane 6), 0.50 mg/mL (lane 7), and 0.75 mg/mL (lane 8) for 24 h. Lane 5 corresponds to untreated cells (control) and lanes 1 and 9 correspond to the protein marker and the molecular weight of each band is presented. . 51

Figure 4.19: SDS-PAGE of cytosolic proteins from Caco-2 cells treated with PG1 0.25 mg/mL (lane 2), 0.50 mg/mL (lane 3), and 0.75 mg/mL (lane 4), and treated with PG2 0.25 mg/mL (lane 6), 0.50 mg/mL (lane 7), and 0.75 mg/mL (lane 8) for 24 h. Lane 5 corresponds to untreated cells (control) and lanes 1 and 9 correspond to the protein marker and the molecular weight of each band is presented. . 52

Figure 4.20: NPC1L1, ABCG5, and ABCG8 bands obtained through Western Blot. HepG2 cells were treated with 1) PG1 0.25 mg/mL, 2) PG1 0.50 mg/mL, 3) PG1 0.75 mg/mL, 4) control, 5) PG2 0.25 mg/mL, 6) PG2 0.50 mg/mL, 7) PG2 0.75 mg/mL for 24h. 53

Figure 4.21: Decrease of NPC1L1, ABCG5, and ABCG8 expression in HepG2 cells treated with 0.25, 0.50, and 0.75 mg/mL of PG1 (A) and PG2 (B) compared to the control (untreated cells)..... 54

Figure 7.22: HPLC-DAD chromatogram of PG1 and water (control) at t0, t2, and t4. 72

Figure 7.23: HPLC-DAD chromatogram of pepsin control (Pep control) at t0, t2, and t4. 73

Figure 7.24: HPLC-DAD chromatogram of pancreatin control (Panc control) at t0, t2, and t4. 73

Figure 7.25: SDS-PAGE of membrane proteins from Caco-2 cells treated with PG1 0.25 mg/mL (lane 2), 0.50 mg/mL (lane 3), and 0.75 mg/mL (lane 4), and treated with PG2 0.25 mg/mL (lane 6), 0.50 mg/mL (lane 7), and 0.75 mg/mL (lane 8) for 24 h. Lanes 1 and 9 correspond to the protein marker and lane 5 corresponds to untreated cells (control). The analyzed bands are marked with horizontal strokes and numbered from 1 to 12. 74

Figure 7.26: SDS-PAGE of cytosolic proteins from Caco-2 cells treated with PG1 0.25 mg/mL (lane 2), 0.50 mg/mL (lane 3), and 0.75 mg/mL (lane 4), and treated with PG2 0.25 mg/mL (lane 6), 0.50 mg/mL (lane 7), and 0.75 mg/mL (lane 8) for 24 h. Lanes 1 and 9 correspond to the protein marker and lane 5 corresponds to untreated cells (control). The analyzed bands are marked with horizontal strokes and numbered from 1 to 19. 74

Abbreviations

PC: phenolic compounds

ROS: reactive oxygen species

RNS: reactive nitrogen species

CM: chylomicrons

VLDL: very-low-density lipoproteins

IDL: intermediate density lipoprotein

LDL: low-density lipoproteins

HDL: high-density lipoproteins

ABCG5/G8: ATP-Binding Cassette G5 and G8

ABC: ATP-Binding Cassette

ABCA1: ATP-Binding Cassette A1

NPC1L1: Niemann-Pick C1-like 1

NPC1: Niemann-Pick C1

SSD: sterol-sensing domain

AP2: adaptor protein 2

ECR: endocytic recycling compartment

ACAT2: acetyl-Coenzyme A acetyltransferase 2

MTP: microsomal triglyceride transfer protein

ER: endoplasmic reticulum

Acetyl CoA: acetyl coenzyme A

HMG-CoA: 3-hydroxy-3-methylglutaryl CoA

HMGR: HMG-CoA reductase

IPP: isopentenyl diphosphate

RCT: reverse cholesterol transport

LCAT: lecithin-cholesterol acyltransferase

CETP: cholesteryl ester transfer protein

CVD: cardiovascular diseases

AChE: acetylcholinesterase

ACh: acetylcholine

AD: Alzheimer's disease

PG1: *P. guajava* aqueous extract

PG2: *P. guajava* ethanolic precipitation supernatant

PG3: *P. guajava* ethanolic precipitation pellet

LC-HRMS-MS: High-Resolution Liquid Chromatography-High-Resolution Tandem Mass Spectrometry

HPLC-DAD: High-performance liquid chromatography with diode array detection

DPPH: 2-diphenyl-1-picrylhydrazyl

ATP: adenosine triphosphate

DMEM: Dulbecco's Modified Eagle Medium

DMSO: dimethyl sulfoxide

DTNB: 5,5'-dithiobis-(2-nitrobenzoic acid)

DTT: dithiothreitol

MTT: 3-(4,5-Dimethylthiazol-2-yl)-2,5-diphenyltetrazolium bromide

PBS: phosphate buffer saline

EDTA: ethylenediamine tetraacetic acid

TFA: trifluoroacetic acid

Tris: tris(hydroxymethyl)aminomethane

NADPH: nicotinamide adenine dinucleotide phosphate hydrogen

HepG2: human hepatoma cell line

Caco-2: human colon carcinoma cell line

BHT: 2,6-ditert-butyl-4-hydroxytoluene

FBS: fetal bovine serum

FTIR: Fourier transform infrared spectroscopy

HBSS: Hank’s balanced salt solution

I(%): inhibition in percentage

IC_{50}: concentration of inhibitor causing 50% inhibition

EC_{50}: effective concentration causing 50% inhibition

General Introduction

Psidium guajava L., commonly known as guava, is a native plant from tropical areas from Central and South America[1] that belongs to the *Myrtaceae* family[2]. It has been used in traditional medicine in Central America, Africa, and Asia, for the prevention and treatment of several diseases and conditions[3]. The most used part of the plant are the leaves, although the whole plant can be used[2]. The leaf decoction was shown to have beneficial effects on health, namely as an antioxidant, hepatoprotective, anti-allergic, anti-microbial, anti-plasmodial, anti-diabetic, and anti-inflammatory[4]. In fact, it was observed that extracts from guava leaf decoction possess strong antioxidant activity[5]. Guava leaves were found to have several bioactive molecules such as phenolic compounds, terpenes, flavonoid derivatives, among others[3,6].

Terpenes are common in nature, being mainly found in fruits, vegetables, and flowers. They have beneficial health effects such as chemopreventive, antimicrobial, antihyperglycemic, and anti-inflammatory activities[7]. Phenolic compounds are the main class of secondary metabolites in plants[8] and they're ubiquitously distributed in most plant tissues[9]. These molecules are responsible for delaying the aging process, decrease the inflammation and oxidative stress that causes degenerative and cardiovascular diseases, and cancer[8,9]. Foods containing these molecules, primarily fruits and beverages, are recommended for the maintenance of a healthy organism[10]. Indeed, it was reported that guava leaves are rich in phenolic compounds[4].

Cardiovascular diseases are among the highest causes of death in the European Union (42%) a trend also registered in Portugal (30%)[11]. One of the main causes is hypercholesterolemia, an imbalance in cholesterol homeostasis. Abnormal cholesterol levels can have serious consequences which may lead to cardiovascular diseases, cancer, metabolic syndrome, and neurodegeneration[12,13]. The first course of action against hypercholesterolemia is a reduction of cholesterol intake and exercise. If this is not enough, patients are prescribed drugs like statins and ezetimibe. Statins inhibit HMG-CoA reductase, the regulatory enzyme of cholesterol biosynthesis, and ezetimibe inhibits cholesterol absorption in the intestine through cholesterol transporters[11]. These drugs, however, may have several adverse effects[14].

It was reported that the consumption of plant infusions rich in phenolic compounds decreased the cholesterol levels in in humans willing to take the drink[14]. *In vitro* studies suggest that this effect is due to the inhibition of HMG-CoA reductase and/or inhibition of cholesterol absorption in the intestine[14]. Another study observed that the consumption of guava leaves aqueous extract by hypercholesterolemic rabbits showed hypolipidemic and hypoglycemic potentials[15]. These observations highlight the pharmacological potential of guava leaves and its possible therapeutic applications.

The aim of this thesis is to evaluate the bioactivity and chemical composition of *P. guajava* leaf decoction responsible for the observed therapeutic effects in traditional medicine. The decoction's influence in the metabolome, proteins, and expression of cholesterol transporters in cells and its effect on cholesterol permeation through the intestinal barrier are assessed.

I. Introduction

1.1. *Psidium guajava*

1.1.1. Botany

Psidium guajava L. (Figure 1.1), commonly known as guava, belongs to the *Plantae* Kingdom, *Magnoliophyta* Division, *Magnoliopsida* Class, *Rosidae* Sub-class, *Myrtales* Order, *Myrtaceae* Family, *Myrtoideae* Sub-family, *Psidium* Genus, and *guajava* species[2]. The Mirtle or *Myrtaceae* family is native from tropical America and is known to contain dicotyledonous plants (flowering plants where the seed has two embryonic cotyledons)[6].

Figure 1.1: *P. guajava* tree (a) and leaves (b). Photographed by Maria Constança Lorena in 01/11/2020 in Queluz, Lisboa, Portugal.

Guava trees are native from Central and South America[1]. It thrives at 2,740 meters above sea level and prefers dry climates. The tree's optimized growth occurs in summer temperatures above 15ºC, though it can't endure intense heat. Additionally, it can't endure intense frost. Climates with distinct winters allow a bigger production of fruit. Although draught resistant, the tree requires an annual rainfall of 1,000 to 20,000 millimeters. The preferred soil is acidic (pH 5-7) with good drainage despite of being able to tolerate different types[2,3]. Notably, this plant is able to grow in tropical and sub-tropical climates, which allows its production around the world[1,16].

P. guajava is a small tree with approximately 10 meters high and has a thin, smooth, patchy, constantly peeling, and reddish-brown bark. The leaves are short with 5 to 15 centimeters long, they are oval with prominent veins, and have a short petiolate. The flowers have whitish petals with up to 2 centimeters long and several stamens. Finally, the fruit is an ovoid berry with approximately 5 centimeters in diameter and has a pink, red, or white fleshy mesocarp with several hard and white seeds[2,6].

1.1.2. Uses of *P. guajava* leaves in traditional medicine

The World Health Organization (WHO) announced that approximately 80% of the population of developing countries still relies on traditional medicine to address their primary health care needs[6].

P. guajava is a versatile plant and has been used for a long time to treat several ailments, by acting as an anti-inflammatory and analgesic, to treat diabetes, hypertension, wounds, and fever[3]. The most used part of the plant are the leaves, although the whole plant can be used[2]. In a randomized, single-blind, clinical trial, it was reported that the addition of guava fruit to the diet along with changes in dietary fatty acids and carbohydrates may decrease lipoprotein metabolism. After 12 weeks, half of the patients had a decrease of 9.9% of serum total cholesterol and 7.7% of triglycerides with an increase of 8% of

HDL[3]. The leaves can be applied orally or topically according to the ailment. The consumption of the decoction is used to treat: cough, gastroenteritis, diarrhea, and dysentery in Colombia and Mexico; diarrhea and stomach ache in Latin America and Mozambique; diabetes mellitus and hypertension in South Africa and Caribbean; diarrhea and diabetes mellitus in China; febrifuge, rheumatism, and convulsions in India; sore throat, laryngitis, and swelling of the mouth in Latin America, in Central and West Africa, and South East Asia. The decoction is also used as an antiseptic in China, as an astringent and antispasmodic in India. The external application of the leaves, as a cataplasm for instance, is used to treat rheumatic pain, wounds, skin ulcers, vaginal irritation and discharge, and toothache in Latin America, in Central and West Africa, and South East Asia. Additionally, the leaves are used as an anti-inflammatory when externally applied hot on inflammations[2,3]. The therapeutic effect of these applications, however, don't have scientific evidence.

1.1.3. Chemical composition *P. guajava* leaves

P. guajava leaves have a lot of components responsible for its therapeutic effects, namely phenolic compounds, flavonoid derivatives, terpenes, and glycosides[3,6]. In fact, it was reported that the leaves are rich in phenolic compounds[4]. The molecules found in literature can be consulted in Annex 1 (Table 7.14). The identified flavonoids were catechin, epicatechin, epigallocatechin, gallocatechin, rutin, epigallocatechin gallate, quercetin, leucocyanidin, reynoutin, and kaempferol. The phenolic acids detected were gallic, protocatechuic, ferulic, syringic, *O*-coumaric, and caffeic acids. Phenolic acid derivatives such as chlorogenic and ellagic acid were found. Resveratrol, a stilbene, was also found. The tannins isostrictinin, strictinin, and guavin (A and B) were identified[3,4,6,16]. Additionally, there can be found glycosides such as guaijaverin (quercetin 3-*O*-L-arabinopyranoside), avicularin (quercetin 3-*O*-L-arabinofuranoside), isoquercitrin (quercetin 3-*O*-β-D-glucoside), hyperoside (quercetin 3-*O*-β-D-galactoside), quercitrin (quercetin 3-*O*-α-L-rhamnoside), quercetin 3-*O*-gentiobioside, and quercetin 4'-glucuronide, astragalin (kaempferol-3-glucoside), cynaroside (luteolin-7-*O*-glucoside), apigenin-7-*O*-glucoside, and morin-3-*O*-α-L-arabinopyranoside[3,6]. Terpenes are another group of molecules found in *P. guajava* leaves. It includes monoterpenes like α-pinene, β-pinene, limonene, eucalyptol, menthol terpenyl acetate; sesquiterpenes such as curcumene, longicyclene, β-bisabolene, farnesene, humulene, selinene, cadinene, azulene, veridiflorene, caryophyllene, τ-cadinol, nerolidol, and caryophyllene oxide; triterpenes like oleanolic, betulinic, ursolic, acetylursolic, eucalyptolic, guavanoic, guavacoumaric, guavenoic, asiatic, guayavolic, guajavanoic, guajanoic, jacoumaric, isoneriucoumaric, psidiumoic, guajadialbetulinic, corosolic, and maslinic acids, goreishic acid I, uvaol, obtusinin, guajavolide, ilelatifol D, psiguanin A-D, and lupeol; meroterpenes, molecules with partial terpenoid structure, such as psiguadial A and B, guajadial, and psidial A-C[3,17–22]. The isolated phytosterols were β-sitosterol, and β-sitosterol-3-O-β-D-glucopyranoside[6]. Other miscellaneous molecules, such as ascorbic acid[3], guavinoside A-C, citric acid, xanthine, glutamic acid, asparagine, malonic acid, *trans*-aconitic acid, maleic acid, cinnamyl alcohol, and methyl cinnamate were also isolated from *P. guajava* leaves[23,24].

1.2. Phenolic compounds

Plants synthetize several organic compounds, namely secondary metabolites which include a group of structurally diverse phytochemicals that accumulate in high concentrations in different plant tissues[25]. Its function in plants includes protection against herbivores and microbial infections, pollinators and seed-dispersing, animals' attraction, allelopathy, UV protection, and signaling molecules for the formation of nitrogen-fixing root nodules in legumes. Some secondary metabolites are used as dyes, fibers, glues, oils, waxes, flavoring agents, drugs and perfumes, and they are viewed as potential sources of new natural drugs, antibiotics, insecticides and herbicides[25].

Phenolic compounds (PC) are the main class of secondary metabolites in plants[8] and the second most abundant group of organic compounds in the plant kingdom[9]. They're ubiquitously distributed in most plant tissues, including edible parts such as fruits, seeds, leaves, stems, and roots[9], and possess strong antioxidant activity, which is an important property of plant extracts that gave yield to extensive studies on the health effects of plants[26].

1.2.1. Role in plants and in human diseases

In plants, PC are responsible for structural support, protection against ultraviolet solar radiation, biotic or abiotic stress, pathogens, and herbivores[9]. They increase the shelf life of food through the antioxidant defense system activation, and also influence the commonly accepted attributes of fruits and vegetables, for instance bitterness, color, and flavor[9].

Oxidative damage can target lipids, proteins, and DNA, impairing its normal function. Many types of reactive oxygen species (ROS) and reactive nitrogen species (RNS) damage these molecules and increase the oxidative stress level of cells. In fact, many chronic degenerative diseases (e.g. cancer, cardiovascular diseases, and diabetes) can be caused by increased exposure to oxidative damage[27].

PC possess strong antioxidant activity resulting from its structural features: hydrogen-donating substituents and the ability to delocalize the resulting free electron, removing its energy to carry on radical reactions[27]. Thus, the consumption of foods rich in PC can prevent chronic degenerative diseases and cancer which are caused by oxidative stress[8,9,27]. In fact, it was observed an inverse correlation between the high consumption of fruits and vegetable and the incidence of chronic diseases in epidemiological studies. This data can be explained by the presence of several antioxidant phytochemicals, which include PC[9].

Another bioactivity of PC worth mentioning is the ability to regulate several cellular processes such as enzyme inhibition, modification of gene expression, and protein phosphorylation[8,9].

1.2.2. Structure and classification

PC have great structural variability, containing at least one aromatic ring with one or more hydroxyl groups attached[9]. According to the number of phenol units in one molecule, PC can be divided in simple phenols or polyphenols. Several classes of PC are described above, namely flavonoids, phenolic acids, tannins, and others.

- **Flavonoids**

Flavonoids are the most bioactive and abundant biomolecules in fruits and vegetables, making up nearly two-thirds of dietary PC. Structurally, flavonoids have a phenyl benzopyran skeleton: two phenyl rings (A and B) joined through a heterocyclic pyran ring (C), as seen in Figure 1.2. Additionally, flavonoids comprise mainly six families of compounds: flavones, isoflavones, flavonols, flavanones, flavanols, and anthocyanidins. In each family, the molecules have a different pattern of hydroxylation and methylation of A, B, and C rings[9].

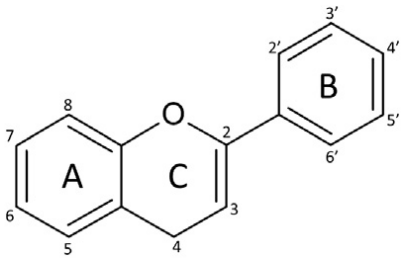

Figure 1.2: Basic flavonoid structure. Two phenyl rings (A and B) are joined by a heterocyclic pyran ring (C); carbon atoms are numbered according to IUPAC nomenclature[9].

Flavones are the most basic structure of flavonoids, containing a keto group in C4, a double bond between C2 and C3, and a B ring is linked to C2 (Figure 1.3A). For instance, they're abundant in herbs and spices, celery, parsley, and thyme. Some fruits and vegetables also contain flavones, such as cantaloupe, watermelon, sweet and hot peppers, Chinese cabbage, and artichokes. The most abundant flavones are apigenin (R_1=H, R_2=OH, R_3=OH, R_4=H, R_5=OH, R_6=H), luteolin (R_1=OH, R_2=OH, R_3=OH, R_4=H, R_5=OH, R_6=H), and their glycosides where a carbohydrate (mono- or disaccharide) is linked to the aglycone through a hydroxyl group[9].

Isoflavones are flavones where the B ring is linked to C3 instead of C2 (Figure 1.3B). This structure shows similarity to estrogens and has mild estrogenic activity. As so, molecules with this structural feature are known as phytoestrogens. Isoflavones are present in small amounts in some legumes, such as beans and peanuts, and are abundant in soybeans and soy products. The most abundant isoflavones are daidzein (R_1=H, R_2=H), genistein (R_1=OH, R_2=H), glycitein (R_1=H, R_2=OCH_3), and their 7-O glycosides (daidzin, genistin, and glycitin, respectively)[9].

Flavonols are flavones hydroxylated in C3 (Figure 1.3C) which increases the stability of the flavonoid radical formed when the molecules act as a radical scavenger. These compounds are the most abundant flavonoids in fruits and vegetables and the most common flavolnols are kaempferol (R_1=H, R_2=H), quercetin (R_1=OH, R_2=H), myricetin (R_1=OH, R_2=OH), and their glycosides. Kaempferol is mainly found in vegetables (leaf greens), herbs (dill and tarragon), beans, and berries. Quercetin can be found in a myriad of fruits and vegetables such as berries, grapes, cherries, apples, artichokes, Chinese cabbage, hot peppers, lettuce, and onion. Myricetin is common in berries and walnuts[9].

Flavanones have a saturated pyrane group, that is no double bond between C2 and C3, in ring C and a keto group in C4 (Figure 1.3D). They are considered minor flavonoids for not being abundant in nature. However, flavanones can be found in citrus fruits and juices and in some herbs, for instance Mexican oregano and peppermint. The most common flavanones are naringenin (R_1=H), eriodictyol (R_1=OH), and hesperetin (R_1=OCH_3)[9].

Flavanols or flavan-3-ols are the most abundant flavonoids in nature, being their polymeric and oligomeric forms the most abundant plant-derived PC. They have a hydroxyl group in C3 and miss the double bond between C2 and C3 and the oxo group in C4 (Figure 1.3E). C2 and C3 are, therefore, the chiral centers since four different groups are attached to each of these carbon atoms. Thus, flavanols can have different configurations. The most common flavanols are catechin (R_1=OH, R_2=H, R_3=H), epicatechin (R_1=H, R_2=OH, R_3=H), gallocatechin (R_1=OH, R_2=H, R_3=OH), epigallocatechin (R_1=H, R_2=OH, R_3=OH), their 3-O-gallates, polymers, and oligomers. Flavanol glycosides are rare. Teas, chocolate, red wine, nuts, and various fruits are rich in these compounds. Epicatechin and catechin can be found in many fruits, for instance grape, strawberry, blackberry, peach, nectarine, apple, and fruit juices[9].

Anthocyanidins also lack a keto group in C4 and have a hydroxyl group in C3 and two double bonds in ring C (Figure 1.3F). Thus, these features make anthocyanidins the only ionic flavonoids that constitute the most important water-soluble plant pigments. Due to its ionic properties, its color changes according to the pH value of the medium: pink at acid pH, purple at neutral pH, greenish-yellow at basic pH, and colorless at very alkaline conditions. Anthocyanidins can appear glycosylated in C3, C7 and C5 in nature, forming anthocyanins. The most common anthocyanidins, that later suffer glycosylation, are pelargonidin (R_1=H, R_2=H), cyanidin (R_1=OH, R_2=H), delphinidin (R_1=OH, R_2=OH), peonidin (R_1=OCH_3, R_2=H), petunidin (R_1=OCH_3, R_2=OH), and malvidin (R_1=OCH_3, R_2=OCH_3). These molecules are common in red wine, berries, grapes, cherries, plum, nectarine, peach, and vegetables like black beans, red lettuce, and red onion[9].

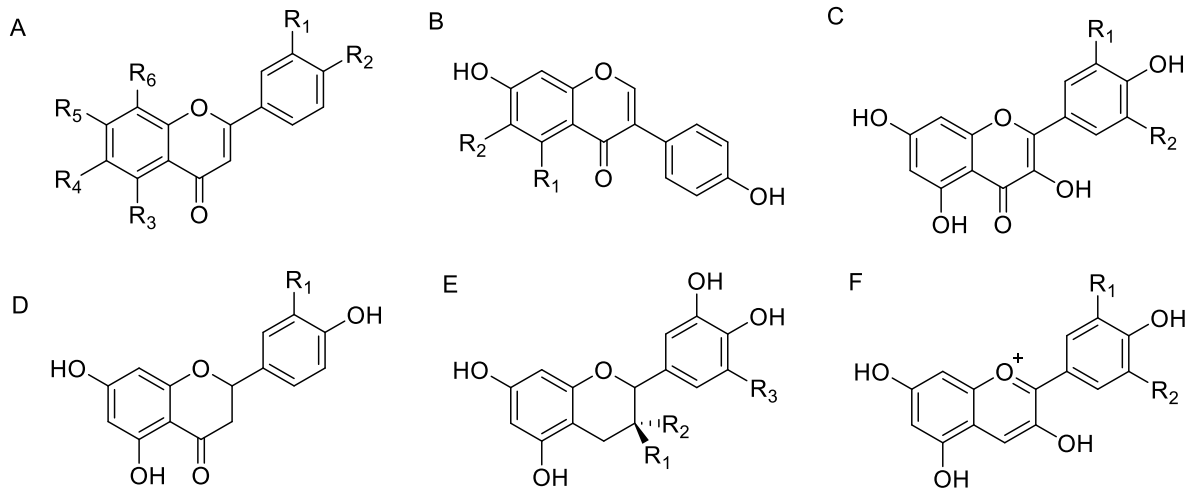

Figure 1.3: The six main families of flavonoids: flavones (A), isoflavones (B), flavonols (C), flavanones (D), flavanols (E), and anthocyanidins (F). The "R"s represent the sites where substituent groups can be added[9].

- **Phenolic acids**

Phenolic acids include molecules with a wide variety of structures where the most part is smaller and simpler than flavonoids. They're composed by a single phenyl group substituted by one carboxylic group and one or more hydroxyl groups. According to the length of the chain that contains the carboxylic group, the phenolic acids group is divided in hydroxybenzoic acids, hydroxycinnamic acids, and other hydroxyphenyl acids. They account for roughly one third of dietary PC[9].

Hydroxybenzoic acids (Figure 1.4A) rarely appear in its free form, instead they appear glycosylated, linked to small organic acids (e.g. quinic, maleic, or tartaric acid), or linked to plant cells structural components (e.g. cellulose, proteins, or lignin). These molecules are found in berries, nuts, tea, chicory, and some spices. Some common hydroxybenzoic acids are protocatechuic acid (R_1=H, R_2=OH, R_3=OH, R_4=H), vanillic acid (R_1=H, R_2=OCH_3, R_3=OH, R_4=H), gallic acid (R_1=H, R_2=OH, R_3=OH, R_4=OH) and syringic acid (R_1=H, R_2=OCH_3, R_3=OH, R_4=OCH_3)[9].

Hydroxycinnamic acids (Figure 1.4B) have a phenylpropanoid basic skeleton and are almost always bound with small or large molecules. Some common hydroxybenzoic acids are *p*-coumaric acid (R_1=H, R_2=H), caffeic acid (R_1=OH, R_2=H), and the methylated forms of ferulic (R_1=OCH_3, R_2=H) and sinapic acid (R_1=OCH_3, R_2=OCH_3). The most common hydroxycinnamic acid derivative in plants is chlorogenic acid, an ester of caffeic and quinic acids, and its isomers. Cranberry, beans, peanuts, maize, and clove are rich in *p*-coumaric acid; caffeic acid is abundant in coffee (mostly as a chlorogenic acid

derivative), berries, herbs, olives, swiss chard leaves, and carrot. Cereals (mainly wheat, maize, and rye), beans, fruits, herbs, and some vegetables are rich in ferulic acid. Sinapic acid can be found in olives, fruits, vegetables, cereal grains, oilseed crops, and some spices[9].

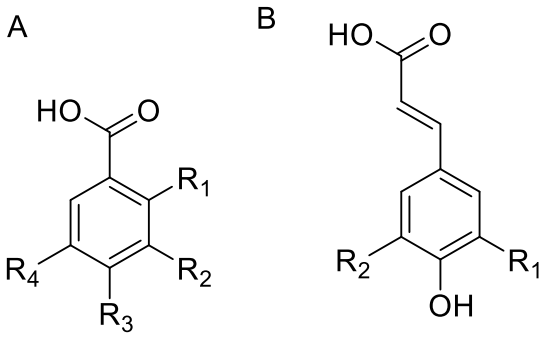

Figure 1.4: The basic structure of the two main groups of phenolic acids: hydroxybenzoic acids, (A), hydroxycinnamic acids (B). The "R"s represent the sites where substituent groups can be added[9].

- **Tannins**

Tannins are molecules whose weight varies between 500 and 3000 Da. They can be classified as hydrolysable tannins and non-hydrolysable or condensed tannins, depending on its chemical structure. The center of hydrolysable tannins consists of a glucose or a polyhydric alcohol partially or completely esterified with gallic acid or hexahydroxydiphenic acid. This results in the formation of gallotannins and ellagitannins, respectivelly. Gallotannins and ellagitannins can go through hydrolysis with acids, bases, and/or enzymes, or condensation with more galoil and hexahydroxydiphenic molecules to form polymers. A common hydrolysable tannin is tannic acid (Figure 1.5A), a gallotannin formed through the esterification of a molecule of pentagalloyl glucose with five units of gallic acid. This molecule can be further esterified with five more gallic acid units. Condensed tannins, as the name suggests, are not easily hydrolyzed and are the main responsible for the astringency of fruits and vegetables. They're polymeric flavonoids mainly composed by catechin and/or leucoanthocyanidin. Condensed tannins can also be called proanthocyanidins[28], and its structure can be seen in Figure 1.5B.

This group of compounds was reported to have antioxidant power, though it's lower than the activity of flavonoids. It was also reported that the antioxidant activity is related to the degree of polymerization, where tannins with higher molecular weight have more activity than simple phenols[28].

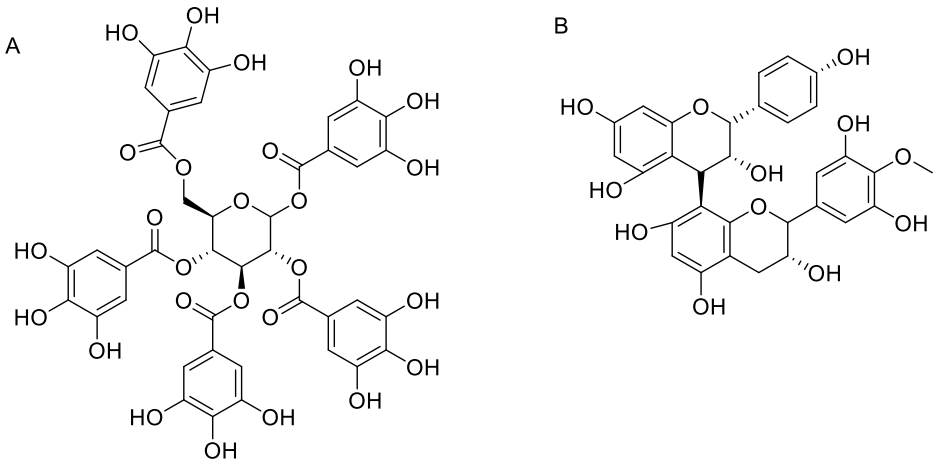

Figure 1.5: Chemical structure of tannic acid (A) and proanthocyanidin (B)[28].

- **Other Phenolic Compounds**

Some nonflavonoids, such as lignans (Figure 1.6A), chalcones (Figure 1.6B) and dihydrochalcones (Figure 1.6C), stilbenes (Figure 1.6D), and furanocoumarins (Figure 1.6E), are not included in the phenolic acids group. They're, nonetheless, characteristic and abundant in certain fruits and vegetables. Lignans are nonflavonoids with two phenylpropanoid units. They're present at low concentration in cereals, fruits, nuts, and vegetables. Some examples of lignans are secoisolariciresinol, matairesinol, lariciresinol, and pinoresinol. Chalcones and dihydrochalcones could be considered as flavonoids, were it not for the absence of the pyran ring. Phloretin and its glycoside phloridzin are the most common dihydrochalcones and are detected in apples and its products. Stilbenes are nonflavonoids mostly found in grapes and wine, although it can also be found in low concentration in berries, peanuts, and pistachio. Resveratrol is known as the most important polyphenol with a stilbene skeleton. Furanocoumarins have a furano benzopyran skeleton and are a class of coumarins. Bergapten and psolaren are furanocoumarins found in celery and parsley[9].

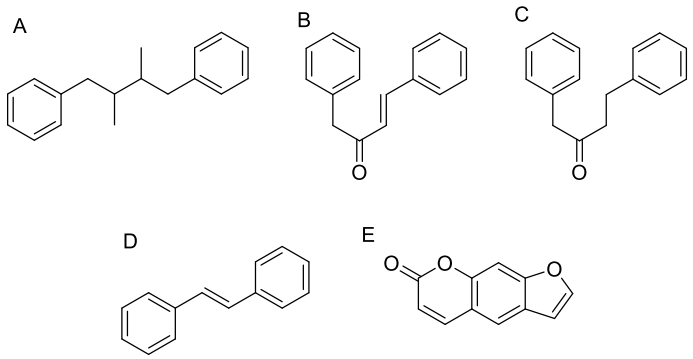

Figure 1.6: Basic chemical structure of other PC: lignans (A), chalcones (B), dihydrochalcones (C), stilbenes (D), and furanocoumarins (E)[28].

1.2.3. Bioavailability of phenolic compounds

As stated above, PC are available in fruits, vegetables, and beverages, such as coffee, tea, wine, and fresh-fruit juices. In fact, Western diet contributes approximately with 1000 mg of flavonoids per day. For instance, the distribution of flavonoids consumed include: 44 mg from cereals; 79 mg from potatoes, bulbs, and roots; 45 mg from peanuts and nuts; and 162 mg from vegetables and herbs. The largest portion, however, is obtained from cocoa, cola, coffee, tea, beer and wine (420 mg per day), and from fruits and juices (290 mg per day)[27].

Phenolic acids account for approximately one-third of the total PC ingested, and the remaining two-thirds are flavonoids[8]. Most flavonoids enter the diet as glycosides[27]. These molecules are modified by food processing through blanching and thermal treatments. When consumed, biomolecules suffer enzymatic reactions along the gastrointestinal tract which influences the intestinal absorption and further metabolism[8]. In the stomach, oligomeric flavonoids are modified by the acid environment[8]. In the small intestine, flavonoid glycosides are hydrolyzed to release the aglycone before absorption[8,27]. The enzymes involved in this process are those with affinity for glucose, xylose, and galactose, lactase phlorizin hydrolase (LPH) and cytosolic glucosidase (CBG) for instance[8]. If flavonoid glycosides are resistant to these enzymatic reactions, they can pass unaltered into the large intestine where they may be cleaved by intestinal bacteria to produce small molecules[8,27]. Additionally, the higher the degree of polymerization results in decrease in bioavailability[27]. Flavonoids metabolism in the small intestine is mainly via conjugation with methyl, glucuronide, or sulfate groups, and via gut microbiome. The

remaining flavonoids that are conjugated with rhamnose are metabolized by α-rhamnosidases synthetized by the colonic microbiome[8].

PC have four possible pathways after absorption: excretion through feces; systemic transport to the liver through portal vein; further conjugation in the liver (with methyl, glucuronide, or sulfate groups) and release in circulation for tissues absorption; excretion through urine[8].

In these processes, PC can lose their bioactivity and convert into secondary compounds. Overall, these factors contribute to the bioavailability of PC, that is the concentration of biomolecules absorbed in the intestine and capable of reaching the circulatory system. Approximately 0.072 to 5 μM of flavonoids (isolated compounds) reach the plasma after intake of 6.4 to 1000 mg/day[8].

1.3. Terpenes in plant extracts

Terpenes are common in nature, being mainly found in fruits, vegetables, and flowers. Since terpenes derive biosynthetically from isoprene units, its basic formula is $(C_5H_8)_n$, where n is the number of isoprene units. The link between units can form a linear chain or can be made to form rings. Oxygen-containing groups, such as hydroxyl, carbonyl, ketone, or aldehyde groups, can be added to the basic hydrocarbon skeleton of terpenes forming molecules called terpenoids. Classification is based in the number of isoprene units: hemiterpenes (one unit), monoterpenes (two units), sesquiterpenes (three units), diterpenes (four units), triterpenes (six units), tetraterpenes (eight units), and polyterpenes (many units)[7].

Terpenes and terpenoids are predominant in plant reproductive structures and foliage during and after flowering, as well as in plant resins. They're typically responsible for the fragrance of many plants, acting as attractants or repellents, and are an important mechanism of protection against herbivores and pathogens as they can be toxic in high concentrations[7].

Dietary terpenes and terpenoids have beneficial health effects that are useful in the prevention and treatment of some diseases, where cancer is an example[7]. Ursolic acid, a pentacyclic triterpenoid, was shown to have antispasmodic and antimicrobial activity, and betulinic acid, another pentacyclic triterpenoid, was reported to have anti-inflammatory, antimalarial, and immunomodulatory properties. Eucalyptol, a monoterpenoid, was found to be antiseptic, mostly for respiratory track conditions. These activities were observed both *in vitro* and *in vivo* models[29].

1.4. Dietary plant peptides

Plant peptides are short chains of amino acids normally with less than 50 residues that mostly derive from a precursor protein hydrolysis with unknown function[30,31]. The precursor protein hydrolysis can be the result of microorganism's activity, gastro-intestinal digestive enzymes, or in vitro procedures where high temperature and extreme pH conditions are employed[32].

Studies *in vitro* and *in vivo* reported that some plant peptides were able to prevent metabolic diseases[33]. In fact, these peptides can act on several systems, namely cardiovascular, digestive, endocrine, nervous, and immune systems. Thus, prevention of hypertension, diabetes, obesity, cancer, and cardiovascular diseases can be achieved[32,33]. Another reported function of peptides present in foods is as an antioxidant, which can prevent DNA damage and lipid peroxidation[33]. However, these therapeutic effects depend on the delivery and bioavailability of plant peptides to the cell. The assessment of health benefits of plant

peptides should include the variety of processes that occur in the consumer's gastrointestinal tract, namely by peptidases and proteases, and the interactions with metabolites and other plant molecules[32].

Highlighting the hypocholesterolemic function of peptides, protein hydrolysates from soy proteins were reported to release peptides with possible hypolipidemic effect in *in vitro*, *ex vivo*, and *in vivo*. This is the result of binding bile acids, micelles disruption, and inhibition of cholesterol absorption in the intestinal tract[33]. The hydrophobic residues, such as leucine, tryptophan, and tyrosine are important for the mentioned functions[32]. In addition, the activity of hepatic and adipocyte enzymes is affected as well as the expression of the enzyme 3-hydroxy-3-methylglutaryl CoA reductase (HMGR). Specifically, the peptides Leu-Pro-Tyr-Pro and Ile-Ala-Val-Pro-Gly-Glu-Val-Ala from soy protein hydrolysates have been reported to inhibit HMGR[33].

1.5. Cholesterol: absorption, metabolism, and role in diseases

Cholesterol is a water-insoluble molecule and it's the most abundant animal sterol, occurring mainly in animal fats, brain, and liver. Besides that, it's also found in animal oils, bile, gallstones, blood, and plasma[34,35]. In addition, cholesterol is the initial molecule of many metabolic pathways due to its steroid backbone, being indispensable as a bile acid precursor; in the synthesis of steroid and sex hormones, such as cortisone and estrogen, respectively, and in the synthesis of vitamin D. It is also important as a cellular membrane component, responsible for cell organization and stability by modulating the fluidity and permeability of membranes[36].

It's a clinically important lipid, along with fatty acids, triglycerides, and phospholipids. The determination of cholesterol levels in the blood is important for the diagnosis and prognosis of cardiovascular diseases, for instance arteriosclerosis, coronary heart disease, stroke, heart attack and peripheral arterial disease, among others[35,36].

Since cholesterol is water-insoluble, it must be transported through blood on water-soluble lipoproteins particles wich are classified by its physical and chemical properties. There are five major types of lipoproteins: chylomicrons (CM), very-low-density lipoproteins (VLDL), intermediate density lipoprotein (IDL), low-density lipoproteins (LDL), and high-density lipoproteins (HDL)[35,37]. They're spherical particles in which the nonpolar lipids (triglycerides and esterified cholesterol) constitute the nucleus while the most polar lipids (free cholesterol and phospholipids) remain on the surface, together with one or more proteins called apoproteins. Apoproteins, are important to maintain the structural integrity of the lipoprotein particle, to activate or inhibit enzymes, and to facilitate lipoprotein recognition by cellular receptors[35,37]. The association between the lipidic core with the polar lipids and apoproteins is secured by hydrogen bonds and van der Waals force, allowing the interconversion of lipoproteins[37]. Lipoproteins are also responsible for the triglyceride transfer from liver to other tissues, where it can be stored or hydrolyzed for energy, and for the reverse cholesterol transport which brings excess cholesterol in extrahepatic tissues back to the liver[35,37].

1.5.1. Cholesterol transporters

- **ATP-Binding Cassette G5/G8 (ABCG5/G8)**

ATP-Binding Cassette G5 and G8 (ABCG5/G8) are members of the superfamily of ATP-Binding Cassette (ABC) transporters, a group of evolutionary highly conserved cellular transmembrane transport proteins that use ATP to allow the transport of metabolites across membranes. They belong to the

structural group of half-transporters that comprises single structural units that form active heterodimers or homodimers[38].

ABCG5 and G8 proteins unite to form a functionally active heterodimer whose function is to protect the body from sterol by restricting the absorption of intestinal cholesterol and to promote biliary excretion of cholesterol[38–40]. These two proteins are highly expressed in the canalicular hepatocyte membrane and small intestine and must be co-expressed to be translocated to the cell membrane[40].

Mutations in ABCG5 or ABCG8 are responsible for causing sitosterolemia. This is a rare disorder in which the plasma levels of plant sterols and cholesterol are increased due to increased absorption and decreased excretion[40].

- **ATP-Binding Cassette A1 (ABCA1)**

ATP-Binding Cassette A1 (ABCA1) a member 1 of the A subfamily of the superfamily of ATP-Binding Cassette (ABC) transporters. Structurally, it belongs to the group of whole-transporters[40]. It mediates the transport of cholesterol, phospholipids, and other lipophilic molecules across the cellular membrane, where they're removed by discoid lipoproteins with apoA-1 and low levels of lipid content[40,41]. This results in the formation of nascent HDL, the initial step in reverse cholesterol transport[42]. Thus, ABCA1 is the involved in cholesterol homeostasis maintenance[40].

ABCA1 is mostly expressed in the liver, adrenal glands, testis, pregnant utero, and placenta[40]. In the liver, ABCA1 is expressed in Kupffer cells, liver's specialized macrophages, and in the basolateral membrane of hepatocytes[40]. Hepatic ABCA1 is also important in the initial lipidation of ApoA-1 and determination and maintenance of plasma HDL concentrations, which is roughly 80% of the plasma HDL pool[43]. Additionally, ABCA1 is highly expressed in macrophages and in atherosclerotic lesions, where it co-localizes with sterol-loaded macrophages[43].

The *ABCA1* gene has a total of 149 kb that comprises 50 exons and encodes an integral membrane protein containing 2,261 amino acids[42]. Mutations in the *ABCA1* gene are responsible for the development of Tangier disease. This is a lipid metabolism disorder characterized by very low plasma HDL and ApoA-1 levels due to impaired cellular efflux of phospholipids and cholesterol. This will lead to an accumulation of cholesterol and cholesteryl esters in macrophage foam cells and many tissues, such as the liver and spleen. Consequently, this impairment will cause peripheral neuropathy, splenomegaly, thrombocytopenia, and increased incidence of cardiovascular disease[40].

- **Niemann-Pick C1-like 1 (NPC1L1)**

Niemann-Pick C1-like 1 (NPC1L1) transporter is a polytopic transmembrane protein composed of 1332 amino acids and is essential in cholesterol absorption in the small intestine. This transporter is mainly found in regions exposed to free cholesterol: the apical membrane of enterocytes and in the canalicular membrane of hepatocytes[44,45]. Here, they facilitate the internalization of unesterified cholesterol into the enterocyte together with adaptor protein 2 (AP2) complex and clathrin[46].

NPC1L1 is a homolog of Niemann-Pick C1 (NPC1) protein, showing 51% similarity and 42% identity. Mutations on NPC1 are responsible for causing Niemann-Pick disease type C1, a genetic disorder that accumulates cholesterol and other lipids in lysosomes[44].

Structurally, this protein has a conserved NPC1 domain in the N-terminal, a typical signal peptide, and an extensive N-linked glycosylation sites which make this protein highly N-glycosylated. Additionally, NPC1L1 is composed by 13 transmembrane domains, 5 of which constitute a sterol-sensing domain (SSD). This domain can be found in other transmembrane proteins responsible for cholesterol metabolism and regulation[44].

Unesterified cholesterol binds to the sterol-binding pocket in the cysteine-rich (18-cysteine) N-terminal domain of NPC1. NPC1L1 N-terminal also contains 18 cysteines. Since these two proteins have high similarity in the N-terminal, one can speculate that the N-terminal of NPC1L1 binds sterols. This matter needs further study, for instance the structure of NPC1L1[44]. The binding between NPC1L1 and cholesterol is yet to be elucidated as well as its mechanism of internalization. One possibility indicates that NPC1L1 N-terminal might be responsible for assisting the movement of extracellular cholesterol to the membrane-localized SSD region. This process may create a raft-like plasma membrane microdomain which promotes the clathrin-mediated endocytic pathway and the internalization of the entire cholesterol-rich microdomain[44].

The regulation of NPC1L1 subcellular localization is a cholesterol-dependent process. When cholesterol is abundant in the cell, NPC1L1 is mainly found in the endocytic recycling compartment. When cholesterol is not abundant in the cell, NPC1L1 will be found in the plasma membrane in order to capture cholesterol for the cell. The SSD region may regulate NPC1L1's intracellular itineraries by sensing membrane cholesterol content[44].

Ezetimibe is a lipid-lowering compound that inhibits cholesterol absorption in the intestine[47]. Briefly, ezetimibe causes: a decrease in the delivery of intestinal cholesterol to the liver; a reduction of hepatic cholesterol stores; and an increase in clearance of cholesterol from the blood[46]. This drug is prescribed as an adjunctive therapy to a healthy diet to lower cholesterol levels in primary hyperlipidemia, mixed hyperlipidemia, homozygous familial hypercholesterolemia, and homozygous sitosterolemia (phytosterolemia)[48]. The mechanism of action of ezetimibe, although not entirely understood, involves primarily the NPC1L1 transporter and selectively inhibits the absorption of cholesterol. The absorption of fat-soluble nutrients such as fat-soluble vitamins, triglycerides, or bile acids is not affected[49].

1.5.2. Cholesterol intestinal absorption

The unesterified free cholesterol found in the lumen of the small intestine comes from the diet, namely meat, egg yolk and sea food[35]. The efficiency of intestinal absorption of cholesterol has a wide range of interindividual variations between 29% and 80% of the total luminal cholesterol[50].

Cholesterol absorption in the small intestine starts with its incorporation in mixed micelles, which contains bile acids, phospholipids, and hydrolytic products of triglycerides. This step allows the solubilization of cholesterol and other hydrophobic nutrients, which is essential for its diffusion through the water layer that lies before the intestinal brush border membrane. Here, unesterified cholesterol is incorporated into the cell membrane of enterocytes, where it binds to the SSD of NPC1L1 and forms a NPC1L1/cholesterol complex. The complex is then internalized or endocytosed by joining with AP2 and clathrin. This forms a vesicle complex that is translocated for storage in the endocytic recycling compartment[44,46].

The unesterified cholesterol that entered the enterocyte via NPC1L1-dependent pathway can be pumped back to the intestinal lumen. This transport is mediated by the ABCG5/ABCG8, an apically localized

heterodimeric sterol efflux transporter. The free cholesterol can also be transported to the basolateral membrane of the enterocyte for the biogenesis of HDL, mediated by the ABCA1 transporter[44].

Inside the enterocyte, most of the free cholesterol is esterified in the endoplasmic reticulum by the acetyl-Coenzyme A acetyltransferase 2 (ACAT2). This enables the incorporation of esterified cholesterol, triglycerides, some unesterified cholesterol, and apolipoprotein B48 into the nascent chylomicron[44]. For this assembly, a microsomal triglyceride transfer protein (MTP) is required. Mature chylomicrons are then released into lymph across the basolateral membrane of enterocytes. Through the lymphatic system, the mature chylomicrons are transported to the bloodstream, where lipoprotein lipase hydrolyses the triglycerides from the chylomicron core for usage and storage by peripheral tissues, for instance fat and muscle. After this enzymatic process remains a chylomicron remnant, which are taken up by the hepatocytes[44].

1.5.3. Cholesterol biosynthesis

The dietary intake of cholesterol is limited. Therefore, cholesterol can be synthetized *de-novo* in multiple tissues in varying amounts, being the liver the major organ involved. The brain is supplied with cholesterol 95% derived from *de novo* synthesis. Cholesterol biosynthesis is an expensive process for the cell as it requires a lot of energy and takes place in the cytoplasm[35,51]. Briefly, units of acetyl coenzyme A (acetyl CoA) are joined to form a 30-carbon molecule. Three carbons are then removed to produce cholesterol, a molecule with 27 carbons[51].

The process starts with the condensation of two molecules of acetyl CoA to form acetoacetyl CoA, which releases CoA in the presence of thiolase. Then, HMG CoA synthase adds a third acetyl CoA to form 3-hydroxy-3-methylglutaryl CoA (HMG CoA). Acetyl-CoA can also be derived from glucose, fatty acids, or amino acids. HMG-CoA is then irreversibly reduced to mevalonic acid by HMG-CoA reductase (HMGR) using two molecules of NADPH and releasing CoA. The HMGR is the regulatory enzyme of the pathway, and is inhibited by statins, a lipid lowering drug. Mevalonic acid is sequentially phosphorylated by two kinases and decarboxylated to form isopentenyl pyrophosphate (IPP), an activated isoprenoid molecule. These three reactions hydrolyze three ATP molecules. Then, IPP (5C) isomerizes to 3,3-dimethylallyl pyrophosphate (5C) by shifting a double bond. The condensation of the IPP isomer with another IPP forms geranyl pyrophosphate (10C). Another isopentenyl diphosphate molecule joins to form farnesyl pyrophosphate (15C). Squalene synthase catalyzes the condensation of two molecules of farnesyl pyrophosphate, yielding squalene (30C). The next reaction, catalyzed by squalene epoxidase, oxidizes squalene to squalene 2,3-epoxide. During the cyclization that will originate lanosterol, a methyl group shifts from C14 to C13 and from C8 to C14. Lanosterol is then converted into cholesterol via a multistep process that requires several enzymes[51].

1.5.4. Reverse cholesterol transport (RCT) and biliary cholesterol secretion

Reverse cholesterol transport (RCT) removes excess cholesterol from peripheral tissues and delivers it to the liver. Here, cholesterol is eliminated through the feces as bile acid, cholesterol, and other catabolism products. Alternatively, cholesterol can be reabsorbed in the intestine and redistributed to other tissues[52,53].

RCT starts with apoA-1 synthesis in apoA-1 -synthetizing organs, such as the liver and intestine, to form discoidal HDL particles, also known as pre-β HDL. These are mainly composed by apoA-1 (around 70%) and phospholipids[53,54]. Pre-β HDL particles are released in the bloodstream and further lipidated

with free cholesterol and phospholipids by interaction with the ABCA1 transporter from peripheral cells, macrophages for instance. The discoidal pre-β HDL will progressively loose its discoid conformation. ApoA-1 is the activating cofactor of lecithin-cholesterol acyltransferase (LCAT), which is responsible for esterification of free cholesterol that makes it impossible for it to re-enter the cells[53]. Finally, a mature and spherical HDL particle is formed (α-HDL)[53]. Additional efflux capacity can be provided by ABCG1 to larger and more mature HDL, but not to lipid-poor pre-β HDL particles[55], and by passive diffusion[52].

There are two ways in which the cholesterol is delivered to the liver: direct and indirect. In the direct pathway, α-HDL interacts with scavenger receptor class B type 1 (SR-B1) in the liver enabling the transfer of its cholesterol content. Afterwards, the remaining α-HDL resumes circulation and repeats the RCT process. In the indirect pathway, α-HDL transfers its cholesterol content to LDL particles in exchange for triglycerides. The reaction is catalyzed by the enzyme cholesteryl ester transfer protein (CETP), which is activated by apoB-100 present in LDL. LDL particles enter the liver through recognition of apoB-100 by its receptors[53]. Additionally, apoE from α-HDL can be recognized by hepatic receptors. In the liver, the esterified cholesterol is hydrolyzed and the free cholesterol is either converted to bile acids or transported by ABCG5/G8 into the bile for excretion[55].

1.5.5. Regulation of cholesterol homeostasis

The maintenance of cellular cholesterol levels is important for cell function and viability[44]. Its levels are tightly transcriptionally and post-transcriptionally regulated by feedback mechanisms[12]. Abnormal levels of cholesterol can have serious consequences for the cells which may lead to cardiovascular diseases, cancer, metabolic syndrome, and neurodegeneration[12,13].

The liver is responsible for the whole-body cholesterol homeostasis that considers: dietary cholesterol; cholesterol biosynthesis, through the rate limiting enzyme HMGR and HMG-CoA synthase; cholesterol secretion and uptake from lipoproteins which is critical for the regulation of the concentration of blood cholesterol; the cholesterol conversion into bile acids, which regulates the efficiency of intestinal absorption of lipids and vitamins; and the RCT, important for cholesterol excretion. All these pathways are protein-mediated processes which are metabolically integrated. This way, it can respond to fluctuations in dietary, systemic, and local cholesterol pools[44].

1.5.6. Hypercholesterolemia

Hypercholesterolemia consist in an abnormally high level of cholesterol in the blood. It can be physiological after meals and pathological when there's a lipoprotein metabolism disorder caused by overproduction, altered clearance, or both[56]. This metabolic alteration is due to high intake of cholesterol, saturated fats, and excessive calories or by genetic factors[36]. Hypercholesterolemia causes atherosclerosis, an accumulation of plaque, in large elastic and muscular arteries, for instance the aorta, coronary, femoral, and carotid arteries as well as in predisposed sites such as bifurcations where there's flow disturbance. It can damage the endothelial lining due to high blood pressure, local injuries, or poor oxygen supply. Therefore, there will be an increased permeability that allows the transport of lipoproteins to the subendothelial space[56]. This is the underlying mechanism for cardiovascular diseases (CVD), the deadliest disease is western countries[36]. CVD include heart attack, premature coronary disease, stroke, and peripheral vascular disease[36,56].

1.5.7. Acetylcholinesterase, Alzheimer's disease, and cholesterol homeostasis

Acetylcholinesterase (AChE; E.C. 3.1.1.7) is an abundant enzyme in the synaptic cleft and it hydrolyzes the neurotransmitter acetylcholine (ACh) in acetate and choline. This is an important process in the activity of the central and peripheral nervous systems[57]. ACh is also responsible for peristaltic contractions and ion transport in gut epithelial cells, and, therefore, water secretion for gut hydration. A proper aqueous environment is essential for enzymatic digestion, nutrient absorption, and for surface lubrification. Surface lubrification and peristaltic movements are necessary to drive intestinal contents. Thus, inhibiting AChE will lead to an increase in ACh and, therefore, an increased gastrointestinal motility[58].

Alzheimer's disease (AD) is a progressive neurodegenerative disorder that responsible for two-thirds of dementia cases[57]. It affects the cerebral cortex and hippocampus, though the first lesions are detected in the frontal and temporal lobes[59]. The structural changes observed in AD include the progressive loss of neurons connections (synapses) and the neurons itself. Thus, the brain appears shrunken in latter stages of the disease. Microscopically, there are two abnormal proteinaceous deposits that characterize AD: accumulation of peptide amyloid-β in plaques, predominant between neurons, and aggregation of the microtubule associated protein tau into neurofibrillary tangles, predominant inside neurons[57,59]. It's also associated with neurotransmitter abnormalities that affect the cholinergic system[59]. Consequently, the first signs of AD include subtle losses of memory and behavior changes. With the disease development, cognitive changes, language disruption, and more pronounced behavior changes appear[57]. Despite the research, the cause and an effective treatment for this impairment is yet to discover[57]. One way to pharmacologically manage the disease is through cognition-enhancing drugs, namely cholinesterase inhibitors. These drugs decrease the extrasynaptic metabolism of the neurotransmitter acetylcholine, increase its lifespan, and enhances the postsynaptic stimulation. Donepezil and Rivastigmine are examples of AChE inhibitors, where the latter one also inhibits butyrylcholinesterase[59].

Epidemiological data have showed that many AD patients suffer from CVD and that high blood cholesterol level is associated with higher risk of developing AD. In a large retrospective cohort study, people with high total cholesterol (> 240 mg/mL) 30 years before the diagnosis of AD, had a 57% higher risk of developing AD than a people with normal total cholesterol level. Based on this observation, it was questioned if there are cholesterol-dependent mechanisms in the pathogenesis of AD. Two examples of reported interactions are presented. Apolipoprotein E (ApoE) is an important cholesterol transporter in the brain and is responsible for the normal catabolism of triglyceride-rich lipoproteins[59,60]. An increased expression of the APOE gene in chromosome 19 is the strongest risk factor for developing AD[59]. Statins, as mentioned, are prescribed to lower the level of blood cholesterol and retrospective clinical studies showed that patients prescribed with statins had a decreased prevalence and incidence of AD[61]. The relationship between the development of AD and cholesterol homeostasis is likely more complex since cholesterol can't cross the blood brain barrier and is synthetized *de novo* in the brain. Nonetheless, this is one of the focus of AD investigation that could provide potential therapeutic targets[60].

II. Objectives

The aim of this thesis is to evaluate the bioactivity and chemical composition of *P. guajava* leaf decoction responsible for the observed therapeutic effects in traditional medicine. Additionally, the decoction's influence in the metabolome, proteins, and expression of cholesterol transporters in cells and its effect on cholesterol permeation through the intestinal barrier are assessed.

Briefly, to approach the main objective, this thesis aimed to:

- Evaluate the bioactivity and chemical composition of *P. guajava* leaf decoction: identification of molecules in the decoction, quantification of known bioactive molecules, and determination of biological activities.
- Understand the influence of *P. guajava* leaf decoction in hepatic cells: cytotoxicity, expression of cholesterol transporters NPC1L1 and ABCG5/ABCG8, and modifications in cell's metabolites.
- Assess the influence of *P. guajava* leaf decoction in intestinal cells: cytotoxicity, cholesterol permeation studies, and modification in total proteins.

III. Materials and Methods

3.1. Reagents

The used reagents were from analytical grade. Ethanol ≥ 99.8%, methanol is from Riedel-de Haën™. Tris(hydroxymethyl)-aminomethane, sodium chloride, sodium nitrite, trifluoroacetic acid, aluminum chloride, sodium carbonate, and milli-Q water (18,2 MΩ·cm resistivity at 25ºC) obtained from a *Milli-Q* Academic water purification system were obtained from Merk. Acetylcholinesterase (149 U/mg solid, 241 U/mg protein), acetylcholine iodine, 5,5-dithio-bis-(2-nitrobenzoic acid), HMG-CoA reductase kit, 2,2-diphenyl-1-picrylhydrazyl (DPPH), hyperoside, gallic acid, quercetin, chlorogenic acid, quercitrin, rutin, cholesterol, bromophenol blue and 2% (w/v), and Folin–Ciocalteu reagent were purchased from Sigma-Aldrich. 3-(4,5-Dimethylthiazol-2-yl)-2,5-diphenyltetrazolium bromide, pre-stained protein molecular weight marker (#26612), Bolt™ MOPS SDS running buffer (B0001), Bolt™ transfer buffer (BT0006), loading buffer (Bolt™ LDS sample buffer; B0007), electrophoresis gels (Bolt™ 4-12% Bis-Tris plus; NW04122BOX), formic acid, water, sodium formate, Mem-PER™ Plus Membrane Protein Extraction Kit (89842Y), and acetonitrile were obtained from Termofisher. Trypsin, Dulbecco's modified Eagle medium (DMEM), glutamine, phosphate-buffered saline, and fetal bovine serum (FBS) were purchased from Lonza. Acetonitrile (ACN) was purchased from Carlo Erba. Sodium hydroxide was purchased from José Manuel Gomes dos Santos, Lda, and catechin from U.S. Pharmacopeia. ABCG8 (NB400-117), ABCG5 (NBP1-95209) and NPC1L1 (NB400-127) antibodies were obtained from Novus Biologicals. Ponceau S stain and TWEEN 20 were purchased from Amresco. The secondary antibody (Amersham™ ECL™ anti-rabbit IgG, horseradish peroxidase-linked species-specific whole antibody from donkey; NA934), nitrocellulose blotting membrane (Amersham™ ECL™ Hybond; RPN2020D), blocking agent (Amersham™ ECL™ blocking agent), and Western Blot detection solution (Amersham™ ECL™ prime Western Blotting detection reagents; RPN2232) were obtained from GE Healthcare. The marker NZYBlue Protein (MB17601) and 5x SDS-PAGE Sample Loading Buffer (MB11701) were purchased from nzytech.

3.2. Decoction and sample preparation

P. guajava leaves were harvested from a home garden in Alhandra, Portugal (38º55'41.8"N 9º00'54.1"W) in July, 2019. Guava leaves (10 g) were boiled in water (300 mL) for 10 min, filtered through Whatman paper no.1, and lyophilized by using a Heto® *PowerDry* LL3000 freeze dryer coupled to Edwards RV3 pump. 1.7 g of extract were obtained. To remove mucilage from the aqueous extract, ethanol (8 mL) was added to 0.5 g of aqueous extract. It stayed for 24h at 4ºC. The mixture was then centrifuged in a Beckman® J2-21M/E centrifuge with a JA-20.1 rotor for 30 min at 4ºC and 3500 g. The pellet was collected and lyophilized. The supernatant was concentrated at 40°C under vacuum in a Büchi® Rotavapor R-200 rotary evaporator Subsequently, the sample was lyophilized. This resulted in 0.3 g of supernatant sample.

The three samples studied were: the aqueous extract called PG1, the supernatant called PG2, and the pellet called PG3. These were all maintained at -20ºC during the work. For every analysis, PG3 was firstly dissolved with 10% methanol and 90% with distilled water and PG2 and PG1 were dissolved with distilled water.

3.3. Quantification of bioactive compounds in *P. guajava* leaf decoction

3.3.1. Quantification of total phenolic content

The quantification of total phenolic content was done with the Folin-Ciocalteu method described by Lee *et al.* (2016)[62], with slight modifications. This method is based on two reactions: the deprotonation of phenolic compounds in alkaline conditions with sodium carbonate (Na_2CO_3), and subsequent redox reaction with the Folin-Ciocalteu reagent (FCR). In the latter reaction, the molybdenum (VI) from the FCR suffers reduction which turns the solution from yellow to blue. Thus, the color of the solution is proportional to the amount of phenolic compounds, which can be spectrophotometrically measured at 760 nm[63].

Briefly, 1350 µL of distilled water, 30 µL of sample (1 mg/mL), and 30 µL of Folin-Ciocalteu reagent were mixed. After agitation and a 3 min incubation at room temperature, 90 µL of sodium carbonate (2%) were added. This mixture was incubated in an orbital agitator for 2h at 4ºC. The absorbance was measured at 760 nm and gallic acid was used as a standard. The total phenolic content was expressed in µg of gallic acid equivalents per mg of extract (GAE/mg extract).

3.3.2. Quantification of flavonoids

The quantification of flavonoids was made using the aluminum chloride colorimetric method described by Tsay *et al.* (2007)[64], with slight modifications. This method is based on the aluminum chloride ability to form acid labile complexes with the orthodihydroxyl groups in the A- or B-ring of flavonoids. Additionally, aluminum chloride forms stable complexes with C-4 keto group and the C-3 or C-5 hydroxyl group of flavones and flavonols[65].

The quantification of flavonoids was made using the aluminum chloride colorimetric method described by Tsay et al. (2007)[64], with some modifications. First, 100 µL of sample, 300 µL of $NaNO_2$ (5%), and 400 mL of distilled water were mixed. After 5 minutes, 30 µL of $AlCl_3$ (10%) were added and, 1 minute later, 200 µL of 1 M NaOH were added. The absorbance was read at 510 nm and rutin was used as a standard. The flavonoid content was expressed as µg of rutin equivalents per mg of extract (µg RE/mg extract).

3.4. Identification and quantification of compounds in *P. guajava* decoction

3.4.1. High-resolution liquid chromatography – high-resolution tandem mass spectrometry (LC-HRMS-MS)

Molecules from guava leaf decoction were identified by High-Resolution Liquid Chromatography-High-Resolution Tandem Mass Spectrometry (LC-HRMS-MS) with the OLE Ultra High-Performance Liquid Chromatography (UHPLC) system. It was interfaced with a Quadrupole Time-of-Flight (QqToF) Impact II mass spectrometer equipped with an Electrospray Ionization (ESI) source (Bruker Daltonics, GmbH, Bremen, Germany). Chromatography separation was carried out on an Intensity Solo 2 C18 (100 x 2.1 mm, 1.8 µm) column (Bruker), at flow rate of 0.25 mL/min. It was injected 5 µL of sample (0.5 mg/mL). The mobile phase is composed of a solution A (0.1% (V/V) of formic acid in water) and B (formic acid in acetonitrile) and was used as follows: 0 min 95% A and 5% B; 1.5 min 25% A and 75% B; 13.5 min 100% B; 21.5 min 95% A and 5% B. The column and the automatic injector were maintained at 35ºC and 10ºC, respectively. The mass spectrometer was operated in the ESI positive and

negative modes, in high resolution mode. The selected parameters were: ion spay voltage of -3.5 kV; end plate offset of 500 V; nebulizer gas (N_2) at 29 psi; dry gas (N_2) -4.0 L/min; dry heater at 200 °C. Internal calibration was performed on the High-Precision Calibration (HPC) mode with sodium formate 10 mM introduced before each acquisition. Acquisition was performed in full scan mode in 50-1500 m/z range with a 3 Hz scanning and in a data-depending mode (auto-MS). Data was processed using Data Analysis 4.4 (Bruker) to extract the mass spectral features from samples raw data.

3.4.2. High-performance liquid chromatography with diode array (HPLC-DAD)

High-performance liquid chromatography with diode array (HPLC-DAD) was carried out in a LaChrom® VWR Hitachi liquid chromatograph VWR Hitachi liquid chromatograph equipped with a LiChroCART® RP-8 (5 µm) column, an automatic injector L-2200, a column oven L-2300, and a Diode array detector L-2455 (VWR, USA). The samples were analyzed by injecting 25 µl (1 mg/ml) and using a gradient composed of solution A (0.05% trifluoroacetic acid), and solution B (methanol) as follows: 0 min 80% A and 20% B; 20 min 20% A and 80% B; 28 min 80% A and 20% B. The flow rate was 1 ml/min and the detection was carried out between 200 and 500 nm. The identified molecules were quantified, both in PG1 and PG2 by relating its peak area with the peak area of the corresponding standard injected with a known concentration.

3.5. Determination of *P. guajava* leaf decoction biological activity

3.5.1. Antioxidant activity

The antioxidant activity was measured using the 2,2-diphenyl-1-picrylhydrazyl (DPPH) method described by Falé *et al.* (2013)[58], with slight modifications. This assay is based on the reduction of the free and stable radical DPPH$^{\bullet}$, naturally purple and absorbs at 516 nm. These properties of DPPH are due to the electron relocation throughout the molecule. When DPPH$^{\bullet}$ is reduced by an antioxidant or a radical, it forms 2,2-difenilpicril-hidrazine (DPPH-H), which is yellow. Thus, the absorbance at 516 nm will decrease according to the intensity of antioxidant activity[63].

To 1 mL of a solution of DPPH (0.002% in methanol), 10 µL of sample were added and the mixture was then incubated for 30 min at room temperature. The reference (100% antioxidant activity) consisted of DPPH solution with water. The absorbance was measured at 517 nm against a blank: methanol with water for the reference and methanol with sample for the sample. The effective concentration providing 50% of antioxidant activity (EC_{50}) was calculated (equation 3.1). Here A_{DPPH} is the absorbance of the DPPH solution against the blank and A_{sample} is the absorbance of the sample against the blank.

$$EC_{50}(\%) = 100 - \frac{A_{sample}}{A_{reference}} * 100 \quad (3.1)$$

3.5.2. Acetylcholinesterase inhibition

In order to study the decoction's influence in the AChE activity, the method described by Falé et al.[58] was used. Firstly, 325 µL of Tris buffer (pH 8.0), 100 µL of sample, and 25 µL of acetylcholinesterase solution (0.26 U/mL) were mixed directly in a cuvette. This mixture was incubated for 15 min at room temperature. 75 µL of a solution of acetylcholine (0.023 mg/mL) and 475 µL of 3 mM Ellman's reagent (DTNB) were added. Immediately, the absorbance of the first 6 minutes of reaction were read at 405

nm. The initial velocity of several concentrations was calculated in order to know the percentage of inhibition. The assays were made using several concentrations to determine the percentage of inhibition with equation 3.2, where I is the percent inhibition of AChE, V_{sample} is the initial velocity of AChE reaction with sample, and $V_{control}$ is the initial velocity of the control reaction.

$$I(\%) = 100 - \frac{V_{sample}}{V_{control}} * 100 \quad (3.2)$$

3.5.3. HMG-CoA reductase inhibition

As stated above, HMG-CoA is the rate limiting enzyme in cholesterol biosynthesis and an important step in cholesterol regulation. This is a nicotinamide adenine dinucleotide phosphate hydrogen (NADPH) dependent enzyme. Thus, the reaction can be spectrophotometrically followed by the decrease of absorbance at 340 nm, which is the NADPH oxidation wavelength.

The enzymatic reaction was made using the method described by the supplier (Sigma, Barcelona, Spain) and the NADPH quantification, through HPLC-DAD, was made using the method described by Mozzicafredo *et al.* (2010)[66], with slight modifications. Briefly, aliquots from 0, 1, 2, 4, and 6 min were collected, and the reaction was stopped by adding 50% methanol. The concentration of NADPH was measured by HPLC-DAD with a LiChroCART® 250-4 LiChrospher® 100 RP-18 (5 µm). For each run it was used a flux of 0.8 mL/min and it was injected 25 µL of each solution. The elution gradient used was composed of solution A (trifluoroacetic acid) and B (acetonitrile) as following: 0 min 95% A and 5% B; 15min 70% A and 30% B; 20 min 20% A and 80% B; 23 min 20% A and 80% B. The detection was made between 200 and 500 nm for 30 min. The assays were made in duplicate and several concentrations of sample were studied. The inhibition corresponds to the percentage of decrease in comparison with the enzyme activity without inhibitor. IC_{50} was calculated with equation 3.2.

3.6. *In vitro* gastrointestinal digestion of *P. guajava* leaf decoction

To evaluate the effect of gastric and pancreatic digestion in the *P. guajava* extract PG1, an *in vitro* gastrointestinal assay was made. Assays were carried out using artificial gastric and pancreatic juices in contact with PG1, as described by Porfirio *et al*. (2010)[67]. A gastric and pancreatic digestion control was made without *P. guajava* extract and another one with water instead of pancreatic and gastric juices.

Firstly, *in vitro* gastric metabolism was performed by adding 4 mg/mL of PG1 to the same volume of gastric juice (3.2 mg/mL of pepsin and 2 mg/mL NaCl at pH 1.2). The mixture was incubated at 37ºC for 4 h in a GFL® 1083 bath. 500 µL were taken at 0 h, 2 h, and 4 h. the reaction was stopped by adding 500 µL of ice-cold methanol. These samples were centrifuged for 5 min at 5000 g and the supernatant was analyzed by HPLC-DAD using the same method described in 3.4.2. The *in vitro* pancreatic metabolism was performed by adding 4 mg/mL of PG1 to the same volume of pancreatic juice (25 mg of pancreatin /mL of potassium phosphate buffer 50 mM at pH 8.0). The mixture was incubated at 37ºC for 4 h. 500 µL were taken at 0 h, 2 h, and 4 h. the reaction was stopped by adding 500 µL of ice-cold methanol. These samples were centrifuged for 5 min at 5000 g and the supernatant was analyzed by HPLC-DAD using the method described in 3.4.2.

3.7. Cell culture

Human hepatoma cell line (HepG2, ATCC®HB-8065) was cultured in Dulbecco's modified Eagle medium (DMEM) supplemented with 10% FBS and 2 mM L-glutamine. Human colon carcinoma cell line (Caco-2, ATCC®HTB-37) was cultured in DMEM supplemented with 20% FBS and 2 mM L-glutamine. Both cell lines were maintained at 37°C in an atmosphere with 5% CO_2 in a *Shel Lab CO_2 Series* from Sheldon Mfg.Inc®. The medium was changed every 72 h before reaching 90% of confluence.

3.8. Cytotoxicity of *P. guajava* leaf decoction

Cytotoxicity was determined using the 3-[4,5-dimethylthiazole-2-yl]-2,5-diphenyltetrazolium bromide (MTT) viability test. Since MTT is positively charged, it can enter viable cells where mitochondrial activity is constant. The activity of dehydrogenases and reducing agents present in metabolically active cells is responsible for the colorimetric reaction in which the MTT, a yellow compound, is reduced to water insoluble formazan crystals, a purple compound[68]. Formazan, however, is lipid soluble and can be dissolved with organic solvents for a homogenous spectrophotometry measurement at 595 nm[68,69]. Thus, the number of viable cells is linearly related to mitochondrial activity and a decrease or increase of viable cells can be detected[69].

Firstly, $2x10^4$ cells/cm^2 were seeded in 96-well plates and incubated for 48 h at 37°C in an atmosphere containing 5% CO_2. After the 48 h, the medium was replaced by different concentrations of *P. guajava* extract (0.05, 0.10, 0.25, 0.50, 1.00, and 2.00 mg/mL) and incubated for 24 h under the same conditions above. The medium was removed, and the cells washed with PBS 1x in order to prepare the cells to be incubated with MTT reagent 1 mg/mL for 2 h at 37°C in an atmosphere containing 5% CO_2. Lastly, the MTT was replaced by DMSO. When the formazan crystals dissolved, the absorbance was read at 595 nm with a reference wavelength of 630 nm in a TECAN®*Sunrise* microplate reader. The control, considered 100% cell viability, consisted of cells incubated with medium only. The percentage of cell death provoked by each concentration of sample was calculated using the IC_{50} equation (equation 1).

3.9. Permeation studies

Permeation studies were performed to evaluate the effect of PG1 and PG2 in cholesterol absorption in a simulated intestinal wall with Caco-2 cells. Caco-2 cells can differentiate spontaneously into polarized monolayers when cells reach confluence on a porous membrane, after approximately three weeks in culture[70].

The permeation was assessed according to Arantes et. al (2016)[71] with minor modifications. Caco-2 cells were seeded at a density of $2\text{-}4x10^4$ cells/cm^2 in 12-well Transwell plate inserts with 10.5 mm of diameter and 0.4 μm of pore size (BD Falcon™). The monolayers were formed till confluence was attained and then differentiated (21–26 days). The medium was replaced every 72 h. Monolayer integrity was evaluated by measuring the transepithelial electrical resistance (TEER) with a Millicell ERS-2 V-Ohm meter from Millipore (Darmstadt, Germany). The membranes were considered fit to permeability studies when the TEER was higher than 250 Ω/cm^2. The cells were then washed with PBS. 0.5 mL of HBSS, 0.5 mL of cholesterol 5 mM dissolved in HBSS, 0.5 mL of PG1/PG2 0.8 mg/mL dissolved in HBSS, and 0.5 mL of PG1/PG2 0.8 mg/mL dissolved in cholesterol 5 mM were applied in the Transwell inserts (apical side of the cells) and 1.5 mL of HBSS was added to the plate well (basolateral side of the

cells). Each sample was made in triplicate. After 6 h of incubation at 37°C in an atmosphere containing 5% CO_2, the apical and basolateral solutions were collected and 25 µL aliquots were analyzed by RP-HPLC-DAD. The quantification of cholesterol was carried out using an isocratic gradient of 50% methanol and 50% acetonitrile for 15 min with a flow of 1 mL/min. The detection was carried out at 210 nm by comparison with a standard. The quantification of molecules from the sample was performed as stated in 3.4.1.

The percentage of permeation (%) was calculated as the amount of material transported divided by the initial amount of material in the apical chamber. The apparent permeability coefficient (P_{app}) was determined using equation 3.3, where dQ/dt represents the rate of compound permeation to the basolateral side, A is the membrane surface area, and C_0 corresponds to the initial concentration of the compound.

$$P_{app} = (dQ/dt)/(AC_0) \quad (3.3)$$

3.10. Fourier-transform infrared spectroscopy (FTIR) analysis of HepG2 cellular components

Fourier-transform infrared (FTIR) spectroscopy is non-destructive and label-free technique that gives insight on the chemical composition of biological samples[72]. Thus, FTIR spectroscopy is a powerful tool for the analysis of cell components such as nucleic acids, proteins, and membranes[73].

FTIR assay was performed as described by André et. al (2019)[74], with minor modifications. A T75 of HepG2 was trypsinised and harvested when it had reached 80-90% confluence. Cells were seeded in calcium fluoride windows at a concentration of 700000 cells in each window and were incubated for 24 h at 37°C in an atmosphere containing 5% CO_2. After 24 h, the medium was replaced by 0.5 mg/mL of PG1 and 0.5 mg/mL of PG2 in FBS free medium. For the control, the medium was replaced with new FBS free medium only. Cells were incubated for 24 h at 37°C in an atmosphere containing 5% CO_2. Then, the cells were washed with PBS 1x and dried under nitrogen flow. FTIR measurements were made using Nicollet™ 6700 FT-IR apparatus from Thermo Electron Corporation® with a DTGS (deuterated triglycine sulfate) detector. The spectra were recorded with 4 cm^{-1} resolution and, for each sample, 128 scans were accumulated in the 4000–900 cm^{-1} spectral range. An empty calcium fluoride window was used as background. Four replicates were used for each condition. FTIR spectra were normalized to Amide II band the ratio values between the intensity of the bands studied were normalized to the control.

3.11. Effect of *P. guajava* decoction in the protein profile of cells

3.11.1. Sodium dodecyl sulfate-polyacrylamide gel electrophoresis (SDS-PAGE) of cytosolic and membrane proteins from Caco-2

To study the HepG2 protein profile, a Sodium dodecyl sulfate-polyacrylamide gel electrophoresis (SDS-PAGE) was made.

After reaching confluence, Caco-2 were incubated for 24 h at 37ºC, in an atmosphere with 5% CO_2, with PG1 or PG2 in a concentration below its IC_{50} (0.25, 0.50, and 0.75 mg/mL). A control was grown in medium only. The cells were then washed three times with cold PBS 1x before adding 1 mL of cold milli-Q water to scrape the cells from the flasks. The obtained cells were lyophilized and maintained at -80ºC. The proteins from Caco-2 cells were extracted using Mem-PER™ Plus Membrane Protein

Extraction Kit. An adaptation of the kit's Protocol 1 (Adherent Mammalian Cells) was made. Briefly, 750 µL of Permeabilization Buffer (plus 1% protease and phosphatase inhibitor and 1% EDTA) was added to 3 mg of dry cells. After using the vortex, a homogenous cell suspension was obtained and incubated for 10 min at 4ºC. The solution was centrifuged for 15 min at 16.000 g and 4ºC to obtain a supernatant rich in cytosolic protein. 500 µL of Solubilization Buffer (plus 1% protease and phosphatase inhibitor and 1% EDTA) were added to the pellet and it was resuspended. Afterwards, the resuspended pellet was incubated at 4ºC and after 30 min it was centrifuged for 15 min at 16.000 g and 4ºC to obtain a supernatant rich in membrane proteins. The samples were stored at -80ºC before use. After protein extraction, the samples were added 5x SDS-PAGE Sample Loading Buffer. SDS-PAGE was done loading per lane an amount of proteins extracted from the same concentration of cells. The electrophoresis went on for 40 min at 200 V. The obtained gel was incubated in Coomassie reagent for 1 h at room temperature. Afterwards, the Coomassie reagent was replaced by destaining solution (10% ethanol and 7.5% acetic acid). Finally, the gels were photographed in ImageQuant™ LAS 500 from GE Healthcare and analyzed in Image Lab™ Version 6.0.0 build 25 (Standard Edition) from Bio-Rad Laboratories, Inc.

3.11.2. Effect of *P. guajava* decoction on cholesterol transporters expression

Western Blot allows the identification and quantification of a specific protein in a complex mixture through indirect detection of protein samples immobilized in a membrane – nitrocellulose or polyvinylidene fluoride (PVDF)[75]. The used method is an adaptation of the one described by Lai et al. (2015)[76].

After reaching confluence, HepG2 were incubated for 24 h at 37ºC, in an atmosphere with 5% CO_2, with PG1 or PG2 in a concentration below its IC_{50} (0.25, 0.50, and 0.75 mg/mL). A control was grown in medium only. The cells were then washed three times with cold PBS 1x before adding 1 mL of cold milli-Q water to scrape the cells from the flasks. The obtained cells were lyophilized and maintained at -80ºC.

Dry HepG2 cells were dissolved in lysis buffer (Igepal 4%, DTT 1%, Urea 6 M). Considering that each cell sample has a different weight, the amount of lysis buffer added aimed to obtain the same concentration of cells. The suspension was sonicated and centrifuged at 10,000 g for 5 min. The supernatant (protein fraction) of each sample was collected. Samples were added loading buffer and SDS-PAGE was done loading per lane an amount of proteins extracted from a same concentration of cells. The electrophoresis went on for 40 min at 200 V. The gel was then transferred to a nitrocellulose blotting membrane and blocked with blocking solution for 1 h. The membranes were incubated with primary antibodies (ABCG8, ABCG5, or NPC1L1) overnight in an orbital agitator at 4ºC. Afterwards, they were washed 4 times with TBS-T (250 mM,1920 mM tris-Glycine, 20% methanol, 70% water, 1% Tween 20; 5 min each wash) and incubated with the secondary antibody conjugated with horseradish peroxidase for 1 h at room temperature with agitation. The membranes were washed 4 times with TBS-T (5 min each wash). Finally, the detection solution was added and after 10 min the blots were visualized in ChemiDoc XRS from Bio-Rad Laboratories, Inc. and analyzed in Image Lab™ Version 6.0.0 build 25 (Standard Edition) from the same company.

3.13. Data analysis

All data were expressed as mean ± standard deviation of three replicates. In cytotoxicity assays, however, it was used 6 replicates. Additional analysis of variance (ANOVA) was performed with α=0.1 for the cholesterol permeation studies and α=0.05 for the other studies. The software Microsoft Excel was used to accomplish this analysis. Additionally, ANOVA analysis was complemented with pair-wise comparisons of sample means via the Tukey HSD test (α=0.1 for the cholesterol permeation studies and α=0.05 for the other studies) in VassarStats website (http://vassarstats.net/ accessed in August 2020).

Principal Components Analysis (PCA) of FTIR spectra was carried out using OriginPro 2020b software. Spectra were truncated to 1800-900 cm^{-1} and 3000-2800 cm^{-1} before PCA. All analyses were conducted with four FTIR spectra for each condition. The analysis was focused on the first two principle components (PC1 and PC2), as they accounted for more than 90% of the variances.

IV. Results and Discussion

4.1. Quantification of bioactive compounds in *P. guajava* leaf decoction: total phenolic and flavonoid content

Three samples were studied: the aqueous extract called PG1, the ethanolic precipitation supernatant called PG2, and the ethanolic precipitation pellet called PG3. In every analysis, PG3 was firstly dissolved with 10% methanol and then 90% distilled water, whereas PG2 and PG1 were dissolved with distilled water.

The three samples, PG1, PG2, and PG3, were analyzed for their total phenolic and flavonoid content and the results can be consulted in Table 4.1.

Table 4.1: *P. guajava* leaf decoction – total phenols, using gallic acid (GA) as standard, and flavonoid content, using rutin (R) and catechin (C) as standards. The same letter indicates no statistical difference at 95% confidence level.

	Total phenolics (GAE/mg extract)	Flavonoids (RE/mg extract)	Flavonoids (CE/mg extract)
PG1	89.58 ± 7.92^{a}	749.42 ± 10.16^{a}	158.72 ± 1.98^{a}
PG2	50.00 ± 0.83^{b}	558.06 ± 12.25^{b}	121.43 ± 2.39^{b}
PG3	50.83 ± 1.67^{b}	503.46 ± 27.38^{b}	110.79 ± 5.34^{b}

The phenolics from the *P. guajava* decoction were quantified by the Folin-Ciocalteau method and expressed as μg of gallic acid equivalents per mg of extract (μg GAE/mg extract). In PG1, it was observed 89.58 ± 7.92 μg GAE/mg of extract, in PG2 50.00 ± 0.83 μg GAE/mg extract, and in PG3 50.83 ± 1.67 μg GAE/mg extract. It is possible to see that PG1 is the sample with more phenolics. Also, PG2 and PG3 aren't significantly different.

PG1, the aqueous extract, was precipitated with ethanol in order to concentrate the phenolic compounds by removing unwanted mucilage, resulting in PG2. Thus, it was expected to quantify higher values of total phenolic content in PG2. This is not observed as the concentration of phenolics from PG2 is 44% lower than in PG1. It seems that several phenolic compounds co-precipitated with the mucilage.

Chen et al. (2006)[5] analyzed the phenolic content of different cultivars of *P. guajava* prepared in similar conditions to PG1. The results ranged from 414 ± 8.2 μg GAE/mg extract to 458 ± 8.1 μg GAE/mg extract. These values are around 80% higher than the PG1 value. This difference can be caused by the leaves maturity, extraction process parameters, the type of cultivar, the environmental conditions such as climate and soil, and harvesting time[77].

The flavonoid quantification was made using the aluminum chloride colorimetric method and expressed as μg of rutin equivalents per mg of extract (μg RE/mg extract). In PG1, it was observed 749.42 ± 10.16 μg RE/mg extract, in PG2 558.06 ± 12.25 μg RE/mg extract, and in PG3 503.46 ± 27.38 μg RE/mg extract. It is possible to see that PG1 is the sample with higher flavonoid content, followed by PG2 and PG3. Additionally, PG2 and PG3 aren't significantly different. Alike the quantification of total phenols, PG2 was expected to contain higher flavonoid concentration in comparison to PG1 due to the precipitation step. Nonetheless, PG2 is 26% lower than PG1. It seems that several flavonoids co-precipitated with the mucilage, alike phenolic compounds.

In order to be able to compare with literature, a catechin calibration curve previously made was used (data not shown). The results are expressed as μg of catechin equivalents per mg of extract (μg CE/mg extract). In PG1, it was observed 158.72 ± 1.98 μg CE/mg extract, in PG2 121.43 ± 2.39 μg CE/mg

extract, and in PG3 110.79 ± 5.34 µg CE/mg extract. These results are like those obtained with the rutin calibration curve.

Pérez-Pérez et al. (2014)[78] analyzed the flavonoid concentration of both young and mature leaves from six individuals chosen from the same population of *P. guajava* plants. They were prepared in similar conditions to PG1 and the results are expressed in µg of catechin equivalents per mg of extract. It was observed that the flavonoid content of young leaves was 28.45 ± 8.09 µg CE/mg extract and for mature leaves was 17.06 ± 4.29 µg CE/mg extract. The justification for the observed difference between literature and experimental results is the same from the phenolic compounds quantification.

In both assays, PG3 was analyzed to assess if the phenolic compounds and flavonoids co-precipitated with the mucilage since they can be glycosylated. PG3 phenolic and flavonoid content ended up being lower than PG1 and alike PG2.

4.2. Identification and quantification of compounds in *P. guajava* leaf decoction

4.2.1. High-resolution liquid chromatography – high-resolution tandem mass spectrometry (LC-HRMS-MS) analysis

High-resolution liquid chromatography – high-resolution tandem mass spectrometry (LC-HRMS-MS) analysis was used to identify the main molecules responsible for the beneficial health effects of guava leaf decoction. Compounds were identified in PG1 and it was carried out by measuring the accurate mass, observation of isotopic patterns on MS spectra, and MS/MS fragmentation pattern. In the negative (Table 4.2) and positive (Table 4.3) ion mode, it was possible to identify several molecules. In these two tables a heat map of peak intensity can be seen where the black corresponds to the highest intensity (289108 A.U. in the negative ion mode and 257790 A.U. in the positive ion mode) and white one to the lowest intensity (12398 A.U. in the negative ion mode and 9076 A.U. in the positive ion mode). The chromatograms can be seen in Figure 4.7a and Figure 4.8b, respectively.

The identified flavonoids were catechin, epigallocatechin, and quercetin, and the identified nonflavonoids were protocatechuic acid, gallic acid, and chlorogenic acid. Both flavonoids and phenolic acids have antioxidants properties which can be related with positive effects on chronic degenerative diseases[8]. In fact, gallic acid and catechin were reported to have three cholesterol-lowering mechanisms *in vitro*: inhibitory activity of pancreatic cholesterol esterase, binding to bile acids, and reduction of cholesterol solubility in micelles[79]. Some flavonoid derivatives were also identified, such as hyperoside, quercitrin, guaijaverin, quercetin 3'-*O*-sulfate, and cyanidin 3-*O*-galactoside. The most abundant MS^2 fragment ion (with 100% intensity) of these molecules corresponds to quercetin (*m/z* 300 and 301). This indicates the loss of the glycoside moiety in hyperoside, quercitrin, and guaijaverin, and sulfate group in quercetin 3'-O-sulfate. The observed low content of total phenols and flavonoids in PG2 can be due to the precipitation of these flavonoid glycosides during the ethanolic precipitation.

Jacoumaric acid, a triterpene, was detected. Triterpenes can be synthetized via mevalonate or 2-C-methyl-D-erythriol 4-phosphate pathway[29]. In fact, 2-C-Methyl-D-erythritol 4-phosphate was identified in the decoction.

It was possible to identify some oligopeptides in the aqueous extract like Thr-Leu-Gly-Tyr, Trp-Thr-His, Asp-Asp-Gly-Gly, Lys-Ala-Pro-Pro, Leu-Gly-Asn-Asn, Pro-Pro-Thr-Phe, Tyr-His-Ala-Ser, Thr-Gln-Ser-Trp, Leu-Cys-Lys-Trp, and Arg-Asn-Val-Arg. Some reported health benefits of plant oligopeptides are blood cholesterol and blood pressure reduction, and antioxidant activity[32]. Hypocholesterolemic peptides include hydrophobic residues in its primary structure like leucine (Leu),

tryptophan (Trp), and tyrosine (Tyr). As so, they're able to establish interactions with lipids and hydrophobic moieties of bile compounds. Antioxidant peptides suppress the damage induced by reactive oxygen species. Thus, it decreases lipid peroxidation of essential fatty acids. Lysine (Lys), histidine (His), methionine (Met), tryptophan (Trp), and tyrosine (Tyr) are residues that can act as radical scavengers[32].

Other identified molecules were: 1-(3,6-Anhydro-5-azido-5-deoxy-alpha-L-idofuranosyl)uracil, a nucleobase derivative; 2-N-(Carboxypropylamino)-2-deoxyglucopyranose, a deoxy sugar; the glycosides (1S,2R,4R,8S)-ρ-Menthane-2,8,9-triol 9-glucoside and (2R,3S,4R,5R)-1-(Octylamino)-5-[(2S,3R,4S,5R,6R)-3,4,5-trihydroxy-6-(hydroxymethyl)oxan-2-yl]oxyhexane-2,3,4,5-tetrol; and 5'-*O*-(Glucopyranosyl)pyridoxine, a vitamin B_6 derivative.

Some miscellaneous organic molecules, including primary metabolites, were found. (2R,4S)-2-[(4R,6R)-4,5-dihydroxy-2,6-dimethyloxan-3-yl]oxy-6-methyloxane-3,4,5-triol, (2R,3R)-2,3-Dihydroxy-4-oxo-4-[(propan-2-yl)oxy]butanoic acid, 3-(Benzoyloxy)-2-hydroxypropyl β-D-glucopyranosiduronic acid (benzoic acid derivative), 5,9-Dihydroxy-7H-furo[3,2-g][1]benzopyran-7-one, Tris(3-hydroxypropil) amine, [2-(3,4-Dihydroxy-5-methoxyphenyl)-6-[2-(4-hydroxy-3-methoxyphenyl)ethyl]oxan-4-yl] acetate, Pyroglutamylserylarginine, L-Alanyl-L-prolyl-O-tert-butyl-L-seryl-N-(6-aminohexanoyl)glycine, and 5,7-Dihydroxy-2-[4-hydroxy-2-methoxy-3-(3-methylbut-2-enyl)phenyl]-6,8-bis(3-methylbut-2-enyl)chromen-4-one were identified.

Table 4.2: Detected molecules in PG1 by LC-HRMS-MS in negative ion mode.

Peak	t_r (min)	Proposed compound	Molecular formula	Accurate $[M-H]^-$ *m/z* (Δ ppm)	MS^2 fragment ions [*m/z* (intensity %)]	Intensity heatmap
1	1.0	(2R,3R)-2,3-Dihydroxy-4-oxo-4-[(propan-2-yl)oxy]butanoic acid	$C_7H_{12}O_6$	191.0565 (-2.0)	126.98 (11); 96.96 (100); 85.02 (32); 75.00 (91)	
1	1.0	2-C-Methyl-D-erythritol 4-phosphate	$C_5H_{13}O_7P^{-2}$	215.0329 (-1.4)	96.96 (100); 79.95 (75)	
2	2.3	Gallic acid	$C_7H_6O_5$	169.0142 (0.0)	125.02 (100); 108.94 (11); 69.05 (10)	
3	4.1	Protocatechuic acid	$C_7H_6O_4$	153.0194 (-0.1)	109.03 (100); 96.96 (31); 80.03 (19)	
4	5.1	Thr-Leu-Gly-Tyr	$C_{21}H_{32}N_4O_7$	451.2190 (1.8)	405.21 (5); 243.16 (5); 233.09 (2); 167.10 (26)	
4	5.1	Trp-Thr-His	$C_{21}H_{26}N_6O_5$	441.1896 (-1.6)	195.06 (100); 180.04 (30); 165.05 (378); 93.03 (21)	
4	5.1	Catechin	$C_{15}H_{14}O_6$	289.0718 (0.0)	203.07 (51); 151.04 (50); 123.04 (40); 109.03 (100)	
5	5.5	Gallocatechin	$C_{15}H_{14}O_7$	305.0698 (-9.2)	225.11 (26); 96.95 (100); 79.97 (16); 59.01 (29)	
6	6.1	3-(Benzoyloxy)-2-hydroxypropyl β-D-glucopyranosiduronic acid	$C_{16}H_{20}O_{10}$	371.0983 (0.2)	249.06 (50); 121.02 (100); 113.02 (16); 89.02 (2); 85.02 (15)	
7	6.3	Quercetin 3-O-sulfate	$C_{15}H_{10}O_{10}S$	380.9924 (0.5)	301.19 (100); 273.03 (3); 171.99 (13); 151.003 (16); 109.02 (5)	
7	6.3	Quercetin	$C_{15}H_{10}O_7$	301.0353 (0.3)	301.00 (100); 178.99 (24); 169.02 (21); 151.00 (85)	

8	6.5	Hyperoside	$C_{21}H_{20}O_{12}$	463.0888 (-1.3)	300.03 (100); 271.03 (30); 151.04 (6); 109.04 (3)	
8	6.5	(2R,4S)-2-[(4R,6R)-4,5-dihydroxy-2,6-dimethyloxan-3-yl]oxy-6-methyloxane-3,4,5-triol	$C_{13}H_{24}O_8$	307.1401 (-0.8)	146.96 (5); 59.01 (7); 44.99 (100)	
9	6.8	Guaijaverin	$C_{20}H_{18}O_{11}$	433.0780 (-0.8)	300.02 (100); 271.02 (16); 243.02 (10);199.03 (3) 148.01 (3)	
10	7.0	Quercitrin	$C_{21}H_{20}O_{11}$	447.0932 (0.2)	300.02 (100); 271.02 (12); 151.00 (2); 148.02 (3)	
10	7.0	Cyanidin-3-galactoside	$C_{21}H_{21}ClO_{11}^{+}$	483.0707 (-1.4)	447.09 (100); 301.03 (55); 271.02 (35); 243.03 (20)	

Table 4.3: Detected molecules in PG1 by LC-HRMS-MS in positive ion mode.

Peak	t_r (min)	Proposed compound	Molecular formula	Accurate $[M-H]^+$ *m/z* (Δ ppm)	MS^2 fragment ions [*m/z* (intensity %)]	Intensity heatmap
1	1.0	5,9-Dihydroxy-7H-furo[3,2-g][1]benzopyran-7-one	$C_{11}H_6O_5$	219.0268 (9.1)	172.94 (71); 125.01 (100); 57.06 (62)	
2	1.1	1-(3,6-Anhydro-5-azido-5-deoxy-alpha-L-idofuranosyl)uracil	$C_{10}H_{11}N_5O_5$	282.0873 (-14.2)	263.06 (9); 212.56 (73); 155.01 (32); 85.02 (92); 73.02 (100)	
2	1.1	Asp-Asp-Gly-Gly	$C_{12}H_{18}N_4O_9$	363.1135 (3.2)	273.08 (100); 263.05 (99); 245.05 (26); 233.08 (15)	
3	1.2	2-N-(Carboxypropylamino)-2-deoxyglucopyranose	$C_{10}H_{19}NO_7$	266.1235 (-0.3)	248.11 (100); 230.10 (21); 194.07 (6)	
4	1.8	Tris(3-hydroxypropil) amine	$C_9H_{21}NO_3$	192.1593 (0.6)	174.14 (100); 156.13 (33); 116.10 (21); 98.09 (80); 59.04 (73)	
4	1.8	5'-O-(Glucopyranosyl)pyridoxine	$C_{14}H_{21}NO_8$	332.1345 (-1.5)	314.12 (47); 170.08 (11); 152.07 (77); 124.07 (25); 108.08 (100)	
5	2.2	Gallic acid	$C_7H_6O_5$	171.0288 (0.0)	135.01 (19); 107.01 (80); 81.03 (100); 51.02 (15)	
6	5.1	Catechin	$C_{15}H_{14}O_6$	291.0863 (0.0)	213.98 (18); 197.01 (31); 167.95 (11); 81.03 (100)	
7	5.2	Chlorogenic acid	$C_{16}H_{18}O_9$	355.1024 (-0.1)	255.07 (15); 235.61 (16); 205.05 (100); 189.05 (15)	
8	6.5	Hyperoside	$C_{21}H_{20}O_{12}$	465.1025 (0.5)	467.23 (8); 465.23 (14); 303.05 (100); 257.06 (2)	
9	6.8	Quercetin	$C_{15}H_{10}O_7$	303.0498 (-2.2)	303.05 (100); 273.04 (5); 153.02 (29); 121.03 (4)	
9	6.8	Guaijaverin	$C_{20}H_{18}O_{11}$	435.0922 (0.0)	303.05 (100); 285.04 (2); 257.05 (2); 73.03 (16)	
10	7.0	Quercitrin	$C_{21}H_{20}O_{11}$	449.1074 (1.0)	303.05 (100); 257.04 (3); 229.05 (2); 153.02 (2)	
11	7.8	(1S,2R,4R,8S)-ρ-Menthane-2,8,9-triol 9-glucoside	$C_{16}H_{30}O_8$	351.2014 (-0.2)	113.05 (100); 69.03 (18); 45.03 (13)	
11	7.8	Pyroglutamylserylarginine	$C_{14}H_{24}N_6O_6$	373.1831 (-0.2)	315.06 (1); 288.15 (1); 201.57 (1); 258.56 (1); 225.10(1); 69.03 (1)	

12	7.9	Lys-Ala-Pro-Pro	$C_{19}H_{33}N_5O_5$	412.2538 (4.0)	395.22 (8); 113.05 (100); 45.03 (1);	
12	7.9	Leu-Gly-Asn-Asn	$C_{16}H_{28}N_6O_7$	417.2091 (0.3)	331.17 (1); 132.04 (1); 58.06 (1)	
12	7.9	[2-(3,4-Dihydroxy-5-methoxyphenyl)-6-[2-(4-hydroxy-3-methoxyphenyl)ethyl]oxan-4-yl] acetate	$C_{23}H_{28}O_8$	433.1833 (5.5)	399.14 (1); 333.01 (1); 127.04 (2); 103.07 (1); 73.02 (2); 57.03 (2)	
13	8.1	(2R,3S,4R,5R)-1-(Octylamino)-5-[(2S,3R,4S,5R,6R)-3,4,5-trihydroxy-6-(hydroxymethyl)oxan-2-yl]oxyhexane-2,3,4,5-tetrol	$C_{20}H_{41}NO_{10}$	456.2801 (0.5)	439.25 (16); 395.23 (1); 333.18 (1); 201.11 (1); 113.05 (100)	
13	8.1	Pro-Pro-Thr-Phe	$C_{23}H_{32}N_4O_6$	461.2354 (-1.2)	440.19 (1); 311.17 (1); 164.59 (1); 133.08 (1); 98.03 (1); 45.03 (1)	
13	8.1	Tyr-His-Ala-Ser	$C_{21}H_{28}N_6O_7$	477.2094 (-0.4)	217060 (1); 160.09 (2); 133.10 (1); 103.03(1); 89.06 (1); 45.03 (2)	
14	8.2	L-Alanyl-L-prolyl-O-tert-butyl-L-seryl-N-(6-aminohexanoyl)glycine	$C_{23}H_{41}N_5O_7$	500.3060 (3.7)	114.06 (6); 113.05 (100); 87.05 (8); 73.02 (1)	
14	8.2	5,7-Dihydroxy-2-[4-hydroxy-2-methoxy-3-(3-methylbut-2-enyl)phenyl]-6,8-bis(3-methylbut-2-enyl)chromen-4-one	$C_{31}H_{36}O_6$	505.2616 (-6.2)	419.22 (3); 285.90 (1); 166.08 (1); 45.03 (1)	
15	8.3	Thr-Gln-Ser-Trp	$C_{29}H_{32}N_6O_8$	521.2354 (-3.4)	502.29 (2); 494.77 (1); 485.25 (2); 171.58 (2)	
15	8.3	Leu-Cys-Lys-Trp	$C_{26}H_{40}N_6O_5S$	549.2877 (-4.1)	463.25 (4); 113.06 (1); 254.14 (1)	
16	8.4	Arg-Asn-Val-Arg	$C_{21}H_{41}N_{11}O_6$	544.3326 (-2.2)	245.13 (6); 130.08 (3); 113.05 (100); 87.06 (12); 45.03 (26)	
17	15.6	Jacoumaric acid	$C_{39}H_{54}O_6$	619.4025 (-5.1)	419.16 (1); 315.18 (1); 300.17 (1); 255.23 (2)	

In addition, the difference between PG1 (Figure 4.7a and Figure 4.8a) and PG2 (Figure 4.7b and Figure 4.8b) peak intensity was assessed. This aims to understand the impact of the ethanolic precipitation in the composition of the decoction. Both negative and positive ion modes were analyzed and a heatmap regarding the relative difference between PG1 and PG2 is presented in Annex 2 Table 4.15 and Table 4.16, respectively. Here black corresponds to the highest value (100% for both ion modes) and white to the lowest one (5% for the positive ion mode and 12% for the negative ion mode). PG3's chromatogram had very low intensity peaks. Thus, it won't be analyzed.

In the negative ion mode, there's a general decrease of peak intensity. Namely, the compounds with *m/*z 215 (metabolite 2-C-Methyl-D-erythritol 4-phosphate), 380 (quercetin 3-*O*-sulphate), and 447 (quercitrin) show the highest intensity decrease of 90%, 92%, and 81%, respectively. Since quercitrin is a quercetin glycoside, it would be expected to see a decrease in its peak intensity due to the ethanolic precipitation. The lowest decrease (12%) was found in *m/z* 169 which corresponds to gallic acid. Protocatechuic acid (*m/*z 153) wasn't found in the PG2 chromatogram.

In the positive ion mode, there's also a general decrease of peak intensity. Specifically, the molecules with *m/z* 332 (5'-*O*-(glucopyranosy)pyridoxine), 355 (chlorogenic acid), and 412 (Lys-Ala-Pro-Pro)) show the highest intensity decrease of 83%, 95%, and 84%, respectively.

The molecules with *m/z* 219 (5,9-Dihydroxy-7H-furo[3,2-g][1]benzopyran-7-one), 282 (1-(3,6-Anhydro-5-azido-5-deoxy-alpha-L-idofuranosyl)uracil), 363 (Asp-Asp-Gly-Gly), 171 (gallic acid), and 619 (jacoumaric acid) weren't found in the chromatogram of PG2.

It was also observed a decrease from PG1 o PG2 in the following molecules: 15% for hyperoside (*m/z* 465), 5% for quercetin (*m/z* 303), 34% for guaijaverin (*m/z* 435), and 32% for quercitrin (*m/z* 449).

These observations suggest that molecules with and without the glycoside moiety suffered co-precipitation. Thus, the lack of total phenols and flavonoids in PG2 can be explained by this phenomenon.

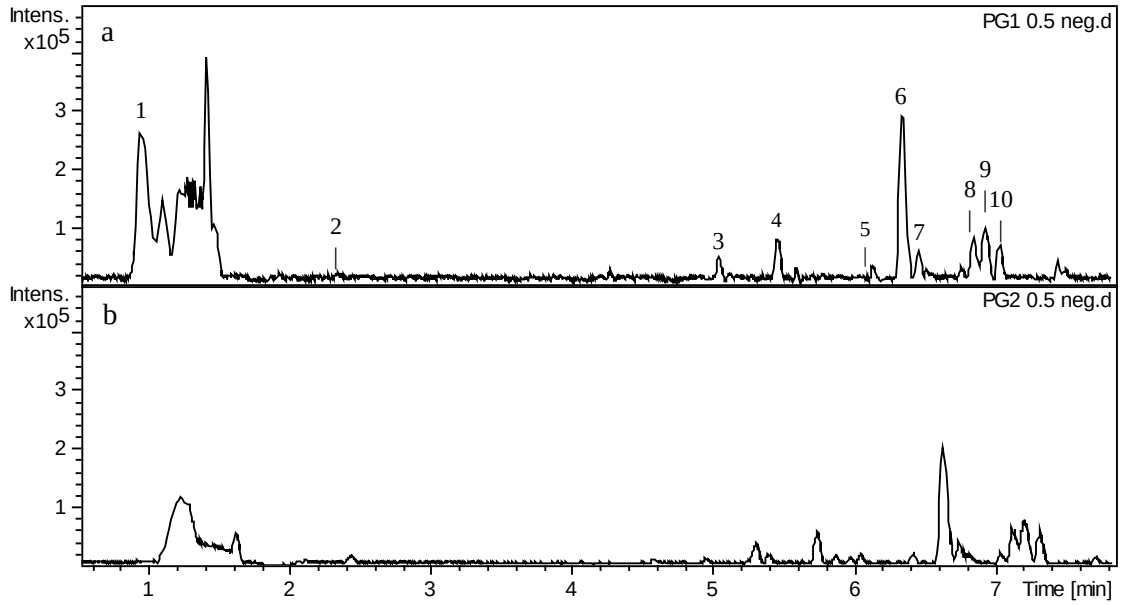

Figure 4.7: LC-HRMS-MS chromatogram of PG1 (a) and PG2 (b) in the negative mode.

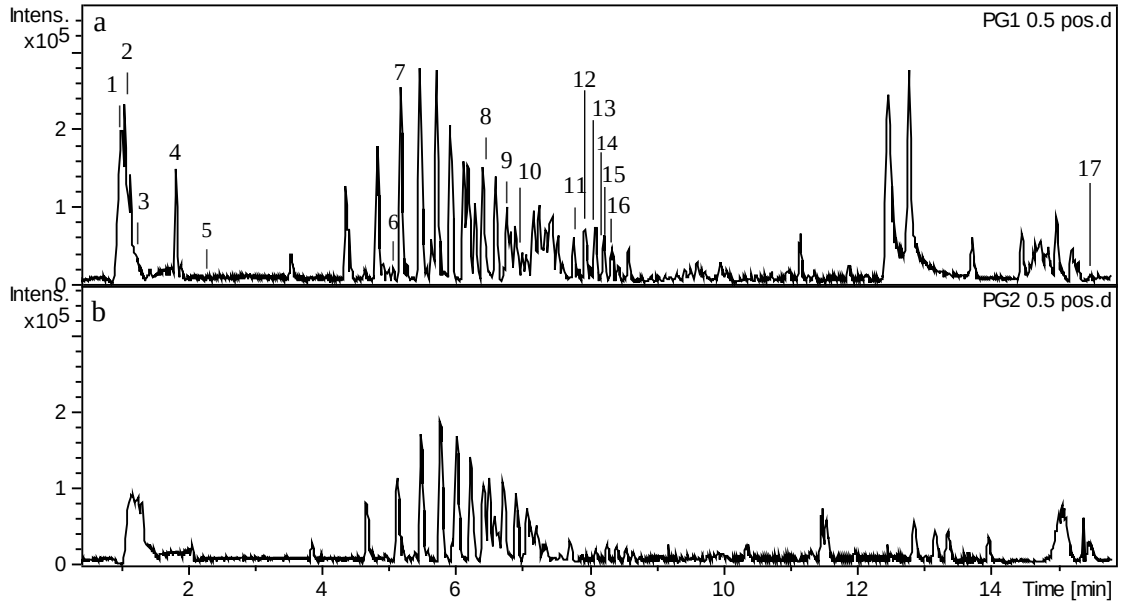

Figure 4.8: LC-HRMS-MS chromatogram of PG1 (a) and PG2 (b) in the positive mode.

4.2.2. High-performance liquid chromatography with diode array (HPLC-DAD) analysis

High-performance liquid chromatography with diode array (HPLC-DAD) was used to quantify the main molecules of PG1 and PG2, found through LC-HRMS-MS. The chromatogram of PG3 is not presented as its peaks had low or no intensity (data not shown). This analysis is based in the retention time of each compound and its UV-Vis absorption spectrum compared to those of standards. The chromatogram can be seen in Figure 4.9, where the last 14 min were rejected since there were no peaks. It's possible to see that PG1 has more intense peaks than PG2. The identified compounds in PG1 and PG2 were: gallic acid at 4.0 min (peak 4), catechin at 6.5 min (peak 9), chlorogenic acid at 8.4 min (peak 12), hyperoside at 13.5 min (peak 17), and quercitrin at 15.0 min (peak 19). The identified molecules were quantified, both in PG1 and PG2 by relating its peak area with the peak area of the corresponding standard injected with a known concentration. The results can be seen in Table 4.4. It's possible to see that the concentration of gallic acid and catechin decreased, which means that these molecules co-precipitated with the mucilage. On the other side, the concentration of chlorogenic acid, hyperoside, and quercitrin seems to have increased in PG2. It would be expected to see the concentration of hyperoside and quercitrin decrease in PG2 since they're flavonoid glycosides, whose glycoside moiety favors its precipitation. Chlorogenic acid too was found with decreased concentration.

Table 4.4: Quantification of the identified molecules in PG1 and PG2.

	Peak number	Concentration (µg/mg of extract)	
		PG1	PG2
Gallic acid	4	1.375	0.669
Catechin	9	1.556	0.798
Chlorogenic acid	12	0.009	0.025
Hyperoside	17	0.298	0.386
Quercitrin	19	4.576	6.277

To further evaluate the precipitation impact, the peaks with the same retention time in PG1 and PG2 were compared and the relative difference of its intensity was calculated. All the peaks were numbered according to its retention time, as seen in Figure 4.9, and its intensity was registered, as seen in Figure 4.9. Additionally, in Table 4.5, a heat map illustrates the difference between the two samples. The highest increase in intensity is colored in black (368%) and the highest decrease in white (82%). In general, there are 11 peaks that decreased in its intensity and 9 that increased. It can be suggested that some molecules suffered co-precipitation while others didn't, which allowed these latter to be more concentrated in the supernatant, PG2.

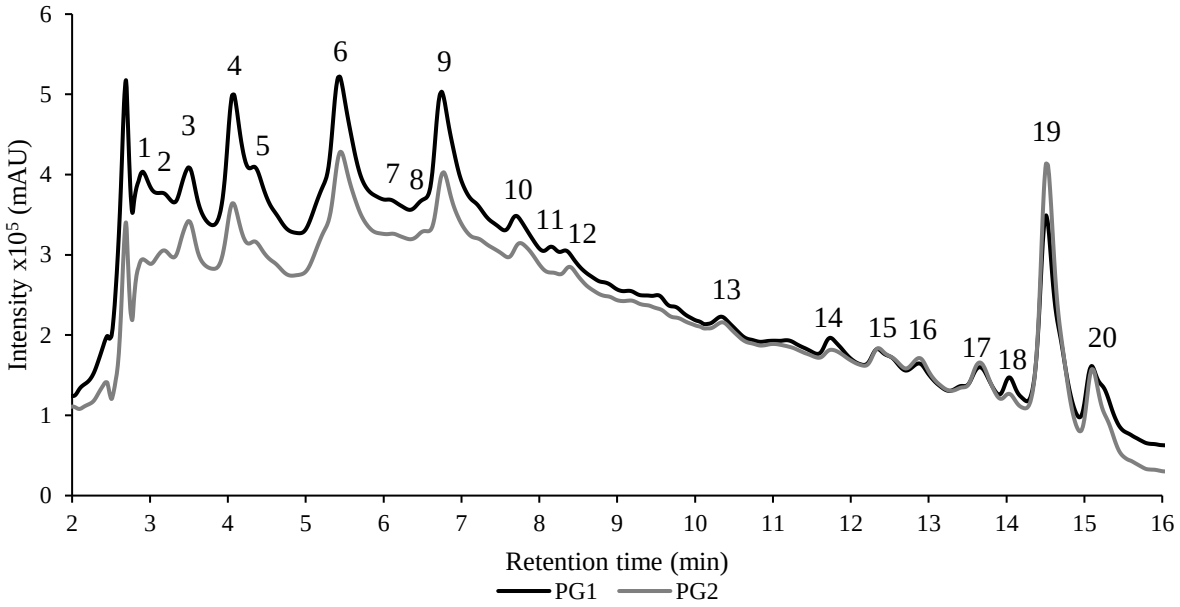

Figure 4.9: HPLC-DAD chromatogram from PG1 and PG2 at 1 mg/mL. Gallic acid (5), catechin (9), chlorogenic acid (12), hyperoside (16), and quercitrin (19).

Table 4.5: HPLC-DAD peak intensity comparison between PG1 and PG2, and heat map of the relative difference (%) normalized to PG1.

#	Retention time (min)	Relative difference between PG1 and PG2 (%)
1	2.907	-82
2	3.200	-25
3	3.493	-10
4	4.053	-50
5	4.320	57
6	5.413	-22
7	6.080	211
8	6.453	13
9	6.720	-46
10	7.733	-2
11	8.133	-68
12	8.373	368
13	10.320	-46
14	11.707	-44
15	12.320	17
16	12.853	127
17	13.680	22
18	14.080	-67
19	14.507	32
20	15.093	27

4.3. Determination of *P. guajava* leaf decoction biological activity

4.3.1. Antioxidant activity

The antioxidant activity was determined using the DPPH scavenging assay and the effective concentration providing 50% of antioxidant activity (EC_{50}) was calculated. Antioxidant activity can be measured by the ability of antioxidants to scavenge free radicals that can damage cell components (proteins, DNA, and lipids) and give rise to diseases[80].

In PG1, it was observed an EC_{50} of 7.45 ± 0.41 µg/mL, in PG2 11.93 ± 0.48 µg/mL, and in PG3 7.26 ± 0.57 µg/mL. These results can be seen in Table 4.6.

Table 4.6: Antioxidant activity (DPPH method) of PG1, PG2, and PG3. The same letter indicates no statistical difference at 95% confidence level.

Sample	DPPH (EC_{50}, µg/mL)
PG1	7.45 ± 0.41^{a}
PG2	11.93 ± 0.48^{b}
PG3	7.26 ± 0.57^{a}

It is possible to see that PG1 and PG3 are the samples with lower EC_{50} and that they're not significantly different. This means that PG1 and PG3 have more antioxidant activity than PG2 (38% and 39% higher, respectively). It was expected to observe a higher antioxidant activity in PG2 due to the precipitation step. As quantified before, PG2 has lower content of some bioactive molecules, as observed in the LC-HRMS-MS analysis and in the quantification of total phenolics and flavonoids Thus, PG2 lower antioxidant activity is justified. The antioxidant activity of the three samples, however, is stronger than the antioxidant standard 2,6-ditert-butyl-4-hydroxytoluene (BHT) that has an EC_{50} of 15.7 ± 0.2 µg/mL[81]. This suggests that PG1, PG2, and PG3 possess strong antioxidant power and, when consumed, can deliver the beneficial effects known to decrease the inflammation and oxidative stress risk associated with several diseases[8,9,27].

PG3 has less phenolic compounds and flavonoids and less intense peaks in LC-HRMS-MS comparing to PG1. Additionally, glycosylated polyphenols were reported to be less effective as antioxidants compared to their free aglycon forms[82]. Thus, it would be normal to see a lower antioxidant activity. This is not observed as PG3 has similar antioxidant activity comparing to PG1. Some of the most antioxidant molecules might have co-precipitated with the mucilage, making the antioxidant activity of PG3 higher.

The observed antioxidant activity can be attributed to phenolic compounds, which have hydrogen-donating substituents and the ability to delocalize the resulting free electron. The resulting radical doesn't have enough energy to carry on radical reactions[27]. Quercetin and gallocatechin were identified in LC-HRMS-MS and their EC_{50} are 2.69 µg/mL and 2.09 µg/mL, respectively[83]. Both molecules have properties that confer this antioxidant activity, namely the presence of both hydroxyl groups 3-OH and 5-OH. Quercetin, however, also has a catechol group in the B ring and the double bond between carbons 2 and 3, together with the 4-keto function, responsible for electron delocalization[27]. Terpenes[29] and small peptides[32] were also reported to possess antioxidant power.

Freire et al. (2014)[84] analyzed the antioxidant activity of *P. guajava* leaves aqueous extract and an EC_{50} of 23.0 ± 0.1 µg/mL was reported. The difference observed between PG1 and this aqueous extract,

around 68%, can be caused by the leaves maturity, extraction process parameters, the type of cultivar, the environmental conditions such as climate and soil, and harvesting time[77].

4.3.2. Acetylcholinesterase inhibition

AChE inhibition was analyzed and the sample concentration that inhibited 50% of AChE activity was determined. For PG1, it was observed an IC_{50} of 48.66 ± 1.39 µg/mL and for PG2 it was observed 63.44 ± 1.13 µg/mL. These results can be seen in Table 4.7. It's possible to see that PG1 has more AChE inhibitory activity than PG2. This difference of around 23% can be explained by the higher total phenol and flavonoid content of PG1. Since PG3 didn't show a correlation between its concentration and the percentage of inhibition, it wasn't possible to calculate the IC_{50}. Considering this observation and the fact that this sample showed low intensity peaks in HPLC-DAD, PG3 won't be used in the subsequent assays.

Table 4.7: AChE inhibitory activity of PG1, PG2, and PG3. The same letter indicates no statistical difference at 95% confidence level.

Sample	AChE (IC_{50}, µg/mL)
PG1	48.66 ± 1.39[a]
PG2	63.44 ± 1.13[b]
PG3	-

The active site of AChE is located at the bottom of a deep and narrow gorge where a catalytic triad of three amino acids hydrolyze ACh (Figure 4.10A) to acetate and choline. This triad includes the residues serine 200 (Ser200), histidine 440 (His440), and glutamine 327 (Glu327). Before arriving to the active site, ACh is trapped through non-covalent π interactions with Trp279 from the peripheral anionic site (PAS). Afterwards, ACh must go through the gorge that is lined with 14 aromatic amino acids and has a large dipole moment oriented along the axis of the gorge. Thus, the positively charged ACh is attracted down to the active site trough cation-π interactions between the quaternary ammonium of ACh and the aromatic amino acid residues. Additionally, the PAS is the binding site of some AChE inhibitors[85].

In fact, small molecules are able to enter the catalytic pocket, though strong binding can´t be achieved[82]. Donepezil (Figure 4.10B) is a selective and potent AChE inhibitor used in the palliative treatment of mild to moderate Alzheimer's disease (AD). It acts by binding to PAS and has an IC_{50} of 2 ng/mL that reflects its shape-complementarity and interactions with AChE[86,87], namely the tertiary amine and aromatic rings that establish π-interactions with PAS[87].

In LC-HRMS-MS analysis was possible to identify some molecules in *P. guajava* decoction decoction that were reported to have AChE inhibitory activity (IC_{50}), namely chlorogenic acid (Figure 4.10C; 196 ± 8 µg/mL), quercitrin (Figure 4.10D; 62 ± 2 µg/mL), and hyperoside (Figure 4.10E; 66 ± 9 µg/mL)[88]. None of these molecules, however, has an IC_{50} as strong as donepezil since they only resemble a fraction of its structure. These three phenolic molecules only establish aromatic-aromatic π interactions with the residues in PAS.

Hyperoside, and quercitrin have similar ability to inhibit AChE and both result from quercetin glycosylation, which makes the molecule larger and consequently increases the difficulty to access the catalytic pocket of AChE[82].

The AChE inhibitory activity of PG2 is similar to that of hyperoside, isoquercitrin, and quercitrin standards and PG1 has more inhibitory potential that the presented standards. Both samples, however, have lower inhibitory activity than donepezil, that was idealized to fit inside AChE's active site.

There are no reports of AChE inhibitory activity for *P. guajava*. Because of this, a set of other medicinal plants was compiled. Falé *et al.* (2013)[58] observed an IC_{50} of 2505 ± 253 µg/mL for *Cynara cardunculos*, 1066 ± 19 µg/mL for *Fraxinus angustifolia*, and 1090 ± 4 µg/mL for *Pterospartum tridentatum*. PG1 has the highest AChE inhibitory activity.

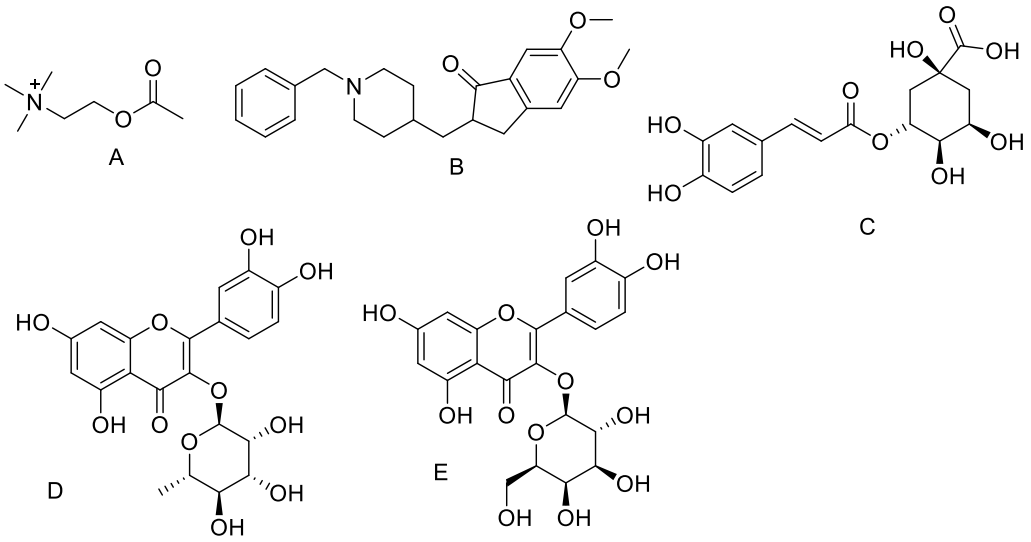

Figure 4.10: Structure of ACh (A), donepezil (B), chlorogenic acid (C), quercitrin (D), and hyperoside (E).

4.4. *In vitro* gastrointestinal digestion of *P. guajava* leaf decoction

To evaluate the effect of gastric and pancreatic digestion in the *P. guajava* decoction, an *in vitro* gastrointestinal assay was made since the different pH values in the gastrointestinal tract can affect the bioactive molecules, inactivating them or the other way around. Only PG1 was analyzed since it's the most bioactive sample, as seen in section 4.3.

The analyzed samples were the control (Control) which only has the extract PG1 and water; the pepsin control (Pep control) that has pepsin and water; the pancreatin control (Panc control) which has pancreatin and water; the digestion assay with pepsin and PG1 (Pep); and the digestion assay with pancreatin with pancreatin and PG1 (Panc). An aliquot of every mentioned sample was collected at 0 min (t0), 2 h (t2), and 4 h (t4). The samples Pep control and Panc control allow the identification of the enzyme peak in the chromatogram.

The heating process and its duration didn't affect the extract composition as the chromatograms are overlapped, as seen in Annex 3 (Figure 7.22). Thus, the modifications detected in the decoction composition under the digestion assay won't be due to the heating process. Since Control t0 didn't undergo the heating process, it corresponds to the chromatogram of PG1 alone alike Figure 4.9 in section 4.2.2.

Alike the Control sample, the heating process and its duration didn't affect Pep control and Panc control chromatogram, as seen in Annex 3 (Figure 7.23 and Figure 7.24, respectively). The chosen temperature for the assay was 37ºC, which is around the normal body temperature for humans[89]. Thus, it's not expected to see modifications in pepsin and pancreatin chromatograms.

In the simulated gastric digestion assay chromatogram, shown in Figure 4.11, it's possible to see that there were no alterations in the extract's chromatogram profile with the increasing incubation time. The molecules present in PG1, mainly flavonoids, were stable under gastric conditions, which agrees with data previously reported[90]. Additionally, pepsin catalyzes the acid hydrolysis of peptide bonds[89], so PC are usually stable under gastric digestion. Although come small peptides were identified in LC-HRMS-MS, its observation in HPLC-DAD can be limited. These results indicate that there's no degradation of *P. guajava* extract induced by the simulated gastric juice nor formation of new molecules.

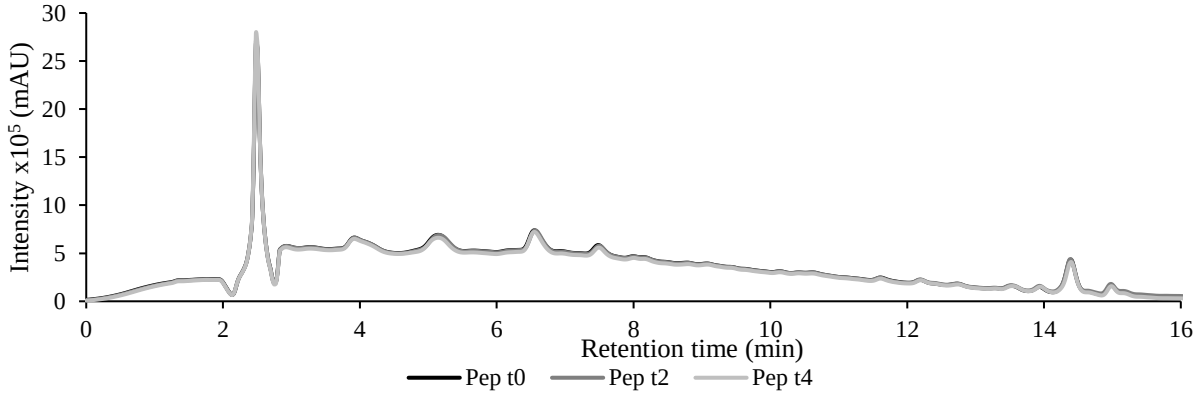

Figure 4.11: HPLC-DAD chromatogram of pepsin digestion assay (Pep) at t0, t2, and t4.

The simulated pancreatic digestion assay chromatogram is shown in Figure 4.12. In general, there are no changes in the chromatogram profile of PG1. The peak at, approximately, 9 min belongs to pancreatin and it's similar to the one in Panc control (Figure 7.24). It's possible to identify a decrease of intensity of some peaks. This can be due to adsorption of molecules to pancreatic juice proteins, which are then removed from solution prior HPLC-DAD analysis[74]. These results indicate that there's no degradation of PG1 induced by the simulated pancreatic juice nor the formation of new molecules. Flavonoids from PG1 were stable under pancreatic conditions, which also agrees with previously reported data[90].

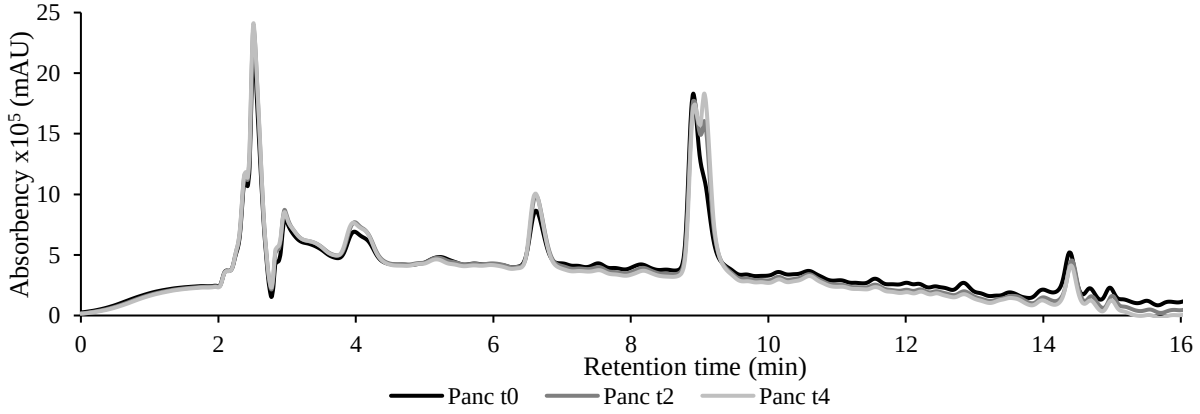

Figure 4.12: HPLC-DAD chromatogram of pancreatin digestion assay (Panc) at t0, t2, and t4.

4.5. Cytotoxicity of *P. guajava* leaf decoction

Cytotoxicity of PG1 and PG2 was determined in Caco-2 and HepG2 cell lines using the MTT method. This assay was made to use a sample concentration bellow the one that kills 50% of cells (IC_{50}) in the subsequent assays. Note that Caco-2 cell line was used as a model of the intestinal wall to evaluate the

cholesterol permeation and HepG2 cell line was used to simulate the liver cells, where cholesterol is mainly synthesized *in vivo*.

PG1 had an IC_{50} of 1.13 ± 0.12 mg/mL in HepG2 and 1.18 ± 0.09 mg/mL in Caco-2. PG2 had an IC_{50} of 0.76 ± 0.15 mg/mL in HepG2 and 0.90 ± 0.08 mg/mL in Caco-2. These results are summarized in Table 4.8. It's possible to see that PG2 has a lower IC_{50} comparing to PG1. Thus, PG2 is more cytotoxic than PG1.

The results showed that these samples do not have any cytotoxic effect on HepG2 and Caco-2 cells since the IC_{50} values were higher than the established one for this type of test, which is 0.1 mg/mL[91]. Note that some chemotherapy drugs, such as doxorubicin and cisplatin, have low IC_{50} values for Caco-2 and HepG2. Specifically, doxorubicin has an IC_{50} value of 18.58 ± 3.10 µg/mL and 2.54 ± 0.59 µg/mL for Caco-2 and HepG2, respectively, whereas cisplatin has an IC_{50} value of 29.02 ± 9.64 µg/mL and 4.48 ± 0.37 µg/mL for Caco-2 and HepG2, respectively[92].

Table 4.8: Cytotoxicity of PG1 and PG2 in HepG2 and Caco-2 cell lines. The same letter indicates no statistical difference at 95% confidence level between samples in each cell line.

Sample	Cytotoxicity (IC_{50} mg/mL)	
	HepG2	Caco-2
PG1	1.13 ± 0.12[a]	1.18 ± 0.09[a]
PG2	0.76 ± 0.15[a]	0.90 ± 0.08[b]

4.6. Effect of *P. guajava* decoction in cholesterol permeation and permeation of phenolic compounds

The hypocholesterolemic effect of guava leaf decoction observed in traditional medicine can be due to a decrease in cholesterol permeation through the intestinal barrier. As so, the influence of PG1 and PG2 in cholesterol permeation through the simulated intestinal barrier was assessed using Caco-2 monolayers. Note that both PG1 and PG2 in the concentration 0.8 mg/mL were not toxic towards Caco-2 cells (see section 4.5) and there were no changes in the chemical composition of PG1 after *in vitro* digestion (see section 4.4). These observations allow the study of cholesterol permeation through Caco-2 cell monolayers. The cholesterol and the mixture of cholesterol plus PG1 or PG2 were applied in the apical compartment and cholesterol quantification was made in the basolateral compartment after 6 h.

It's possible to see, in Table 4.9, that PG1 induced a decreased of 55.1% of cholesterol permeation when compared with the blank test, which was done without plant samples. On the other hand, PG2 caused a decrease of 24.4% of cholesterol permeation. These results can be due to the chemical composition of PG1 and PG2. Specifically, the molecules found in PG1 and PG2 can be responsible for interfering with the cholesterol transporters in the cell membrane or with the membranes itself. Either way, a limitation of cholesterol transport or diffusion occurs.

These observations agree with previous results obtained with other leaf decoctions such as *Annona cherimola*[11], *Peumus boldos*, and *Pterospartum tridentatum*[14]. In fact, membrane transporter proteins were reported to suffer interferences in the presence of phenolic compounds[11,93]. Specifically, quercetin was reported to inhibit intestinal cholesterol absorption mediated by NPC1L1[94]. In addition, a polyphenol-rich grape seed and red wine extracts were shown to inhibit cholesterol uptake[95].

Falé et. al (2013)[11] evaluated the effect of the drug ezetimibe (100 µM) in cholesterol permeation and the percentage of cholesterol found in the basolateral compartment was 5.2 ± 3.1 %, which corresponds

to a decrease of 76% of cholesterol permeation. Although PG1 can't inhibit cholesterol permeation so strongly as ezetimibe, its effect is still satisfying.

Table 4.9: Permeation of cholesterol in Caco-2 cells in the absence and presence of PG1 and PG2. The same superscript letter indicates no statistical difference at 90% confidence level.

Sample	Permeation (%)	P_{app} ($x10^{-6}$ cm/s)	Reduction of cholesterol permeability (%)
Cholesterol	33.6 ± 0.7^{a}	70.2 ± 3.9^{a}	-
Cholesterol + PG1	15.1 ± 3.5^{b}	52.3 ± 6.1^{b}	55.1
Cholesterol + PG2	28.9 ± 0.5^{c}	51.4 ± 3.9^{b}	24.4

The hypocholesterolemic effect of guava leaf decoction can also be the result of an interference in cholesterol biosynthesis, namely the inhibition of HMGR. For this to happen, however, the phenolic compounds from the decoction must permeate the intestinal barrier. To evaluate if the molecules found in HPLC-DAD analysis (section 4.2.2.) permeate the intestinal barrier, Caco-2 cell monolayers were also used. The permeation (%) and the coefficient of apparent permeability (P_{app}) were calculated for gallic acid, catechin, chlorogenic acid, hyperoside, and quercitrin.

In Table 4.10 is possible to see that all phenolic compounds from PG1 permeated the simulated intestinal barrier, ranging from 0.21% to 9.95%. Only chlorogenic acid, hyperoside, and quercitrin from PG2 permeated the intestinal barrier. Thus, these molecules can be absorbed and transported through the blood flow to access other therapeutic targets.

In addition, chlorogenic acid, hyperoside, and quercitrin quantified in section 4.2.2. showed an increased concentration in PG2, while gallic acid and catechin showed a decreased concentration. Nonetheless, the permeation of compounds is similar between PG1 and PG2.

Table 4.10: Permeation of the molecules found in PG1 and PG2 through Caco-2 cell monolayers.

	PG1		PG2	
Compound	Permeation (%)	P_{app} $x10^{-6}$ (cm/s)	Permeation (%)	P_{app} $x10^{-6}$ (cm/s)
Gallic acid	9.95 ± 7.90	18.49 ± 12.84	0.00 ± 0.00	0.00 ± 0.00
Catechin	2.37 ± 0.23	4.97 ± 1.92	0.00 ± 0.00	0.00 ± 0.00
Chlorogenic acid	0.21 ± 0.19	0.85 ± 0.70	0.07 ± 0.05	0.10 ± 0.08
Hyperoside	1.15 ± 1.21	4.00 ± 10.36	1.73 ± 1.03	0.62 ± 0.09
Quercitrin	2.84 ± 0.48	4.47 ± 0.95	2.53 ± 1.99	0.68 ± 0.48

Ozeki et. al (2015) determined that, for a molecule to have high permeability, its P_{app} should be higher than $10x10^{-6}$ cm/s[96]. By analyzing the P_{app} values (Table 4.10), gallic acid seems to be the compound with the best permeability. The other molecules are all bellow the stipulated value. Note that in Table 4.9, cholesterol has a P_{app} value above $10x10^{-6}$ cm/s, which suggests that cholesterol has high permeability. Both samples seem to decrease the cholesterol P_{app} which agrees with the decreased cholesterol permeation when cells are incubated with PG1 and PG2. In addition, the same authors proposed that the P_{app} should be lower than $2.8x10^{-7}$ cm/s to allow passive diffusion of molecules through the membrane[96]. Since almost all molecules are above this value, its permeation through the intestinal barrier is facilitated by membrane transported, namely ABC transporters. This type of transporters were reported to play a role in the active transport of molecules like glycoside derivatives[97]. Chlorogenic acid from PG2, however, seems to be able to cross the membrane through passive diffusion.

Falé et. al (2014)[14] reported the permeation and P_{app} of chlorogenic acid from two different plant extracts through the simulated intestinal barrier: 18.18 ± 0.12 % and 46.76 ± 0.31 $x10^{-7}$ cm/s for *Cynara cardunculus;* 4.12 ± 0.67 % and 10.60 ± 1.72 $x10^{-7}$ cm/s for *Fraxinus angustifolia*. By observing these reported data and the results from the quantification of chlorogenic acid in HPLC-DAD (0.009 µg/mL), it's expected to see such a lower value of bioavailability of chlorogenic acid in the basolateral compartment.

4.7. HMGR inhibition

Since the compounds from the samples can permeate the simulated intestinal barrier (section 4.6.), the HMGR inhibitory activity of PG1 was evaluated. The sample concentration that inhibited 50% of enzymatic activity was determined. PG1 was the only analyzed sample since it's the one with more bioactivity and content of phenols and flavonoids. It was observed an IC_{50} of 8.40 ± 0.51 µg/mL. Since simvastatin has an IC_{50} of 198 ± 15 ng/mL[14], one can suggest that the aqueous extract can act as a cholesterol reducing agent, probably by a statin-like mechanism, though with less efficiency.

One of the molecules found in LC-HRMS-MS analysis of PG1 was chlorogenic acid and it was reported to have an IC_{50} of 4.57 ± 0.18 µg/mL[14]. Although structurally different from simvastatin, chlorogenic acid (Figure 4.10C) can establish few hydrogen bonds or electrostatic interactions with the hydrophobic pocket of HMGR. In fact, this molecule is regarded as an HMGR inhibitor and docking studies reported that it can fit in the enzyme active site. This may explain how chlorogenic acid inhibits cholesterol biosynthesis[71].

There are no reports of HMGR inhibitory activity for *P. guajava*. Because of this, a set of other medicinal plants was compiled. Falé *et al.* (2013)[14] observed an IC_{50} of 152.66 ± 15.99µg/mL for *Cynara cardunculos*, 95.32 ± 4.69 µg/mL for *Fraxinus angustifolia*, and 329.04 ± 21.24 µg/mL for *Pterospartum tridentatum*. PG1 has the highest HMGR inhibitory activity of them all.

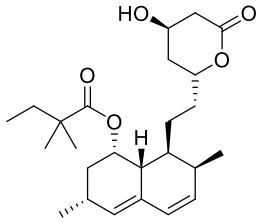

Figure 4.13: Structure of simvastatin.

4.8. Fourier-transform infrared (FTIR) spectroscopy analysis of HepG2 cellular components

FTIR spectroscopy was used to provide information on the global effect of *P. guajava* decoction on HepG2 cellular components. To do so, the assay was carried out in HepG2 cells treated with PG1 and PG2, comparatively to untreated cells and the analysis was performed in the spectral range of 3000-950 cm^{-1}. Note that the drying process of cells is known to introduce experimental artifacts in FTIR spectroscopy analysis. Samples were normalized to amide II. Analysis was performed in the spectral range 3000-900 cm^{-1} (Figure 4.14 and Figure 4.15) and the absorption in the 3200-3500 cm^{-1} region was not considered for further analysis due to strong water signal.

The signals at 3000-2800 cm^{-1} are due to symmetric and asymmetric stretching vibrations of CH_2 (~2923 cm^{-1}) and CH_3 (~2956 cm^{-1}) groups found in acyl chains of lipids and amino acid side chains. Additionally, the absorption signals in 1800-1700 cm^{-1} are characteristic of lipids and proteins as well, being the band at ~1741 cm^{-1} attributed to the C=O ester stretching band, mainly found in membrane phospholipids and triglycerides[98]. The vibrations of peptide bonds in proteins, namely C=O and C–N stretching and N–H bending modes, result in the Amide I (1652 cm^{-1}) and Amide II (1540 cm^{-1}) bands. These are very sensitive to the secondary structure of proteins. In the spectral region of 1300-900 cm^{-1} is possible to detect absorptions resulting from carbohydrates as well as phosphates. The vibrational mode of C-OH of carbohydrates is mainly found at ~1050 cm^{-1} and glycogen (glyco) at ~1025 cm^{-1}. The asymmetric and symmetric phosphodiester vibrations (PO_2^-asym and PO_2^-sym, respectively) of nucleic acids are found at ~1238 and 1081 cm^{-1}, respectively. Specifically, cell DNA is related to the intensity of the symmetric PO_2^- band[99] While RNA absorbs at ~1120 that results from the ribose C–O stretching[100].

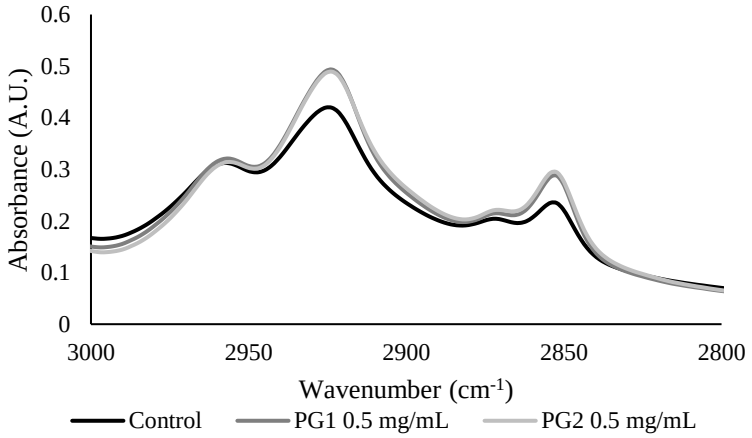

Figure 4.14: FTIR spectra between 3000 and 2800 cm^{-1} of HepG2 cells and HepG2 cells exposed to 0.5 mg/mL of PG1 and exposed to 0.5 mg/mL of PG2.

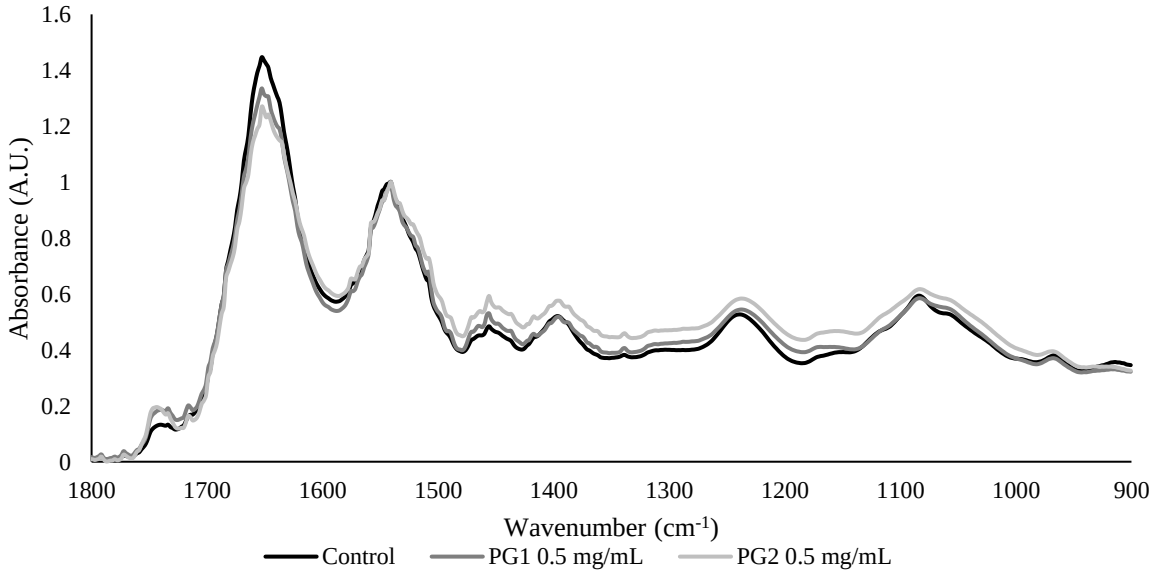

Figure 4.15: FTIR spectra between 1800 and 900 cm^{-1} of HepG2 cells and HepG2 cells exposed to 0.5 mg/mL of PG1 and exposed to 0.5 mg/mL of PG2.

The calculated ratios CH_3/CH_2, CH_2/COOH, CH_2/AmideII, AmideI/AmideII, COOH/AmideII, DNA/AmideII, glyco/AmideII, glyco/DNA, PO_2^-asym/PO_2^-sym, RNA/DNA, and protein/RNA from the FTIR spectra are presented in Figure 4.16 and it's possible to see that there are some significant differences between the control and the cells treated with samples at 95% confidence level, except for the CH_2/COOH one. Additionally, a heatmap is presented in Table 4.11 to illustrate the relative difference between PG1 and control, and between PG2 and control. The highest increase in intensity is colored in black (40% for PG1 and 46% for PG2) and the highest decrease in white (36% for PG1 and 41% for PG2).

The ratio CH_3/CH_2 (2956/2923 cm^{-1}) gives insight on the length of hydrocarbon chains of lipids[74] and its saturation level[101] and, by looking at Figure 4.16, it's possible to see that this ratio showed a slight decrease from untreated cells to cells treated with PG1 or PG2. Thus, the treated cells have shorter hydrocarbon chains and are less saturated. These results may suggest that the membrane fluidity suffered modifications[73], becoming more fluid with the decreased saturation level.

The ratio CH_2/AmideII (2920/1540 cm^{-1}) analyzes the number of total lipids normalized to Amide II band, representing the total protein in the cell[72,74]. This ratio increased, which means that the treated cells have more lipids than the ones untreated. The ratio COOH/AmideII (1741/1540 cm^{-1}) is attributed to the C=O ester stretching band normalized to Amide II band, whereas CH_2/COOH (2920/1741 cm^{-1}) gives insight on the number of acyl chains[74]. As mentioned, CH_2/COOH ratio is unaltered from untreated to treated cells, which means that the number of acyl chains remains the same. COOH/AmideII ratio increased when cells were treated with PG1 or PG2. This suggests that there's an increase of phospholipids and triglycerides in treated cells, which agrees with the observation of the CH_2/AmideII ratio.

AmideI/AmideII (1652/1540 cm^{-1}) ratio allows the detection of changes in cell protein pattern[102]. It's possible to see that the untreated cells present the highest ratio, PG1 treatment is intermediary, and PG2 treatment has the lowest value. The three are significantly different. These results suggest that the cell proteome suffers modifications which is an indication of disordered secondary structure[103]. In fact, PG2 was the most cytotoxic sample and it can justify the higher secondary structure disorder of PG2. Note that water has a dominant contribution to the Amide I band[102]. Nonetheless, the cells were dried prior to analysis so that the water contribution is minimized.

DNA/AmideII ratio (1081/1540 cm^{-1}) is related with modifications on the cell's DNA normalized to the total amount of cell proteins whereas RNA/AmideII (1120/1540 cm^{-1}) is related to RNA and cell proteins. A decrease in the first ratio is observed in the cells treated with PG1 or PG2. This suggests that the samples can inhibit DNA replication[98]. For RNA/AmideII ratio, PG1 and PG2 induced a slight decrease in the amount of RNA. The ratio RNA/DNA (1081/1120 cm^{-1}) of PG1 and PG2 treated cells also decreased comparing to untreated cells. This observation together with the one from the RNA/AmideII ratio, indicates that there's a lower transcription level[101] in treated cells. The ratio PO2-asym/PO2-sym (1238/1081 cm^{-1}) gives insight on the phosphorylative process in the cell[101]. Note that the DNA (PO_2^-sym) per total cell protein decreases. As so, it's expected to see the increase in the ratio PO2-asym/PO2-sym.

Both glyco/AmideII (1025/1540 cm^{-1}) and glyco/DNA (1025/1081 cm^{-1}) ratios refer to glycogen levels in the cell[101] normalized for the total amount of cell proteins and cell DNA, respectively. Glycogen is a way for cells to store glucose to obtain energy[100]. The two ratios decrease when the cells are treated with PG1 or PG2.

Through FTIR spectroscopy analysis, it was possible to see that the *P. guajava* decoction induced some changes in HepG2 cells components. Modifications were seen in nucleic acids, proteins, lipids, and in carbohydrates.

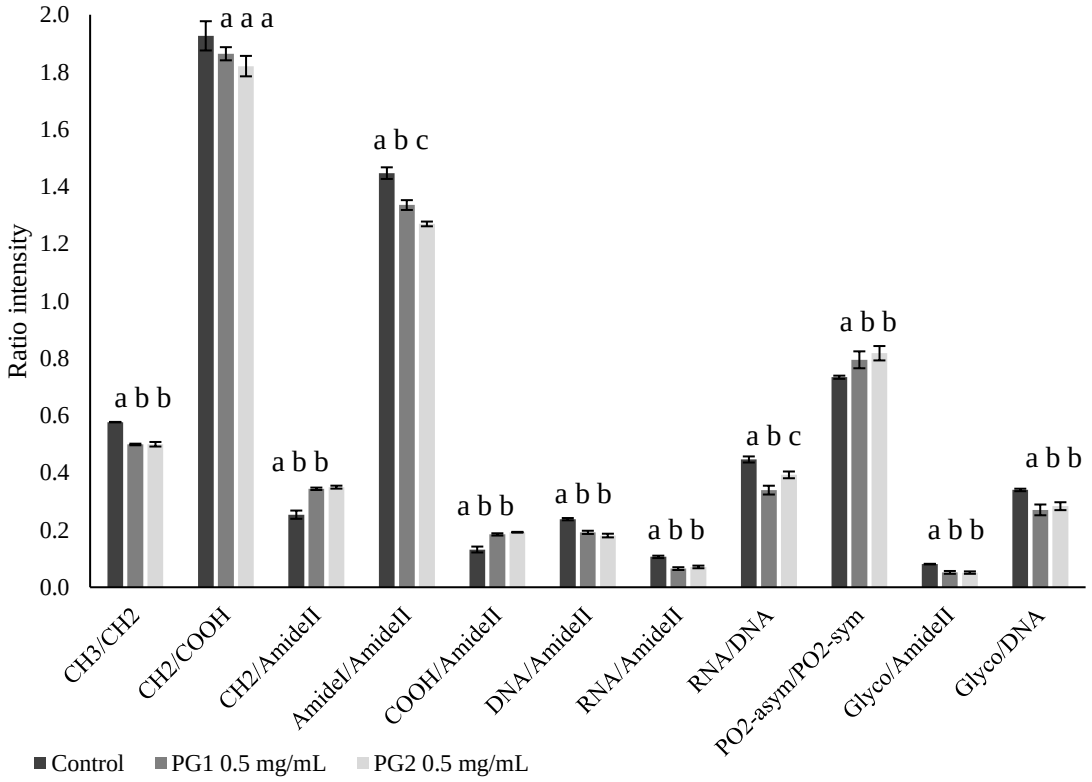

Figure 4.16: Comparison between the ratios CH3/CH2, CH2/COOH, CH2/AmideII, AmideI/AmideII, COOH/AmideII, DNA/AmideII, RNA/AmideII, RNA/DNA, PO2-asym/PO2-sym, glyco/AmideII, and glyco/DNA resulting from FTIR analysis of control cells, cells exposed to 0.5 mg/mL of PG1 and cells exposed to 0.5 mg/mL of PG2. The ratios were normalized according to the intensity of control. Different letters (a-c) correspond to values in the same ratio that can be considered statistically different with 95% confidence level.

Table 4.11: Heatmap of the relative difference between PG1 and control, and PG2 and control for the analyzed ratios in FTIR spectroscopy.

	Relative difference (%) normalized to the control	
Ratio	PG1	PG2
CH3/CH2		
CH2/COOH		
CH2/AmideII		
AmideI/AmideII		
COOH/AmideII		
DNA/AmideII		
RNA/AmideII		
RNA/DNA		
PO2-asym/PO2-sym		
Glyco/AmideII		
Glyco/DNA		

To further clarify differences between spectra of cells exposed to different conditions, and to identify main sources of variation, the analysis was complemented with Principal Component Analysis (PCA). PCA is a multivariate regression method for constructing variables to explain the co-variance between reference data and the spectra[104]. It identifies directions, that is Principal Components (PCs), along which the variance of the data is maximized. The effect of this process is to concentrate the sources of variability in the data into the first few PCs[105]. Positive scores correspond to positive loadings for each PC and negative scores correspond to negative loadings for that PC. Thus, the molecular components of the spectra depicted by the PC positive loadings would be present in larger amount for samples showing positive scores. Whereas the molecular components related to the spectral features showing negative loadings would be in present in lower amount for samples showing negative scores[74].

Spectra were separated in two regions for PCA, that are characteristic of different cell components vibrations. PCA of control and treated cells are shown in Figure 4.17.

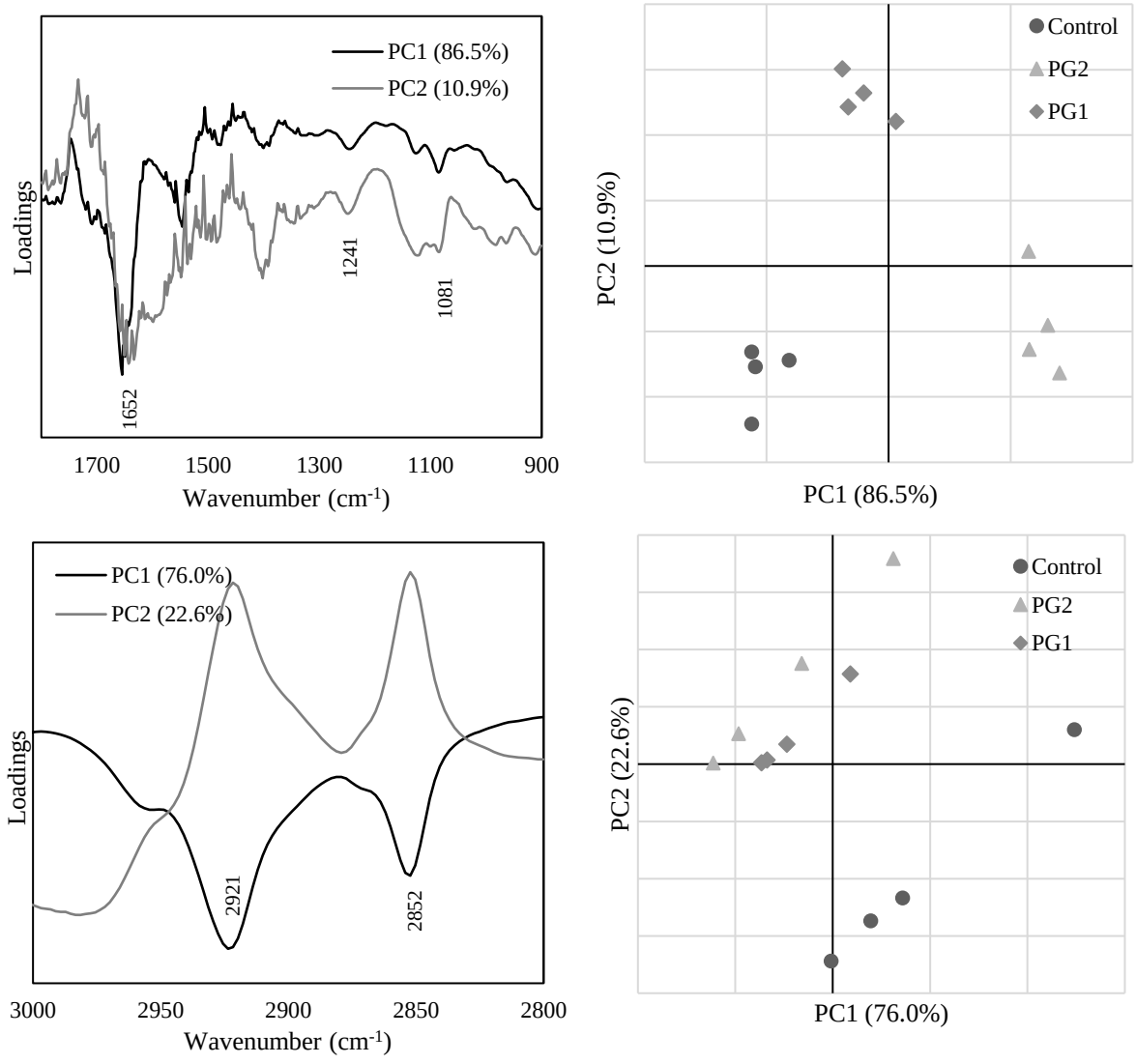

Figure 4.17: Analysis of FTIR spectra of control and treated cells with PCA. Two spectral regions were considered for analysis: 1800-900 and 3000-2800 cm^{-1}. PC loadings are represented on the left and score scatter plots of the corresponding PC1 and PC2 are represented on the right.

The region 1800-900 cm^{-1} shows a dominating PC1 explaining 86.5% of the variation in the set of spectra, which gave a clear separation of cells treated and control. For instance, PC1 highlighted small

changes showing negative loadings at 1081, 1241, and 1652 (Amide I) cm^{-1}. PC2 also highlighted changes at 1150-950 cm^{-1} associated with changes in carbohydrates and phosphorylated cellular compounds[106]. Thus, The PC2 loadings plot showed similar features with negative loadings at 1081 and 1240 cm^{-1} (sym/asym PO_2^- vibrations). Control cells and treated cells form discrete clusters, presenting the highest amount of sym/asym PO_2^- vibrations α-helix-rich proteins for PG2 and an intermediate position for PG1 treated cells between control and PG2 treated cells.

The region of 3000-2800 cm^{-1} corresponds to C–H stretching, mainly associated with aliphatic chains of fatty acids in cells. The scores scatter plot PC1 vs. PC2 shows a clear separation of cell groups along the PC1 (76.0% of variance) and the PC2 (22.6%). The PC1 and showed negative loadings at 2852 and 2921 cm^{-1} which correspond to the CH2asym/sym stretching vibrations whereas PC2 showed similar features but positive. Compared to the control, PG1 and PG2 treated cells present lower value (negative scores) for PC1 and higher value (positive scores) for PC2. Control cells formed a group presenting the highest amount of lipids, while PG1 treated cells formed an intermediate group between control and PG2 treated cells showing that PG2 has the lowest amount of lipids.

4.9. Effect of *P. guajava* decoction in proteins

4.9.1. SDS-PAGE of cytosolic and membrane proteins from Caco-2

The effect of PG1 and PG2 on Caco-2 protein profile was evaluated through SDS-PAGE since the compounds from the samples permeated the simulated intestinal. Proteins extracted from Caco-2 cell line were separated in two different fractions: membrane and cytosolic proteins. The resulting gels can be seen in Figure 4.18 and Figure 4.19, respectively, and the most intense bands were analyzed for its intensity and molecular weight. The bands numbering can be consulted in Annex 4, in Figure 7.25 and Figure 7.26, respectively.

In Figure 4.18 it's possible to notice subtle changes in the membrane protein profile of cells treated with PG1 (lanes 2, 3, and 4) and PG2 (lanes 6, 7, and 8) compared with untreated cells (lane 5). The intensities of the most prominent bands (12 in total) were analyzed to quantify the relative difference (%) between treated and untreated cells. A heatmap illustrates these results in Table 4.12 where black indicates the highest decrease value (99%) and white the highest increase (96%). There's a general decrease in band intensity when cells are treated with PG1 and PG2. The bands that showed the biggest decrease were: band 1 when cells were treated with PG2 0.50 (94.9%) and 0.75 mg/mL (97.4%), band 5 when cells were treated with PG2 0.75 mg/mL (96.8%), band 9 when cells were treated with PG1 0.25 mg/mL (97.2%) and PG2 0.75 mg/mL (98.5%), and band 12 when cells were treated with PG1 0.25 mg/mL (90.3%) and PG2 0.25 mg/mL (99.1%). An increase was observed in bands 8 and 10 of PG1 0.25 and 0.50 mg/mL as well as in PG2 0.25 mg/mL; bands 2, 8, and 10 of PG1 0.75 mg/mL; and bands 2 and 11 of PG2 0.75 mg/mL.

Since this is the membrane proteins fraction, we can search for the cholesterol membrane transporters NPC1L1, ABCG8, and ABCG5. In fact, the calculated molecular weight of band 1 was 138.0 ± 2.1 kDa, which is near the molecular weight of NPC1L1, that is 140 kDa. Thus, it can be suggested that this bands corresponds to NPC1L1 (relative error 1.43%). This band showed a decrease when cells were treated with PG1 and PG2 and the higher the sample concentration, the greater the decrease, although PG2 0.50 and 0.75 mg/mL showed a similar variation (94.9 and 97.4, respectively). ABCG5 and ABCG8 have similar mass (73 and 70 kDa, respectively), which makes it difficult to distinguish. The protein in band 6 was determined to have 71.4 ± 0.9 kDa and may be suggested that the protein in this band corresponds to ABCG5 or ABCG8. This band decreases in intensity when cells were treated with PG1 and PG2. This

is a preliminary evaluation of cholesterol transporters expression and a more precise method, such as Western Blot, is necessary to correctly assess the influence of PG1 and PG2 in these proteins.

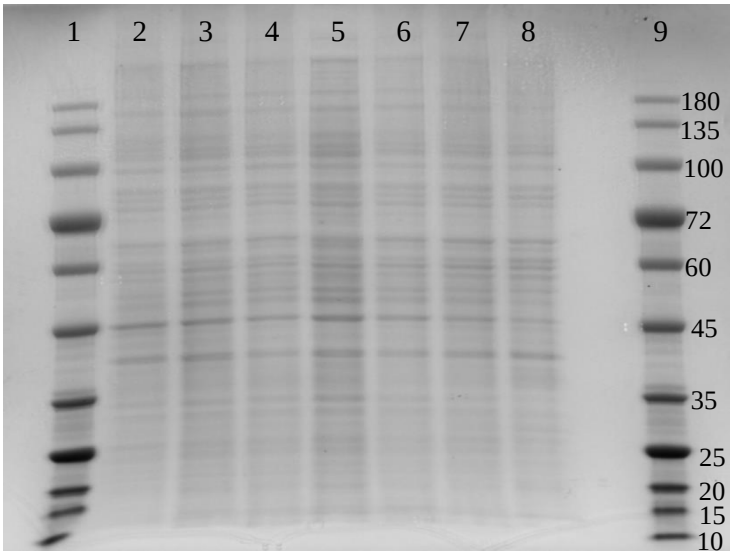

Figure 4.18: SDS-PAGE of membrane proteins from Caco-2 cells treated with PG1 0.25 mg/mL (lane 2), 0.50 mg/mL (lane 3), and 0.75 mg/mL (lane 4), and treated with PG2 0.25 mg/mL (lane 6), 0.50 mg/mL (lane 7), and 0.75 mg/mL (lane 8) for 24 h. Lane 5 corresponds to untreated cells (control) and lanes 1 and 9 correspond to the protein marker and the molecular weight of each band is presented.

Table 4.12: Calculated molecular weight and relative difference between bands from membrane proteins of treated (PG1 0.25, 0.50,and 0.75 mg/mL, and PG2 0.25, 0.50, and 0.75 mg/mL for 24 h) and untreated Caco-2 cells.

		Relative difference (%)					
Band number	Calculated Mr (kDa)	PG1 0.25 mg/mL	PG1 0.50 mg/mL	PG1 0.75 mg/mL	PG2 0.25 mg/mL	PG2 0.50 mg/mL	PG2 0.75 mg/mL
1	138.0 ± 2.1						
2	103.9 ± 1.5						
3	93.0 ± 1.3						
4	85.9 ± 1.1						
5	81.7 ± 1.1						
6	71.4 ± 0.9						
7	63.0 ± 0.8						
8	55.8 ± 0.6						
9	53.3 ± 0.6						
10	48.4 ± 0.5						
11	40.6 ± 0.4						
12	32.5 ± 0.3						

In Figure 4.19, regarding cytosolic proteins, protein expression seems to be similar between treatments. Nonetheless, the assessment of band intensity must be made to quantify the variations in protein expression according to the cell treatment: PG1 (lanes 2, 3, and 4) and PG2 (lanes 6, 7, and 8). In fact, it was observed a general decrease in band intensity that can be seen in the heatmap in Table 4.13. Again, black indicates the highest decrease value (122%) and white the highest increase (76%). The bands that showed the biggest decrease were band 3 with PG1 0.25 mg/mL treatment (98.2%), band 2 with PG2 0.50 mg/mL treatment (101.5%), band 1, 2, 3, 11, and 19 with PG2 0.75 mg/mL treatment (84.2%, 103.9%, 107.5%, 103.2%, and 122.1%, respectively). An increase in protein expression was observed

in bands 4, 9, and 10 from PG1 0.25 mg/mL; bands 1, 5, 7, 8, 9, and 14 from PG1 0.50 mg/mL; bands 1 and 16 from PG1 0.75 mg/mL; bands 4, 10, 14, and 17 from PG2 0.25 mg/mL, bands 4, 8, and 10 from PG2 0.50 mg/mL; and band 10 from PG2 0.75 mg/mL.

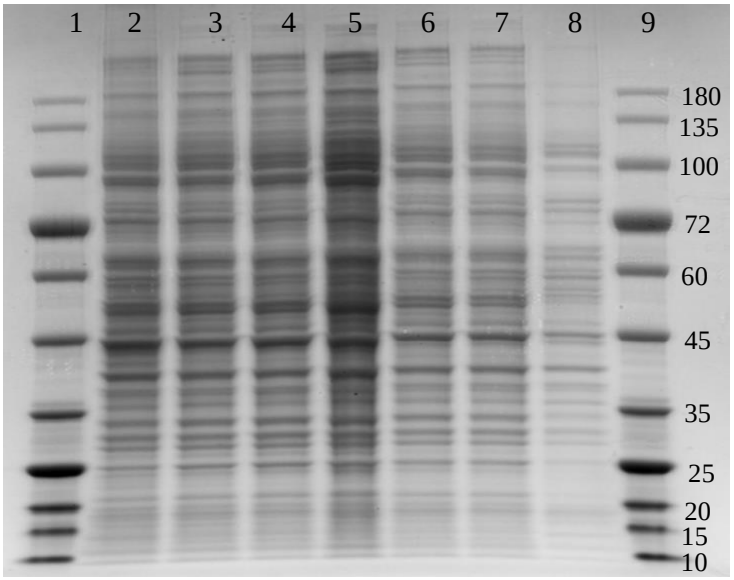

Figure 4.19: SDS-PAGE of cytosolic proteins from Caco-2 cells treated with PG1 0.25 mg/mL (lane 2), 0.50 mg/mL (lane 3), and 0.75 mg/mL (lane 4), and treated with PG2 0.25 mg/mL (lane 6), 0.50 mg/mL (lane 7), and 0.75 mg/mL (lane 8) for 24 h. Lane 5 corresponds to untreated cells (control) and lanes 1 and 9 correspond to the protein marker and the molecular weight of each band is presented.

Table 4.13: Calculated molecular weight and relative difference between bands from cytosolic proteins of treated (PG1 0.25, 0.50,and 0.75 mg/mL, and PG2 0.25, 0.50, and 0.75 mg/mL for 24 h) and untreated Caco-2 cells.

		Relative difference (%)					
Band number	Calculated Mr (kDa)	PG1 0.25 mg/mL	PG1 0.50 mg/mL	PG1 0.75 mg/mL	PG2 0.25 mg/mL	PG2 0.50 mg/mL	PG2 0.75 mg/mL
1	136.9 ± 2.1						
2	124.3 ± 1.8						
3	113.2 ± 1.6						
4	102.2 ± 1.4						
5	98.0 ± 1.4						
6	91.2 ± 1.2						
7	76.0 ± 1.0						
8	63.2 ± 0.8						
9	58.5 ± 0.7						
10	57.1 ± 0.7						
11	50.4 ± 0.6						
12	43.1 ± 0.5						
13	37.3 ± 0.4						
14	33.0 ± 0.3						
15	30.0 ± 0.3						
16	28.2 ± 0.2						
17	27.1 ± 0.2						
18	24.7 ± 0.2						
19	21.4 ± 0.2						

These results indicate that PG1 and PG2 induce modifications in the expression of membrane and cytosolic proteins from Caco-2 cells. In fact, flavonoids were reported to interfere with Caco-2 cell cycle[107] which confirms the observations from this assay. The most cytotoxic sample, PG2, was the one that affected protein expression the most, although LC-HRMS-MS analysis indicated that this sample had less bioactive compounds.

Falé et al. (2012) reported modifications in the protein profile of HeLa cell line when cells where treated with phenolic compounds from *Peumus boldus* aqueous extract[108].

4.9.2. Effect of *P. guajava* decoction on cholesterol transporters

The effect of PG1 and PG2 on cholesterol transporter proteins, namely NPC1L1, ABCG5, and ABCG8, was analyzed by Western Blot in HepG2 cells. The abundance of transporters was analyzed with specific antibodies and the band intensities (Figure 4.20) were quantified using Image Lab software in order to calculate the decrease of protein expression (%), as seen in Figure 4.21. Assays were done in duplicate for NPC1L1 and ABCG5 where ABCG8 protein expression was evaluated without replicates.

Western Blot has a limitation which is the standardization of the protein content in the gel and α-tubulin is normally used as an internal standard. Nonetheless, some authors reported that phenolic compounds could modify the cell's protein content, thus, the total protein content can't be used to standardize the Western Blot measurements[98,108,109]. Due to this, the same concentration of cells was used instead.

A decrease in the abundance of all cholesterol transporter proteins can be seen and this trend seems to follow a dose-dependent fashion. Additionally, there were no protein expression in lane 3, 6, and 7 of NPC1L1 and in the lane 7 of ABCG8. These results agree with the general decreased protein expression observed in section 4.9.1.

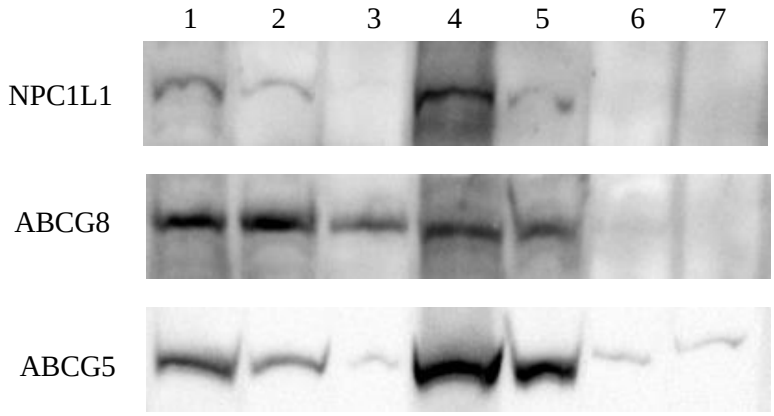

Figure 4.20: NPC1L1, ABCG5, and ABCG8 bands obtained through Western Blot. HepG2 cells were treated with 1) PG1 0.25 mg/mL, 2) PG1 0.50 mg/mL, 3) PG1 0.75 mg/mL, 4) control, 5) PG2 0.25 mg/mL, 6) PG2 0.50 mg/mL, 7) PG2 0.75 mg/mL for 24h.

NPC1L1's expression decreased 16.1 ± 0.7 %, 74.2 ± 2.9 %, and 94.2 ± 3.0 % when cells were treated with 0.25, 0.50, and 0.75 mg/mL of PG1, respectively. With 0.25 mg/mL of PG2, it decreased 76.1 ± 19.7 %. Cells in contact with 0.50 and 0.75 mg/mL of PG2 show a total inhibition of this protein's expression. Several phenolic compounds were identified in LC-HRMS-MS analysis. Namely, quercetin was reported to inhibit the expression of NPC1L1 in Caco-2 cells[94]. In the same cell line, NPC1L1's expression decreased when cells were treated with catechin and chlorogenic acid[110].

As mentioned above, the inhibition of NPC1L1 is an important mechanism to decrease blood cholesterol since it mediates cholesterol absorption[44]. This fact, together with the obtained results, suggests that PG1 and PG2 can decrease blood cholesterol levels by inhibiting the expression of NPC1L1 cholesterol transporter.

ABCG8's expression decreased 24.3%, 30.4%, and 36.7% when cells were treated with 0.25, 0.50, and 0.75 mg/mL of PG1, respectively. With PG2 0.25 and 0.50 mg/mL, the protein expression decreased 57.9% and 80.0%, respectively. Total protein inhibition was observed in PG2 0.75 mg/mL. Catechin and chlorogenic acid were reported to increase the expression of ABCG8 in Caco-2 cells[111].

ABCG5's expression decreased 27.7 ± 17.1 %, 72.1 ± 4.4 %, and 97.7 ± 1.5 % when cells were treated with 0.25, 0.50, and 0.75 mg/mL of PG1, respectively. With PG2 0.25, 0.50, and 0.75 mg/mL, the transporter's expression decreased 28.1 ± 5.8 %, 97.3 ± 1.9 %, and 94.5 ± 1.4 %, respectively.

ABCG8 and ABCG5 promote cholesterol efflux from the body through hepatobiliary secretion[55]. Its overexpression is desired to decrease blood cholesterol levels. Since the expression of both transporters decreased, when cells were treated with PG1 and PG2, this is not the mechanism by which PG1 and PG2 decrease blood cholesterol level.

Another observation to have in mind is that FTIR spectrometry results suggested that there's a decrease in DNA replication and in transcription when cells were treated with PG1 and PG2. Thus, the decrease of NPC1L1 and ABCG8 expression observed in Western Blot can be justified with these results from FTIR spectroscopy.

Additionally, the effect of drugs used to treat hypercholesterolemia, by inhibiting cholesterol *de novo* synthesis, on cholesterol transporter proteins was evaluated by some authors. Statins, such as pravastatin induced a decrease of 70% and 80% in NPC1L1's and ABCG5/8's expression, respectively[112]. PG1 0.50 mg/mL and PG2 0.25 mg/mL seem to be able to inhibit the cholesterol transporters like pravastatin.

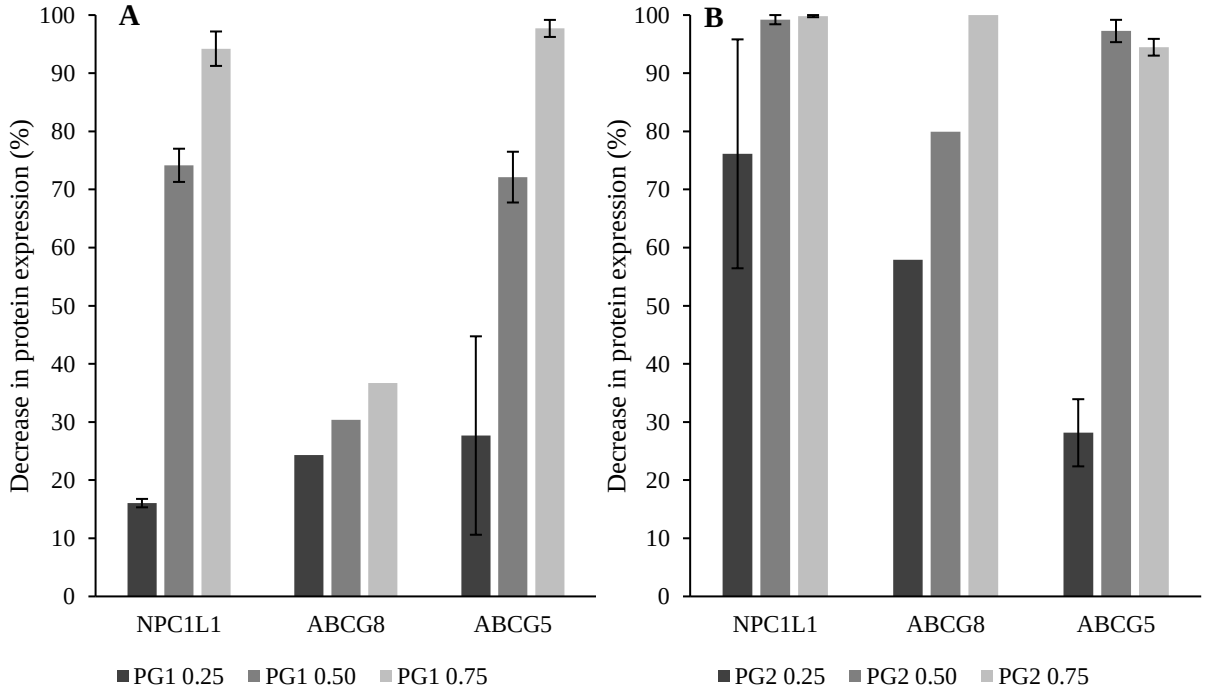

Figure 4.21: Decrease of NPC1L1, ABCG5, and ABCG8 expression in HepG2 cells treated with 0.25, 0.50, and 0.75 mg/mL of PG1 (A) and PG2 (B) compared to the control (untreated cells).

V. Conclusions and Perspectives

5.1. Conclusions

P. guajava leaf decoction has been used in traditional medicine due to its beneficial health effects, both in the prevention and treatment of diseases, namely hypercholesterolemia.

Three samples were assessed in this study, namely the aqueous extract called PG1, the ethanolic precipitation supernatant called PG2, and the ethanolic precipitation pellet called PG3. The decoction's chemical composition was determined through LC-HRMS-MS analysis and several molecules were identified, namely catechin, quercetin, epigallocatechin, protocatechuic acid, gallic acid, chlorogenic acid, hyperoside, quercitrin, guaijaverin, and jacoumaric acid. It's also relevant to note that PG2 had less concentration of some compounds. PG3's chromatogram didn't show peaks. The biological activity of guava leaf decoction was evaluated by the antioxidant and acetylcholinesterase (AChE) inhibitory activity. In both assays, PG1 showed the best activity with IC_{50} values of 7.5 ± 0.4 µg/mL for DPPH assay and 48.7 ± 1.4 µg/mL for AChE inhibition. PG2 had 11.9 ± 0.5 µg/mL and 63.4 ± 1.1 µg/mL, respectively. PG3 had antioxidant activity (7.26 ± 0.57 µg/mL) and didn't have AChE inhibitory activity, so it wasn't used in the subsequent assays. Since PG1 didn't show any modifications induced by the simulated gastric and pancreatic juice, the permeation of molecules from the decoction can be assessed. It was observed the permeation of gallic acid (10.0 ± 7.9 %), catechin (2.4 ± 0.2 %), chlorogenic acid (0.2 ± 0.2 %), hyperoside (1.2 ± 1.2 %), and quercitrin (2.8 ± 0.5 %). Thus, these molecules can be absorbed and transported through the blood to access other possible therapeutic targets. The liver is responsible for the majority cholesterol synthesis which is modulated by the activity of 3-hydroxy-3-methylglutaryl coenzyme A reductase (HMGR). PG1 was able to inhibit the activity of HMGR with an IC_{50} of 8.4 ± 0.5 µg/mL and this may be one of the mechanisms by which guava leaf decoction decreases blood cholesterol. Another way to decrease blood cholesterol is through the reduction of cholesterol permeation in the intestinal barrier. In fact, both PG1 and PG2 were able to decrease the permeation of cholesterol through Caco-2 cell monolayers by 55% and 24%, respectively. To understand how cholesterol permeation decreases, the expression of cholesterol transporters NPC1L1, ABCG5, and ABCG8 was evaluated under the influence of PG1 and PG2. HepG2 were used as a model of hepatocytes and it was possible to see a decrease in the expression of the three transporters. The decrease of NPC1L1 indicates a decreased absorption of cholesterol and this may be another mechanism by which guava leaf decoction decreases blood cholesterol. The decrease in ABCG5/G8 expression suggests a reduced efflux of cholesterol. FTIR analysis suggested that the samples induce modifications in HepG2 metabolite profile and that the decreased expression of several proteins may be related to the changes in the RNA transcription. The SDS-PAGE of Caco-2 cells also indicated a subtle decrease in protein expression when cells were treated with PG1 and PG2.

Overall, the *P. guajava* leaf decoction was able to interfere in the absorption and metabolism of cholesterol. This effect results from the inhibition of cholesterol synthesis in the liver, through HMGR inhibition, and decrease of dietary cholesterol permeation in the intestine, through NPC1L1's expression modulation. These observations help to understand the rationale behind the use and justify the effects of *P. guajava* leaf decoction observed in traditional medicine.

5.2. Perspectives

The results presented in this study allow me to propose the continuation of this study. Thus, it is considered important to:

- Study the metabolome of HepG2 and Caco-2 under the decoction's influence through LC-HRMS-MS and perform a Principal Component Analysis (PCA).
- Further study the protein modifications through bidimensional electrophoresis followed by proteins collection the from the gel for identification.
- Perform Western Blot for cholesterol transporters from differentiated Caco-2 cells used in the permeation assay.
- Study the interaction of statins and guava leaf decoction.
- Develop a supplemented drink with guava leaf decoction extract PG1 and evaluate its bioactivity and effect in cholesterol metabolism.

VI. References

1. Díaz-de-Cerio, E., Verardo, V., Gómez-Caravaca, A. M., Fernández-Gutiérrez, A. & Segura-Carretero, A. Health effects of Psidium guajava L. Leaves: An overview of the last decade. *Int. J. Mol. Sci.* **18**, 1–31 (2017).

2. Gupta, G. K., Chahal, J. & Arora, D. Psidium Guajava Linn : Current Research and Future Prospects Available online through Psidium guajava Linn : Current Research and Future Prospects. *J. Pharm. Res.* **4**, 42–46 (2011).

3. Gutiérrez, R. M. P., Mitchell, S. & Solis, R. V. Psidium guajava: A review of its traditional uses, phytochemistry and pharmacology. *J. Ethnopharmacol.* **117**, 1–27 (2008).

4. Simão, A. A., Marques, T. R., Marcussi, S. & Corrêa, A. D. Aqueous extract of Psidium guajava leaves: phenolic compounds and inhibitory potential on digestive enzymes. *An. Acad. Bras. Cienc.* **89**, 2155–2165 (2017).

5. Chen, H.-Y. & Yen, G.-C. Antioxidant activity and free radical-scavenging capacity of extracts from guava (Psidium guajava L .) leaves. *Food Chem.* **101**, 686–694 (2007).

6. Ngbolua, J.-P. K.-N. *et al.* A review on the Phytochemistry and Pharmacology of Psidium guajava L. (Myrtaceae) and Future direction. *Discov. Phytomedicine* **5**, 7–13 (2018).

7. Paduch, R., Kandefer-Szerszeń, M., Trytek, M. & Fiedurek, J. Terpenes: Substances useful in human healthcare. *Arch. Immunol. Ther. Exp. (Warsz).* **55**, 315–327 (2007).

8. Minatel, I. O. *et al.* Phenolic Compounds: Functional Properties, Impact of Processing and Bioavailability. in *Phenolic Compounds - Biological Activity* 1–24 (2017). doi:10.5772/66368.

9. de la Rosa, L. A., Moreno-Escamilla, J. O., Rodrigo-García, J. & Alvarez-Parrilla, E. Phenolic Compounds. in *Postharvest Physiology and Biochemistry of Fruits and Vegetables* (eds. Yahia, E. & Carrillo-Lopez, A.) 253–271 (Elsevier Inc., 2019). doi:10.1016/b978-0-12-813278-4.00012-9.

10. Scalbert, A., Manach, C., Morand, C., Rémésy, C. & Jiménez, L. Dietary Polyphenols and the Prevention of Diseases. *Crit. Rev. Food Sci. Nutr.* **45**, 287–306 (2005).

11. Falé, P. L. *et al.* Evaluation of cholesterol absorption and biosynthesis by decoctions of Annona cherimola leaves. *J. Ethnopharmacol.* **150**, 718–723 (2013).

12. Goedeke, L. & Fernández-Hernando, C. Regulation of cholesterol homeostasis. *Cell. Mol. Life Sci.* **69**, 915–930 (2012).

13. Luo, J., Yang, H. & Song, B. L. Mechanisms and regulation of cholesterol homeostasis. *Nat. Rev. Mol. Cell Biol.* **21**, 225–245 (2020).

14. Falé, P., Ferreira, C., Rodrigues, A. M., Frazo, F. N. & Serralheiro, M. L. M. Studies on the molecular mechanism of cholesterol reduction by Fraxinus angustifolia, Peumus boldus, Cynara cardunculus and Pterospartum tridentatum infusions. *J. Med. Plants Res.* **8**, 9–17 (2014).

15. Akinloye, O., Akinmoladun, A. C. & Farombi, E. O. Modulatory effect of Psidium guajava linn and Ocimum gratissimum linn on lipid profile and selected biochemical indices in rabbits fed high cholesterol diet. *J. Complement. Integr. Med.* **7**, (2010).

16. Wang, F. *et al.* Chemical Components and Bioactivities of Psidium guajava. *Int. J. Food Nutr. Saf.* **5**, 98–114 (2014).

17. Begum, S., Hassan, S. I. & Siddiqui, B. S. Two new triterpenoids from the fresh leaves of Psidium guajava. *Planta Med.* **68**, 1149–1152 (2002).

18. Begum, S., Hassan, S. I., Ali, S. & Siddiqui, B. S. Chemical Constituents of the Leaves of Psidium guajava. *Nat. Prod. Res. Former. Nat. Prod. Lett.* **18**, 135–140 (2004).

19. Begum, S. *et al.* Triterpenoids from the leaves of Psidium guajava. *Phytochemistry* **61**, 399–403 (2002).

20. Begum, S., Ali, S. N., Hassan, S. I. & Siddiqui, B. S. A new ethylene glycol triterpenoid from the leaves of Psidium guajava. *Nat. Prod. Res. Former. Nat. Prod. Lett.* **21**, 742–748 (2007).

21. Shao, M. *et al.* Four new triterpenoids from the leaves of Psidium guajava. *J. Asian Nat. Prod. Res.* **14**, 348–354 (2012).

22. Weli, A. *et al.* Chemical composition and biological activities of the essential oils of Psidium guajava leaf. *J. King Saud Univ. - Sci.* (2018) doi:10.1016/j.jksus.2018.07.021.

23. Barbalho, S. M. Psidium Guajava (Guava): A Plant of Multipurpose Medicinal Applications. *Med. Aromat. Plants* **01**, (2012).

24. Kim, S. H. *et al.* Metabolic profiling and predicting the free radical scavenging activity of guava (Psidium guajava L.) leaves according to harvest time by 1H-nuclear magnetic resonance spectroscopy. *Biosci. Biotechnol. Biochem.* **75**, 1090–1097 (2011).

25. Crozier, A., Jaganath, I. B. & Clifford, M. N. Phenols, Polyphenols and Tannins: An Overview. in *Plant Secondary Metabolites: Occurrence, Structure and Role in the Human Diet* 1–24 (2007). doi:10.1002/9780470988558.ch1.

26. Neagu, E., Radu, G. L., Albu, C. & Paun, G. Antioxidant activity, acetylcholinesterase and tyrosinase inhibitory potential of Pulmonaria officinalis and Centarium umbellatum extracts. *Saudi J. Biol. Sci.* **25**, 578–585 (2018).

27. Murkovic, M. Phenolic Compounds. in *Encyclopedia of Food Sciences and Nutrition* (ed. Caballero, B.) 4507–4514 (Academic Press, 2003). doi:10.1201/b17244-10.

28. Giada, M. de L. R. Food Phenolic Compounds: Main Classes, Sources and Their Antioxidant Power. in *Oxidative Stress and Chronic Degenerative Diseases - A Role for Antioxidants* (ed. Morales-González, J. A.) 87–112 (InTech, 2013).

29. Ludwiczuk, A., Skalicka-Woźniak, K. & Georgiev, M. I. Terpenoids. in *Pharmacognosy: Fundamentals, Applications and Strategies* (eds. Badal, S. & Delgoda, R.) 233–266 (Academic Press, 2017). doi:10.1016/B978-0-12-802104-0.00011-1.

30. Marmiroli, N. & Maestri, E. Plant peptides in defense and signaling. *Peptides* **56**, 30–44 (2014).

31. Hu, Z., Zhang, H. & Shi, K. Plant peptides in plant defense responses. *Plant Signal. Behav.* **13**, (2018).

32. Maestri, E., Marmiroli, M. & Marmiroli, N. Bioactive peptides in plant-derived foodstuffs. *J. Proteomics* **147**, 140–155 (2016).

33. Mazorra-Manzano, M. A., Ramírez-Suarez, J. C. & Yada, R. Y. Plant proteases for bioactive peptides release: A review. *Crit. Rev. Food Sci. Nutr.* **58**, 2147–2163 (2018).

34. Sheppard, A. J., O'Dell, R. G. & Pennington, J. A. T. Cholesterol | Properties and Determination. in *Encyclopedia of Food Sciences and Nutrition* (ed. Caballero, B.) 1220–1226 (Academic Press, 2003). doi:10.1016/b0-12-227055-x/00224-8.

35. Arnold, D. R. & Kwiterovich, P. O. Cholesterol | Absorption, Function, and Metabolism. in *Encyclopedia of Food Sciences and Nutrition* (ed. Caballero, B.) 1226–1237 (Academic Press, 2003). doi:10.1016/b0-12-227055-x/00225-x.

36. Röhrl, C. & Stangl, H. Cholesterol metabolism—physiological regulation and pathophysiological deregulation by the endoplasmic reticulum. *Wiener Medizinische Wochenschrift* **168**, 280–285 (2018).

37. Burtis, C. A., Ashwood, E. R. & Bruns, D. E. *Tietz Textbook of Clinical Chemistry and Molecular Diagnostics*. (Elsevier Health Sciences, 2012).

38. Ye, D. *et al.* Hepatic cell-specific ATP-binding cassette (ABC) transporter profiling identifies putative novel candidates for lipid homeostasis in mice. *Atherosclerosis* **196**, 650–658 (2008).

39. Méndez-González, J. *et al.* ATP-binding cassette G5/G8 deficiency causes hypertriglyceridemia by affecting multiple metabolic pathways. *Biochim. Biophys. Acta - Mol. Cell Biol. Lipids* **1811**, 1186–1193 (2011).

40. Manautou, J. E., Campion, S. N. & Aleksunes, L. M. Regulation of Hepatobiliary Transporters during Liver Injury. *Compr. Toxicol. Second Ed.* **9**, 175–220 (2010).

41. Oram, J. F. & Heinecke, J. W. ATP-binding cassette transporter A1: A cell cholesterol exporter that protects against cardiovascular disease. *Physiol. Rev.* **85**, 1343–1372 (2005).

42. Vaisman, B. L. *et al.* ABCA1 overexpression leads to hyperalphalipoproteinemia and increased biliary cholesterol excretion in transgenic mice. *J. Clin. Invest.* **108**, 303–309 (2001).

43. Guerin, M. Reverse Cholesterol Transport in HDL Metabolism: Relevance to Atherosclerosis Progression and Cardiovascular Diseases. in *The HDL Handbook: Biological Functions and Clinical Implications* (ed. Komoda, T.) 97–119 (Academic Press., 2017). doi:10.1016/B978-0-12-812513-7.00005-7.

44. Jia, L., Betters, J. L. & Yu, L. Niemann-pick C1-like 1 (NPC1L1) protein in intestinal and hepatic cholesterol transport. *Annu. Rev. Physiol.* **73**, 239–59 (2014).

45. Betters, J. L. & Yu, L. NPC1L1 and Cholesterol Transport. *FEBS Lett.* **584**, 2740–2747 (2010).

46. Phan, B. A. P., Dayspring, T. D. & Toth, P. P. Ezetimibe therapy: Mechanism of action and clinical update. *Vasc. Health Risk Manag.* **8**, 415–427 (2012).

47. Garcia-Calvo, M. *et al.* The target of ezetimibe is Niemann-Pick C1-Like 1 (NPC1L1). *Proc. Natl. Acad. Sci. U. S. A.* **102**, 8132–8137 (2005).

48. FDA Approved Drug Products: Zetia (ezetimibe) oral tablets. https://www.accessdata.fda.gov/drugsatfda_docs/label/2012/021445s033lbl.pdf.

49. Nutescu, E. A. & Shapiro, N. L. Ezetimibe: A Selective Cholesterol Absorption Inhibitor. *Pharmacotherapy* **23**, 1463–1474 (2003).

50. Malhotra, P., Gill, R. K., Dudeja, P. K. & Alrefai, W. A. Diabetes Mellitus and Intestinal Niemann-Pick C1-Like 1 Gene Expression. in *Molecular Nutrition and Diabetes: A Volume in the Molecular Nutrition Series* (ed. Mauricio, D.) 277–290 (Academic Press, 2016). doi:10.1016/B978-0-12-801585-8.00022-1.

51. Kumari, A. Cholesterol Synthesis. in *Sweet Biochemistry: Remembering Structures, Cycles, and Pathways by Mnemonics* (ed. Kumari, A.) 27–31 (Academic Press, 2018). doi:10.1016/b978-0-12-814453-4.00007-8.

52. Maranhão, R. C., Casela Filho, A., Sigal, G. A., Chagas, A. C. P. & da Luz, P. L. HDL and Endothelium. in *Endothelium and Cardiovascular Diseases: Vascular Biology and Clinical Syndromes* (eds. Luz, P. L. Da, Libby, P., Chagas, A. C. P. & Laurindo, F. R. M.) 297–317 (Academic Press, 2018). doi:10.1016/B978-0-12-812348-5.00022-2.

53. Marques, L. R. *et al.* Reverse cholesterol transport: Molecular mechanisms and the non-medical approach to enhance HDL cholesterol. *Front. Physiol.* **9**, 1–11 (2018).

54. Structure, H. D. L., Brufau, G., Groen, A. K. & Kuipers, F. Reverse Cholesterol Transport Revisited. *Arterioscler. Thromb. Vasc. Biol.* **31**, 1726–1733 (2011).

55. Ouimet, M., Barrett, T. J. & Fisher, E. A. HDL and reverse cholesterol transport: Basic mechanisms and their roles in vascular health and disease. *Circ. Res.* **124**, 1505–1518 (2019).

56. Reckless, J. P. D. & Lawrence, J. M. Hyperlipidemia (Hyperlipidaemia). in *Encyclopedia of Food Sciences and Nutrition* (ed. Caballero, B.) 3183–3192 (Academic Press, 2003). doi:10.1016/b0-12-227055-x/00613-1.

57. Drew, L. An age-old story of dementia. *Nature* **559**, S2–S3 (2018).

58. Falé, P. *et al.* Antioxidant and anti-acetylcholinesterase activity of commercially available medicinal infusions after in vitro gastrointestinal digestion. *J. Med. Plants Res.* **7**, 1370–1378 (2013).

59. Masters, C. L. *et al.* Alzheimer's disease. *Nat. Rev. Dis. Prim.* **1**, 1–18 (2015).

60. Wanamaker, B. L., Swiger, K. J., Blumenthal, R. S. & Martin, S. S. Cholesterol, Statins, and Dementia: What the Cardiologist Should Know. *Clin. Cardiol.* **38**, 243–250 (2015).

61. Huttunen, H. J. & Kovacs, D. M. ACAT as a Drug Target for Alzheimer's Disease. *Neurodegener. Dis.* **5**, 212–214 (2008).

62. Lee, C.-H. *et al.* Antioxidant Activity of Brown Soybean Ethanolic Extracts and Application to Cooked Pork Patties. *Korean J. Food Sci. An* **36**, 359–368 (2016).

63. De Oliveira, A. C. *et al.* Fontes vegetais naturals de antioxidantes. *Quim. Nova* **32**, 689–702 (2009).

64. Tsai, P. J., Tsai, T. H. & Ho, S. C. In vitro inhibitory effects of rosemary extracts on growth and glucosyltransferase activity of Streptococcus sobrinus. *Food Chem.* **105**, 311–316 (2007).

65. Chang, C. C., Yang, M. H., Wen, H. M. & Chern, J. C. Estimation of total flavonoid content in propolis by two complementary colometric methods. *J. Food Drug Anal.* **10**, 178–182 (2002).

66. Mozzicafreddo, M., Cuccioloni, M., Eleuteri, A. M. & Angeletti, M. Rapid reverse phase-HPLC assay of HMG-CoA reductase activity. *J. Lipid Res.* **51**, 2460–2463 (2010).

67. Porfírio, S. *et al.* Antiacetylcholinesterase and antioxidant activities of Plectranthus barbatus tea, after in vitro gastrointestinal metabolism. *Food Chem.* **122**, 179–187 (2010).

68. Stockert, J. C., Blázquez-Castro, A., Cañete, M., Horobin, R. W. & Villanueva, Á. MTT assay for cell viability: Intracellular localization of the formazan product is in lipid droplets. *Acta Histochem.* **114**, 785–796 (2012).

69. Van Meerloo, J., Kaspers, G. J. L. & Cloos, J. Cell senstitivity assays: The MTT assay. in *Cree I. (eds) Cancer Cell Culture: Methods and Protocols* vol. 731 237–245 (Humana Press, 2011).

70. Hu, M., Ling, J., Lin, H. & Chen, J. Use of Caco-2 Cell Monolayers to Study Drug Absorption and Metabolism. in *Optimization in Drug Discovery* 19–35 (Humana Press, 2004). doi:10.1385/1-59259-800-5:019.

71. Arantes, A. A. *et al.* Inhibition of HMG-CoA reductase activity and cholesterol permeation through Caco-2 cells by caffeoylquinic acids from Vernonia condensata leaves. *Rev. Bras. Farmacogn.* **26**, 738–743 (2016).

72. Falé, P. L., Altharawi, A. & Chan, K. L. A. In situ Fourier transform infrared analysis of live cells' response to doxorubicin. *Biochim. Biophys. Acta - Mol. Cell Res.* **1853**, 2640–2648 (2015).

73. Mihoubi, W., Sahli, E., Gargouri, A. & Amiel, C. FTIR spectroscopy of whole cells for the monitoring of yeast apoptosis mediated by p53 over-expression and its suppression by Nigella sativa extracts. *PLoS One* **12**, 1–16 (2017).

74. André, R. *et al.* Action of euptox A from Ageratina adenophora juice on human cell lines: A top-down study using FTIR spectroscopy and protein profiling. *Toxicol. Vitr.* **57**, 217–225 (2019).

75. Alegria-Schaffer, A., Lodge, A. & Vattem, K. Performing and Optimizing Western Blots with an Emphasis on Chemiluminescent Detection. in *Methods in Enzymology* (eds. Burgess, R. R. & Deutscher, M. P.) vol. 463 573–599 (Academic Press Inc., 2009).

76. Lai, S. H. *et al.* Cytotoxic activity, DNA damage, cellular uptake, apoptosis and western blot analysis of ruthenium(II) polypyridyl complex against human lung decarcinoma A549 cell. *J. Inorg. Biochem.* **152**, 1–9 (2015).

77. Nantitanon, W., Yotsawimonwat, S. & Okonogi, S. Factors influencing antioxidant activities and total phenolic content of guava leaf extract. *LWT - Food Sci. Technol.* **43**, 1095–1103 (2010).

78. Pérez-Pérez, E. *et al.* Determinación de fenoles y flavonoides totales en hojas de guayabo (Psidium guajava L.). *Rev. la Fac. Agron.* **31**, 60–77 (2014).

79. Ngamukote, S., Mäkynen, K., Thilawech, T. & Adisakwattana, S. Cholesterol-lowering activity of the major polyphenols in grape seed. *Molecules* **16**, 5054–5061 (2011).

80. Henriques, J. *et al.* Valorization of kiwifruit production: leaves of the pruning branches of Actinidia deliciosa as a promising source of polyphenols. *Eur. Food Res. Technol.* **243**, 1343–1353 (2017).

81. Mata, A. T. *et al.* Antioxidant and antiacetylcholinesterase activities of five plants used as Portuguese food spices. *Food Chem.* **103**, 778–786 (2007).

82. Ressaissi, A., Attia, N., Falé, P. L. V, Pacheco, R. & Teixeira, V. H. Aqueous extracts from Nopal (Opuntia ficus-indica): antiacetylcholinesterase and antioxidant activity from phenolic bioactive compounds. *Int. J. Green Herb. Chem.* **5**, 337–348 (2016).

83. Okawa, M., Kinjo, J., Nohara, T. & Ono, M. DPPH (1,1-Diphenyl-2-Picrylhydrazyl) Radical Scavenging Activity of Flavonoids Obtained from Some Medicinal Plants. *Biol. Pharm. Bull.* **24**, 1202–1205 (2001).

84. Freire, J. M., de Abreu, C. M. P., Duarte, S. M. da S., de Paula, F. B. A. & Lima, A. R. Evaluation of the protective effect of guava fruits and leaves on oxidative stress. *Acta Sci. - Biol. Sci.* **36**, 35–40 (2014).

85. Fisher, S. K. & Wonnacott, S. Acetylcholine. *Basic Neurochem.* 258–282 (2012) doi:10.1016/B978-0-12-374947-5.00013-4.

86. Guedes, L. *et al.* Bioactivities of Centaurium erythraea (Gentianaceae) Decoctions: Antioxidant activity, enzyme inhibition and docking studies. *Molecules* **24**, 3795 (2019).

87. Colovic, M. B., Krstic, D. Z., Lazarevic-Pasti, T. D., Bondzic, A. M. & Vasic, V. M. Acetylcholinesterase Inhibitors: Pharmacology and Toxicology. *Curr. Neuropharmacol.* **11**, 315–335 (2013).

88. Hernandez, M. F., Falé, P. L. V, Araújo, M. E. M. & Serralheiro, M. L. M. Acetylcholinesterase inhibition and antioxidant activity of the water extracts of several Hypericum species. *Food Chem.* **120**, 1076–1082 (2010).

89. Raufman, J.-P. Pepsin. in *Encyclopedia of Gastroenterology* 147–148 (Elsevier, 2004). doi:10.1016/b0-12-386860-2/00561-x.

90. Bouayed, J., Deußer, H., Hoffmann, L. & Bohn, T. Bioaccessible and dialysable polyphenols in selected apple varieties following in vitro digestion vs. their native patterns. *Food Chem.* **131**, 1466–1472 (2012).

91. Okonogi, S., Duangrat, C., Anuchpreeda, S., Tachakittirungrod, S. & Chowwanapoonpohn, S. Comparison of antioxidant capacities and cytotoxicities of certain fruit peels. *Food Chem.* **103**, 839–846 (2007).

92. Nurcahyanti, A. D. R. & Wink, M. L-Canavanine potentiates the cytotoxicity of doxorubicin and cisplatin in arginine deprived human cancer cells. *PeerJ* **2016**, (2016).

93. Falé, P. L., Ascensão, L. & Serralheiro, M. L. M. Effect of luteolin and apigenin on rosmarinic acid bioavailability in Caco-2 cell monolayers. *Food Funct.* **4**, 426–431 (2013).

94. Nekohashi, M. *et al.* Luteolin and quercetin affect the cholesterol absorption mediated by epithelial cholesterol transporter Niemann-Pick C1-Like 1 in Caco-2 cells and rats. *PLoS One* **9**, 1–9 (2014).

95. Leifert, W. R. & Abeywardena, M. Y. Grape seed and red wine polyphenol extracts inhibit cellular cholesterol uptake, cell proliferation, and 5-lipoxygenase activity. *Nutr. Res.* **28**, 842–850 (2008).

96. Ozeki, K. *et al.* Evaluation of the appropriate time range for estimating the apparent permeability coefficient (Papp) in a transcellular transport study. *J. Chem. Inf. Model.* **52**, 1833–1841 (2012).

97. Li, D. *et al.* Structure-based design and screen of novel inhibitors for class II 3-hydroxy-3-methylglutaryl coenzyme a reductase from Streptococcus pneumoniae. *J. Chem. Inf. Model.* **52**, 1833–1841 (2012).

98. Ressaissi, A., Attia, N., Pacheco, R., Falé, P. L. & Serralheiro, M. L. M. Cholesterol transporter proteins in HepG2 cells can be modulated by phenolic compounds present in Opuntia ficus-indica aqueous solutions. *J. Funct. Foods* **64**, (2020).

99. Benedetti, E. *et al.* Infrared Characterization of Nuclei Isolated from Normal and Leukemic (B-CLL) Lymphocytes: Part III. *Appl. Spectrosc.* **40**, 39–43 (1986).

100. Sabbatini, S., Conti, C., Orilisi, G. & Giorgini, E. Infrared spectroscopy as a new tool for studying single living cells: Is there a niche? *Biomed. Spectrosc. Imaging* **6**, 85–99 (2017).

101. Giorgini, E. *et al.* FTIR microspectroscopic characterization of Spitz nevi. *Spectrochim. Acta - Part A Mol. Biomol. Spectrosc.* **141**, 99–103 (2015).

102. Mitri, E. *et al.* Time-Resolved FT-IR Microspectroscopy of Protein Aggregation Induced by Heat-Shock in Live Cells. *Anal. Chem.* **87**, 3670–3677 (2015).

103. Saulou, C. *et al.* Synchrotron FTIR microspectroscopy of the yeast Saccharomyces cerevisiae after exposure to plasma-deposited nanosilver-containing coating. *Anal. Bioanal. Chem.* **396**, 1441–1450 (2010).

104. Davies, A. & Fearn, T. Back to Basics: The Principles of Principal Component Analysis. *Spectrosc. Eur. Tony Davies Column* **16**, 20–23 (2005).

105. Bonnier, F. & Byrne, H. J. Understanding the molecular information contained in principal component analysis of vibrational spectra of biological systems. *Analyst* **137**, 322–332 (2012).

106. Altharawi, A., Rahman, K. M. & Chan, K. L. A. Towards identifying the mode of action of drugs using live-cell FTIR spectroscopy. *Analyst* **144**, 2725–2735 (2019).

107. Salucci, M., Bugianesi, R., Maiani, G., Stivala, L. A. & Vannini, V. Flavonoids uptake and their effect on cell cycle of human colon adenocarcinoma cells (Caco2). *Br. J. Cancer* **86**, 1645–1651 (2002).

108. Falé, P. L. *et al.* Acetylcholinesterase inhibition, antioxidant activity and toxicity of Peumus boldus water extracts on HeLa and Caco-2 cell lines. *Food Chem. Toxicol.* **50**, 2656–2662

(2012).

109. Böhl, M., Czupalla, C., Tokalov, S. V., Hoflack, B. & Gutzeit, H. O. Identification of actin as quercetin-binding protein: An approach to identify target molecules for specific ligands. *Anal. Biochem.* **346**, 295–299 (2005).

110. Kobayashi, S. The effect of polyphenols on hypercholesterolemia through inhibiting the transport and expression of niemann–pick C1-like 1. *Int. J. Mol. Sci.* **20**, 1–14 (2019).

111. Liu, S., You, L., Zhao, Y. & Chang, X. Wild Lonicera caerulea berry polyphenol extract reduces cholesterol accumulation and enhances antioxidant capacity in vitro and in vivo. *Food Res. Int.* **107**, 73–83 (2018).

112. Kawase, A., Hata, S., Takagi, M. & Iwaki, M. Pravastatin modulate niemann-pick C1-like 1 and ATP-binding cassette G5 and G8 to influence intestinal cholesterol absorption. *J. Pharm. Pharm. Sci.* **18**, 765–772 (2015).

VII. Annex

Annex 1: Identified molecules in *P. guajava* decoction in the bibliography

Table 7.14: Molecules identified in *P. guajava* leaves from literature.

Name	Molecular formula	Molecular weight (g/mol)	Reference
(+)-gallocatechin	$C_{15}H_{14}O_7$	306.270	6
Acetylursolic acid	$C_{32}H_{50}O_4$	498.700	21
Apigenin-7-*O*-glucoside	$C_{21}H_{20}O_{10}$	432.400	6
Ascorbic acid	$C_6H_8O_6$	176.120	3
Asiatic acid	$C_{30}H_{48}O_5$	488.700	19
Asparagine	$C_4H_8N_2O_3$	132.120	24
Astragalin	$C_{21}H_{20}O_{11}$	448.400	3
Avicularin	$C_{20}H_{18}O_{11}$	434.350	6
Azulene	$C_{10}H_8$	128.170	3
Betulinic acid	$C_{30}H_{48}O_3$	456.700	23
Caffeic acid	$C_9H_8O_4$	180.160	3
Cadinene	$C_{15}H_{24}$	204.350	6
Caryophyllene	$C_{15}H_{24}$	204.350	6
Caryophyllene oxide	$C_{15}H_{24}O$	220.350	6
Catechin	$C_{15}H_{14}O_6$	290.271	4
Chlorogenic acid	$C_{16}H_{18}O_9$	354.310	3
Cinnamyl alcohol	$C_9H_{10}O$	134.170	3
Cis-aconitic acid	$C_6H_6O_6$	174.110	24
Citric acid	$C_6H_8O_7$	192.120	24
Corosolic acid	$C_{30}H_{48}O_4$	472.700	19
Curcumene	$C_{15}H_{22}$	202.330	6
Cynaroside	$C_{21}H_{20}O_{11}$	448.400	6
Ellagic acid	$C_{14}H_6O_8$	302.190	3
Epicatechin	$C_{15}H_{14}O_6$	290.270	16
Epigallocatechin gallate	$C_{22}H_{18}O_{11}$	458.372	4
Eucalyptol	$C_{10}H_{18}O$	154.250	3
Eucalyptolic acid	$C_{40}H_{56}O_7$	648.900	21
Farnesene	$C_{15}H_{24}$	204.350	6
Ferulic acid	$C_{10}H_{10}O_4$	194.180	3
Gallic acid	$C_7H_6O_5$	170.120	3
Glutamic acid	$C_5H_9NO_4$	147.130	24
Goreishic acid I	$C_{30}H_{46}O_4$	470.700	19
Guaijaverin	$C_{20}H_{18}O_{11}$	434.350	6
Guajanoic acid	$C_{40}H_{56}O_6$	632.408	6
Guajavanoic acid	$C_{37}H_{53}O_6$	593.811	18
Guajavolide	$C_{30}H_{46}O_6$	502.681	17
Guavacoumaric acid	$C_{39}H_{54}O_7$	634.800	19
Guavanoic acid	$C_{32}H_{51}O_6$	530.361	19
Guavenoic acid	$C_{30}H_{46}O_6$	502.681	17
Guavin A	$C_{56}H_{40}O_{32}$	1224.900	6
Guavin B	$C_{33}H_{26}O_{17}$	694.500	6
Guavinoside A	$C_{30}H_{34}O_5$	474.600	23

Guavinoside B	$C_{30}H_{36}O_6$	492.600	[23]
Guavinoside C	$C_{30}H_{36}O_6$	492.600	[23]
Humulene	$C_{15}H_{24}$	204.350	[6]
Hyperoside	$C_{21}H_{20}O_{12}$	464.380	[6]
Ilelatifol D	$C_{30}H_{46}O_4$	470.700	[19]
Isoneriucoumaric acid	$C_{39}H_{54}O_6$	618.800	[19]
Isoquercitrin	$C_{21}H_{20}O_{12}$	464.380	[6]
Isostrictinin	$C_{27}H_{22}O_{18}$	634.500	[6]
Jacoumaric acid	$C_{39}H_{54}O_6$	618.800	[19]
Kaempferol	$C_{15}H_{10}O_6$	286.230	[6]
Leucocyanidin	$C_{15}H_{14}O_7$	306.270	[3]
Limonene	$C_{10}H_{16}$	136.238	[6]
Longicyclene	$C_{15}H_{24}$	204.350	[6]
Lupeol	$C_{30}H_{50}O$	426.700	[23]
Maleic acid	$C_4H_4O_4$	116.070	[24]
Malonic acid	$C_3H_4O_4$	104.060	[24]
Maslinic acid	$C_{30}H_{48}O_4$	472.710	[6]
Menthol	$C_{10}H_{20}O$	156.269	[6]
Methyl cinnamate	$C_{10}H_{10}O_2$	162.180	[3]
Morin-3-*O*-α-L-arabinopyranoside	$C_{20}H_{18}O_{11}$	434.350	[3]
Nerolidol	$C_{15}H_{26}O$	222.370	[6]
Obtusinin	$C_{15}H_{18}O_6$	294.300	[6]
O-coumaric acid	$C_9H_8O_3$	164.160	[4]
Oleanolic acid	$C_{30}H_{48}O_3$	456.711	[18]
Protocatechuic acid	$C_7H_6O_4$	154.120	[3]
Psidial A	$C_{30}H_{34}O_5$	474.600	[23]
Psidial B	$C_{30}H_{36}O_6$	492.600	[23]
Psidial C	$C_{30}H_{36}O_6$	492.600	[23]
Psidiumoic acid	$C_{32}H_{52}O_5$	516.752	[20]
Psiguadial A	$C_{30}H_{34}O_5$	474.600	[23]
Psiguadial B	$C_{30}H_{34}O_5$	474.600	[23]
Psiguanin A	$C_{30}H_{48}O_4$	472.700	[21]
Psiguanin B	$C_{30}H_{50}O_6$	506.710	[21]
Psiguanin C	$C_{30}H_{50}O_6$	506.710	[21]
Psiguanin D	$C_{30}H_{50}O_6$	506.710	[21]
Quercetin	$C_{15}H_{10}O_7$	302.236	[6]
Quercetin 3-*O*-gentiobioside	$C_{27}H_{30}O_{17}$	626.500	[6]
Quercetin 4'-glucuronoide	$C_{21}H_{18}O_{13}$	478.400	[6]
Quercitrin	$C_{21}H_{20}O_{11}$	448.380	[6]
Resveratrol	$C_{14}H_{12}O_3$	228.230	[4]
Reynoutin	$C_{20}H_{18}O_{11}$	434.300	[23]
Rutin	$C_{27}H_{30}O_{16}$	610.521	[16]
Selinene	$C_{15}H_{24}$	204.350	[6]
Strictinin	$C_{27}H_{22}O_{18}$	634.500	[6]
Syringic acid	$C_9H_{10}O_5$	198.174	[4]
Trans-aconitic acid	$C_6H_6O_6$	174.110	[24]

Ursolic acid	$C_{30}H_{48}O_3$	456.700	[18]
Uvaol	$C_{30}H_{50}O_2$	442.700	[18]
Veridiflorene	$C_{16}H_{26}$	282.109	[16]
Xanthine	$C_5H_4N_4O_2$	152.110	[24]
α-pinene	$C_{10}H_{16}$	136.238	[6]
β-bisabolene	$C_{15}H_{24}$	204.350	[6]
β-pinene	$C_{10}H_{16}$	136.238	[6]
β-sitosterol	$C_{29}H_{50}O$	414.718	[18]
β-sitosterol-3-*O*-β-D-glucopyranoside	$C_{60}H_{100}O_7$	933.400	[19]
τ-cadinol	$C_{15}H_{26}O$	222.370	[16]

Annex 2: Identification of compounds in *P. guajava* leaf decoction through LC-HRMS-MS analysis

Table 4.15: Relative difference heatmap between peak intensities from PG1 and PG2, in the negative ion mode.

	Negative ion mode		
Accurate $[M-H]^-$ *m/z*	PG1	PG2	Relative difference (%)
191.0565	139718	81038	
215.0329	139718	14178	
169.0142	19888	17554	
153.0194	17588	0	
451.219	52982	29370	
441.1896	46162	27964	
289.0718	12398	7494	
305.0698	81774	19014	
371.0983	24316	6566	
380.9924	289108	23112	
301.0353	289108	177110	
463.0888	50724	33540	
307.1401	63316	46238	
433.078	47862	13556	
447.0932	62208	11662	
483.0707	72720	49010	

Table 4.16: Relative difference heatmap between peak intensities from PG1 and PG2, in the positive ion mode.

	Positive ion mode		
Accurate $[M-H]^+$ *m/z*	PG1	PG2	Relative difference (%)
219.0268	174938	0	
282.0873	153798	0	
363.1135	153798	0	
266.1235	49994	27946	
192.0593	29378	13380	
332.1345	150440	25520	
171.0288	9076	0	
291.0863	23578	10250	
355.1024	257790	11750	
465.1025	38708	32998	
303.0498	55364	52370	
435.0922	70908	46858	
449.1074	42576	29114	
351.2014	62466	13220	
373.1831	37382	22382	
412.2538	69944	11044	
417.2091	69944	26822	
433.1833	69944	26822	
456.2801	72376	20476	
461.2354	72376	25934	
477.2094	72376	25934	
500.306	65832	23804	
505.2616	65832	19010	
521.2354	65832	23804	
549.2877	13852	13100	
544.3326	36332	16334	
619.4025	9942	0	

Annex 3: *In vitro* gastrointestinal digestion of *P. guajava* leaf decoction

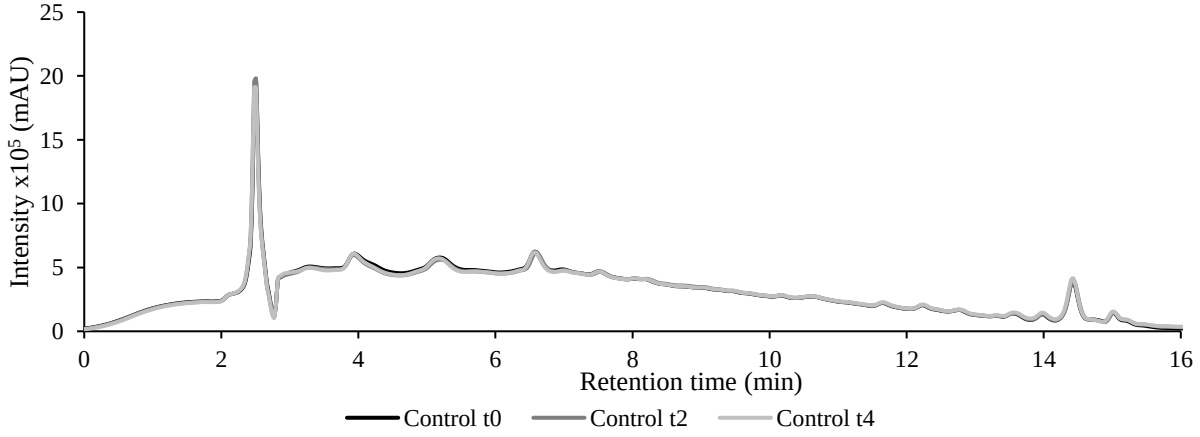

Figure 7.22: HPLC-DAD chromatogram of PG1 and water (control) at t0, t2, and t4.

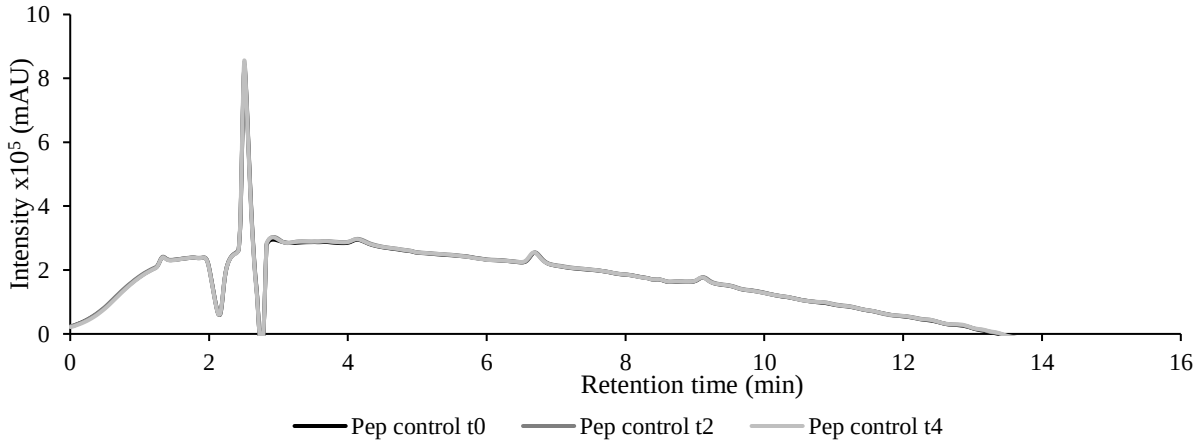

Figure 7.23: HPLC-DAD chromatogram of pepsin control (Pep control) at t0, t2, and t4.

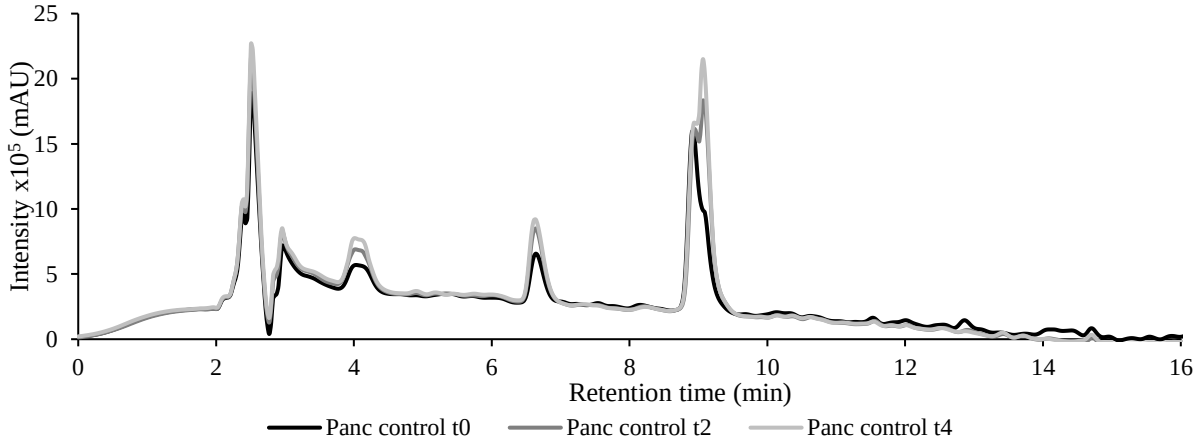

Figure 7.24: HPLC-DAD chromatogram of pancreatin control (Panc control) at t0, t2, and t4.

Annex 4: SDS-PAGE of membrane and cytosolic proteins from Caco-2

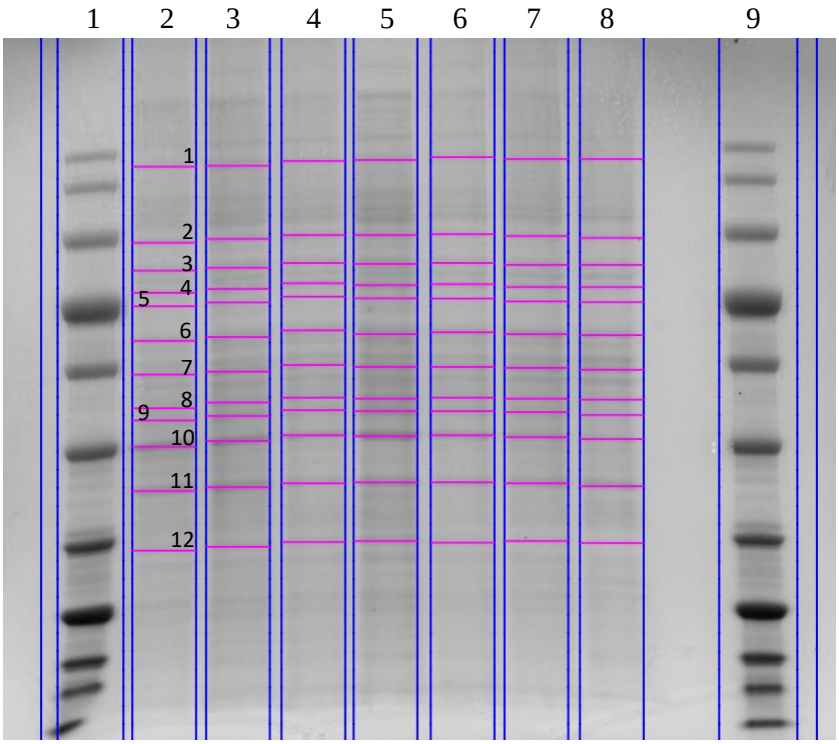

Figure 7.25: SDS-PAGE of membrane proteins from Caco-2 cells treated with PG1 0.25 mg/mL (lane 2), 0.50 mg/mL (lane 3), and 0.75 mg/mL (lane 4), and treated with PG2 0.25 mg/mL (lane 6), 0.50 mg/mL (lane 7), and 0.75 mg/mL (lane 8) for 24 h. Lanes 1 and 9 correspond to the protein marker and lane 5 corresponds to untreated cells (control). The analyzed bands are marked with horizontal strokes and numbered from 1 to 12.

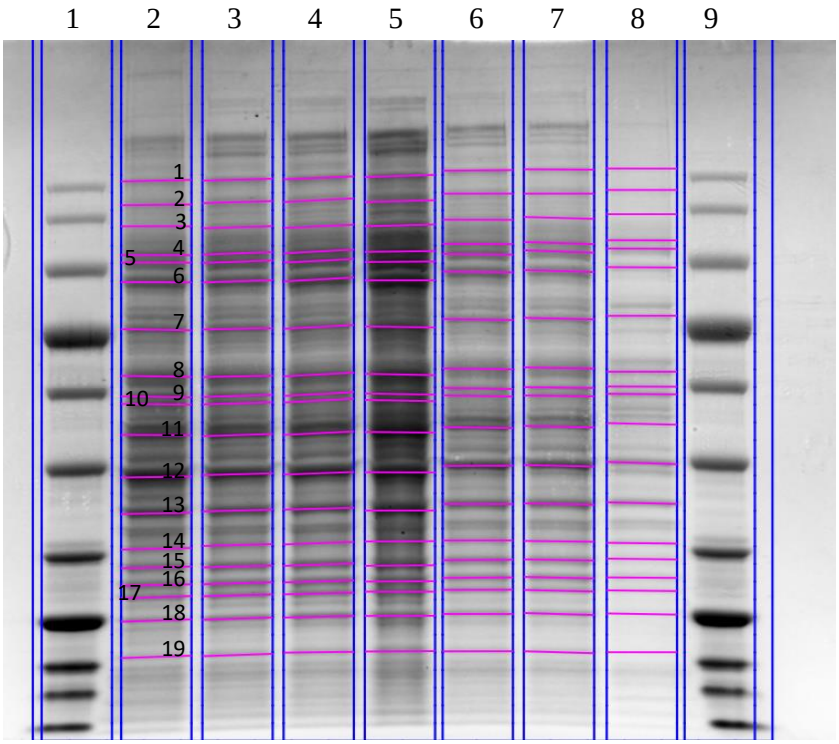

Figure 7.26: SDS-PAGE of cytosolic proteins from Caco-2 cells treated with PG1 0.25 mg/mL (lane 2), 0.50 mg/mL (lane 3), and 0.75 mg/mL (lane 4), and treated with PG2 0.25 mg/mL (lane 6), 0.50 mg/mL (lane 7), and 0.75 mg/mL (lane 8) for 24 h. Lanes 1 and 9 correspond to the protein marker and lane 5 corresponds to untreated cells (control). The analyzed bands are marked with horizontal strokes and numbered from 1 to 19.